The Pennsylvania State University

The Graduate School

Department of Physiology

MULTIPLE MECHANISMS OF ODC REGULATION BY ACTIVATED RAS: STUDIES IN AN EPITHELIAL CELL MODEL

A Thesis in

Physiology

By

Sofia S. Origanti

© 2007 Sofia S. Origanti

Submitted in Partial Fulfillment
of the Requirements
for the Degree of

Doctor of Philosophy

May 2007

The thesis of Sofia S. Origanti was reviewed and approved* by the following:

Lisa M. Shantz
Associate Professor of Cellular and Molecular Physiology
Thesis Advisor
Chair of Committee

Gary A. Clawson
Professor of Pathology, and Biochemistry and Molecular Biology

Scot R. Kimball
Professor of Cellular and Molecular Physiology

Anthony E. Pegg
Evan Pugh Professor of Cellular and Molecular Physiology, and Pharmacology
J. Lloyd Huck Professor of Cellular and Molecular Biology

Stephen R. Rannels
Associate Professor of Cellular and Molecular Physiology

Leonard S. Jefferson, Jr.
Evan Pugh Professor and Chair of Cellular and Molecular Physiology Department

* Signatures are on file in the Graduate School

ABSTRACT

A majority of human cancers carry activating mutations in the Ras oncogene. One of the key effectors of Ras that is essential for its tumorigenic properties is Ornithine Decarboxylase (ODC). Studies characterizing the effects of Ras on ODC synthesis have thus far been carried out in fibroblasts. However, since most Ras-activated cancers are epithelial in origin, we aimed to determine the regulation of ODC by activated Ras using an epithelial cell model, RIE-1 cells. Ras transformation greatly induced ODC activity, which was predominantly regulated at the level of RNA stability. Increased RNA stability correlated with increased levels of ODC RNA associated with the polysomes. Treatment with the mTOR inhibitor Rapamycin surprisingly inhibited this increase in RNA stability without affecting transcription or efficiency of ODC translation. Analysis of the ODC 5'UTR in control and Ras12V-transfected cells revealed the presence of four splice variants of variable length, with the presence or absence of two intronic sequences. The variants containing intronic sequences were more abundant in the Ras-transformed cells. All splice variants supported internal ribosome entry site (IRES)-mediated translation, and this activity was markedly elevated in cells transformed by Ras, which was further increased by dephosphorylation of eIF4E by inhibiting either MEK or its kinase Mnk even in RIE-1 cells. When both the Raf-kinase and PI3K /mTOR pathways were inhibited in normal cells, ODC IRES activity was very low, and most cells arrested in G1. However, when these pathways were inhibited in Ras-transformed cells, cell cycle arrest did not occur and ODC IRES activity increased, thus maintaining the high levels of ODC activity. In conclusion, our study for the first time shows that Ras predominantly regulates ODC synthesis both at the level of RNA degradation and also by a novel

mechanism involving IRES-mediated translation. Understanding the regulation of ODC will help us to develop better therapeutic strategies to treat Ras-activated cancers.

TABLE OF CONTENTS

LIST OF FIGURES

LIST OF TABLES

LIST OF ABBREVIATIONS

AdoMetDc	S-adenosylmethionine decarboxylase
APC	Adenomatous polyposis coli
AZ	Antizyme
AMPK	AMP activated protein kinase
ActD	Actinomycin D
Cdkn2b	Cyclin dependent kinase inhibitor 2b
DFMO	α–diflouromethylornithine
DMEM	Dulbecco's modified essential medium
DMSO	Dimethyl Sulfoxide
Dsh	Dishevelled
4EBP1	eIF4E binding protein1
EGFR	Epidermal Growth Factor Receptor
Egr-1	Early growth response 1
eIF4E	eukaryotic Initiation Factor 4E
eIF4G	eukaryotic Initiation Factor 4G
eIF4A	eukaryotic Initiation Factor 4A
eIF4B	eukaryotic Initiation Factor 4B
eIF4F	eukaryotic Initiation Factor 4F
eIF2	eukaryotic Initiation Factor 2
eIF3	eukaryotic Initiation Factor 3
eIF5	eukaryotic Initiation Factor 5
EMCV	Encephalomyocarditis virus

EMT	Epithelial to Mesenchymal Transition
ERK	Extracellular Signal-regulated kinase
Fzd	Frizzled
GEF	Guanine nucleotide Exchange Factor
GAP	GTPase activating protein
HLH/LZ	helix-loop-helix/leucine –zipper structure
HuR	HU-antigen R
IRES	Internal Ribosome Entry Site
ITAF's	IRES Transacting Factors
K5	Keratin 5
K6	Keratin 6
K14	Keratin 14
KSR1	Kinase suppressor of Ras
MAPK	Mitogen Activated Protein Kinase
MEK	Mitogen-activated protein kinase/extracellular signal-regulated kinase
MM	Mis Match
MYC	Myelocytomatosis viral oncogene homolog
Max	Myc-associated factor X
Mad	Max dimerization protein
Mnk	MAPK interacting kinase
Mnt	Max binding protein
mTOR	mammalian target of Rapamycin

ODC	Ornithine Decarboxylase
ORS	Outer root sheath
ORF	Open reading frame
PABP	Poly A tail binding protein
PAGE	Polyacrylamide gel electrophoresis
PDK1	Phosphoinositide-dependent protein kinase 1
PI	Phosphoinositides
PI3K	Phosphatidyl Inositol 3-Kinase
PM	Perfect Match
PTB	Polypyrimdine tract binding protein
PTEN	Phosphatase and tensin homolog deleted on chromosome ten
Raf	murine leukemia viral oncogene homologue
Rheb	Ras homolog enriched in brain
RIE-1	Rat intestinal epithelial cell-1
S6K	Ribosomal protein S6 kinase
SNP	Single nucleotide Polymorphism
Tgfβ1	Tumor growth factor beta1
Tiam1	T-lymphoma and metastasis invasion protein
TOP	Terminal Oligo Pyrimidine
TPA	12-O-tetradecanoyl-phorbol-13-acetate
TSC	Tuberous Sclerosis Complex
TTP	Tristetraprolin
Unr	Upstream of N-Ras

uORF	Upstream open reading frame
Wnt	Wingless-type MMTV integration site family member
5’UTR	5’ Untranslated region
3’UTR	3’ Untranslated region

ACKNOWLEDGEMENTS

"At times our own light goes out and is rekindled by a spark from another person. Each of us has cause to think with deep gratitude of those who have lighted the flame within us" (Albert Schweitzer).

There are not enough words to express my gratitude for my mentor, Lisa Shantz. The confidence that Lisa has given me has been invaluable and something I would cherish for life. She has taught me how to be a good mentor and researcher. She gave me all the freedom to pursue my thoughts, yet she made sure I stayed on track. I can't thank her enough for guiding me with the utmost patience and care for all these years.

I express my gratitude to the members of my committee; Anthony Pegg, Scot Kimball, Gary Clawson and Steve Rannels for their excellent guidance and support, and scientific input that helped me better understand my project.

I thank Suzie Kuhn for all her help and encouragement. She made the lab feel like home away from home. I thank all the members of the Pegg lab especially Dave Feith, Diane McCloskey and Sreenivas Kanugula for their excellent suggestions and for donating their time to help me with my project, my thesis, and all my presentations. I thank Pat Welsh and Chethana Gowda for their excellent technical expertise with the mice work. I express my gratitude to An Do and Dave Williamson for their invaluable guidance with the polysomal work.

I thank my friends Reena, Aley and Kelly for their constant support and encouragement. I express my gratitude to my family; mom, dad, brother and sister for encouraging and supporting me all these years. I thank my mom and dad especially for

the innumerable things they sacrificed just so I could have a good education. Finally I thank my husband Edwin for his support and for just holding my hand through it all.

Dedicated to those who were ever afflicted by this disease
And to my Family

Chapter I

Introduction

Overview of the polyamine biosynthetic pathway

Polyamines are positively charged organic molecules essential for cell growth (Ignatenko et al., 2004; Marton & Pegg, 1995; Pegg, 1988). Due to their cationic nature, polyamines are generally found bound to the negatively charged nucleic acids DNA and RNA in the cell (Marton & Pegg, 1995; Pegg, 1988). Their discovery dates back to the 17th century with the identification of crystals in semen that were later determined to be the polyamine spermine (reviewed in Ignatenko et al., 2004). This was followed by the identification of two other polyamines putrescine and spermidine (reviewed in Marton & Pegg, 1995; Pegg, 1988). Synthesis of polyamines is a highly regulated and complex process. Cells need polyamines for normal growth and survival, but when the levels of polyamines exceed a threshold the consequence is catastrophic, resulting in diseases such as cancer.

Synthesis of polyamines begins with the conversion of the precursor ornithine to the diamine putrescine, which is catalyzed by the enzyme ornithine decarboxylase (ODC) (Fig 1.1) (Marton & Pegg, 1995; Pegg, 1988). Putrescine is then converted into the polyamines spermidine and spermine through the enzymes spermidine synthase and spermine synthase, which catalyze the transfer of aminopropyl groups (Marton & Pegg, 1995; Pegg, 1988). These aminopropyl groups are donated by decarboxylated S-adenosylmethionine generated by the action of S-adenosylmethionine decarboxylase (AdoMetDc) (Fig 1.1) (Pegg, 1988; Pegg et al., 2003). Both spermidine and spermine are converted back to putrescine by acetylation, which is mediated by the enzyme

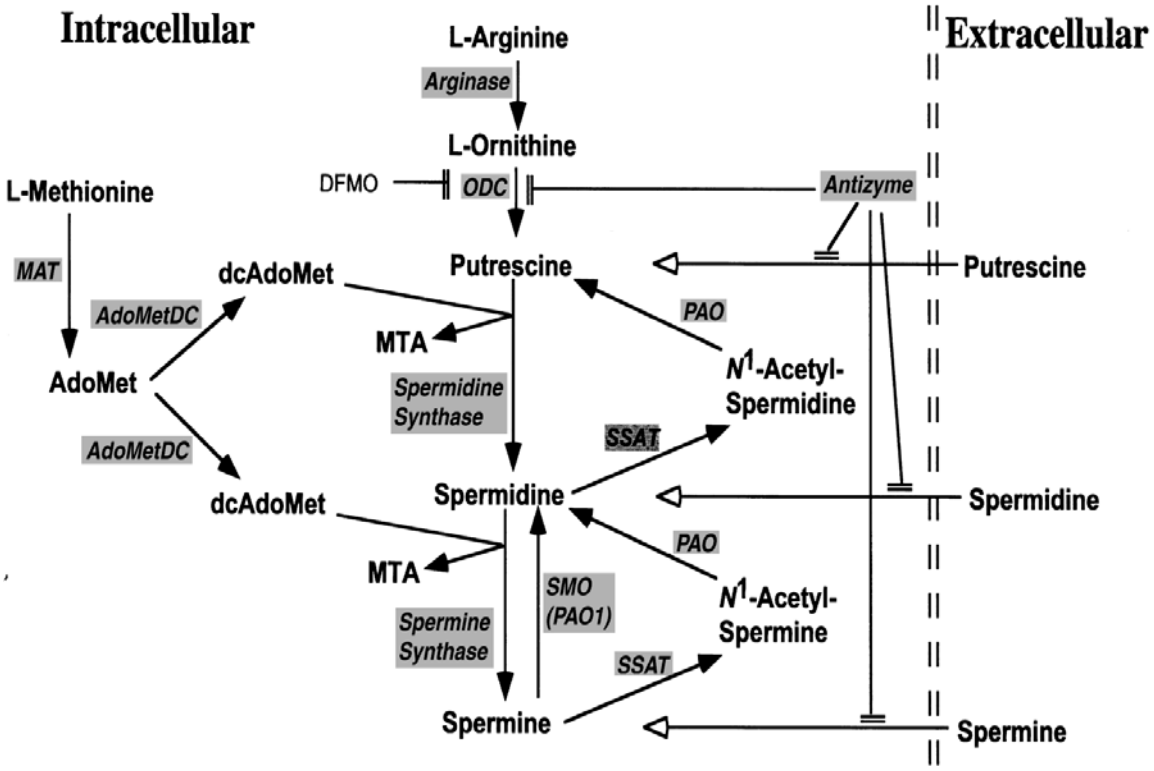

Figure 1.1. Polyamine biosynthetic pathway (Pegg et al., 2003)

See text for details

spermidine/spermine N^1acetyl transferase (SSAT) followed by the action of polyamine oxidase (Fig 1.1) (Ignatenko et al., 2004; Pegg, 1988). The synthesis of polyamines is a highly regulated process swayed by two critical enzymes; ODC and AdoMetDC (Pegg, 1988). Both these enzymes are also essential for mouse development, as homozygous knock out of either ODC or AdoMetDC results in embryonic lethality (Nishimura et al., 2002; Pendeville et al., 2001). Since the main aim of our project is to understand the regulation of ODC, this introduction will primarily focus on the regulation of ODC and its role in carcinogenesis.

ODC and cancer

While there is some evidence to suggest that polyamines are involved in regulating molecular functions such as transcription, translation and ion channel activity, the exact role of polyamines has still remained an obscurity (Lopatin et al., 1994; Park et al., 1993; Pollard et al., 1999). However, it cannot be disputed that polyamines have a critical role in cancer formation and progression. Reports of polyamines and cancer date back to the 1960's, with the observation of increased levels of ODC in several tumors (Russell & Snyder, 1968). Levels of polyamines themselves were found to be elevated in cancers such as hepatomas and sarcomas (Andersson & Heby, 1972). To link ODC to cancer, studies by Boutwell et. al., showed that epidermal ODC is induced in response to treatment with tumor promoting agents such as 12-O-tetradecanoyl-phorbol-13-acetate (TPA), correlating ODC with skin carcinogenesis (O'Brien et al., 1975). Studies show that ODC activity is induced in cancers of an epithelial origin such as prostrate cancer, skin cancers and colon cancers carrying mutations in the tumor suppressor gene adenomatous polyposis coli (APC) (Giardiello et al., 1997; Mohan et al., 1999; O'Brien et

al., 1975).

Functions of polyamines in cancer were predominantly determined by inhibition of ODC activity using the irreversible inhibitor α–difluoromethylornithine (DFMO). DFMO reacts with the active site of ODC and irreversibly inhibits its activity (Kingsnorth, 1986; Pegg, 1988). DFMO treatment results in the decreased synthesis of the polyamines putrescine and spermidine without a significant effect on the levels of spermine (Pegg, 1988; Pera et al., 1986). Its effects were found to be specific for polyamines, as they could be reversed by the administration of putrescine (Pegg, 1988; Pera et al., 1986). A causative role for polyamines in cancer was provided by studies using DFMO, which showed that tumor growth could be successfully reversed in several *in vivo* models of carcinogenesis by affecting several cellular processes such as cell-proliferation, apoptosis and, cell invasiveness (Fong et al., 2001; Sunkara & Rosenberger, 1987; Zirvi et al., 1989). Inhibition of cell invasiveness was observed when treatment with DFMO resulted in a reduction of pulmonary metastases of melanomas, breast and liver cancers and successfully inhibited pulmonary invasiveness of lung cancer cells injected subcutaneously into mice (Sunkara et al., 1989; Sunkara & Rosenberger, 1987; Zirvi et al., 1989). Also, DFMO prevented angiogenesis in several cancers, which was attributed to the inhibited proliferation of endothelial cells (Takigawa et al., 1990; Yunmbam, 1998). While all these studies demonstrated the promise of DFMO as an effective cancer drug, clinical trials failed to establish the anti-tumorigenic properties of DFMO in humans.

The causes for the lack of effectiveness of DFMO in humans still remain unclear, although a few potential explanations include that DFMO has a cytostatic rather than a

cytotoxic response, its effect on ODC is compensated by other enzymes in the pathway, it is not effectively transported into the cell or its failure to affect spermine levels in cells (Pegg, 1988). Although DFMO is not effective for cancer treatment, it is used for other medicinal purposes. For example it is being developed as the drug Vaniqa to treat unwanted facial hair in women, and it is also used to treat African sleeping sickness (trypanosomiasis) (Gerner & Meyskens, 2004). Though not effective for cancer treatment, studies in mouse models of skin and colon cancers showed that DFMO can reduce cancer risk, suggesting that it could be used as a chemopreventive agent (Tang et al., 2004; Tempero et al., 1989). Also, since clinical trials showed that even very high doses of DFMO could be tolerated in humans with reversible side effects such as hearing loss and gastrointestinal problems, DFMO is currently in clinical trials as a chemopreventive agent for colon, skin and cervical cancers (Marton & Pegg, 1995; Pegg, 1988).

ODC has a critical role in carcinogenesis, hence it is important to understand the complete workings of ODC synthesis, especially under cancerous conditions. This would not only help us develop a novel approach to target ODC, but also may help determine potential drugs that can be used in combination with DFMO.

Regulation of ODC by AZ

Induction of ODC elevates polyamine synthesis, and in turn polyamines inhibit ODC levels, thus maintaining a steady pool of polyamines. In the 1970's, a cellular inhibitor of ODC was identified that was induced in response to polyamines

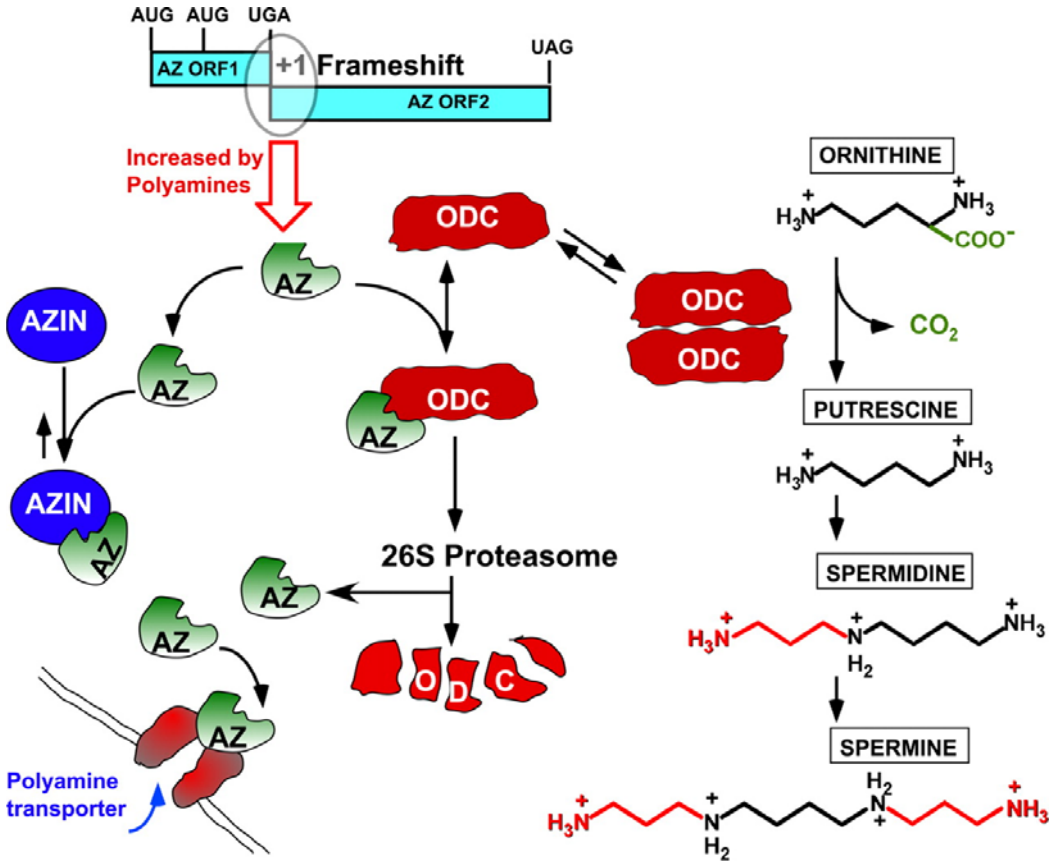

Pegg, A. E. J. Biol. Chem. 2006;281:14529-14532

Figure 1.2. Regulation of ODC and polyamines by AZ (Pegg, 2006)

See text for details

(Heller et al., 1976). This endogenous inhibitor was termed anti-enzyme or antizyme (AZ). AZ is a unique protein that is induced in response to polyamines and in turn checks their levels by inhibiting synthesis and transport of polyamines (Fig 1.2) (Coffino, 2001b). What makes AZ unique is the mechanism by which it responds to polyamines. AZ is encoded by two open reading frames (ORF). The first ORF (ORF1) contains two AUG start codons to initiate translation but ends very shortly at UAG, a conserved stop codon. The second ORF (ORF2) encodes most of the protein but it does not contain a start site (Fig 1.2) (Matsufuji et al., 1995). ORF2 interestingly can only be translated from one of the start codons in ORF1 by a +1 frame shift at the UAG stop codon that results in the synthesis of the entire protein (Fig 1.2) (Matsufuji et al., 1995). The frame shift mechanism is induced by the elevated levels of polyamines, especially by spermidine and spermine more so than putrescine (Fig 1.2) (Matsufuji et al., 1995). While the exact mechanism involved in the polyamine induced frame shifting remains unclear, it has been shown that the secondary structure, a conserved element 5' to the frame-shift site and the stop codon are critical for the polyamine response (Petros et al., 2005).

Synthesis of AZ in response to increased levels of polyamines results in the degradation of ODC. AZ degrades ODC by targeting it to the 26S proteasome and it makes ODC an interesting exception in this process since, unlike other proteins, ODC does not require ubiquitination (Fig 1.2) (Murakami et al., 1992). Degradation of ODC is initiated by the binding of AZ to the ODC monomer, thus disrupting the formation of the enzymatically active ODC homodimers (Fig 1.2) (Coffino, 2001b). AZ bound ODC is then targeted to the 26S proteasome, a process that requires the carboxyl terminus of ODC (Coffino, 2001b). Once ODC is targeted for degradation, AZ is recycled and is

available to dimerize with additional ODC monomers. Thus, in response to high levels of polyamines AZ is induced, resulting in increased ODC degradation and inhibition of polyamine transport, which in turn brings down polyamine levels, thus maintaining cellular homeostasis.

The functions described above are all characterized for one of the AZ isoforms AZ1. There are two other family members AZ2 and AZ3 whose functions still remain obscure (Pegg, 2006). There are also several forms of AZ1, which result when translation is initiated from the first or the second AUG start codon in ORF1 resulting in proteins of sizes 29 KDa and 24.5 KDa, with the 24.5 KDa being the most abundant form. Recent studies have also identified another protein termed AZ inhibitor that binds to AZ with a higher affinity than ODC (Pegg, 2006). However, AZ inhibitor does not have any ODC enzyme properties and its effects on ODC and polyamines are yet to be determined.

Few studies have established the antitumorigenic properties of AZ *in vivo*. Expression of AZ in mouse epidermis using keratin promoters reduced susceptibility to skin carcinogenesis induced by chemical tumor initiation and promotion protocols (Feith et al., 2001). Studies using mice over-expressing AZ and MEK (an effector of the Ras oncogene) have shown that AZ expression delays and decreases spontaneous tumors formed by MEK activation (Feith et al., 2006). Also, expression of AZ in the fore stomach of zinc deficient mice reduced their susceptibility to tumor formation in a chemical carcinogenesis model, and the effects of AZ involved inhibition of cell proliferation and induction of apoptosis (Fong et al., 2003). While these studies implicate AZ as a tumor suppressor, the question still remains whether the functions of AZ are

solely mediated by regulating polyamines. AZ has been shown to be involved in the degradation of other proteins, such as Cyclin D1 and Smad1 (Gruendler et al., 2001; Newman et al., 2004). Over-expression of AZ in cell culture models reduced the levels of the cell-cycle regulator Cyclin D1 suggesting that some of the effects of AZ on cell growth could be mediated by Cyclin D1(Newman et al., 2004). However, further studies have to be carried out to determine the generality of AZ effects on targets other than ODC and their contributions to the tumor suppressing functions of AZ. We have attempted to address some of these questions by a genomic study on tumors induced by MEK also over-expressing AZ and, some of the preliminary results are described in chapter V.

Transcriptional regulation of ODC

Several growth promoting stimuli such as hormones, tumor promoting agents and oncogenes induce transcription of ODC (Shantz, 2004; Zhao & Butler, 2001). Several motifs have been identified in the ODC promoter such as the GC-rich SP1 binding sites, c-AMP response elements, TATA motifs, CAAT and AP-1 and AP-2 motifs that respond to hormones and tumor promoting agents (Qin et al., 2004; Zhao & Butler, 2001). One of the well characterized transcriptional activators of ODC is Myc. Myc belongs to a family of oncogenes (Myc, L-Myc, N-Myc) that are activated in many cancers either directly or by increased action of other oncogenes (Vita & Henriksson, 2006). Myc functions in both activation of cell-proliferation and induction of apoptosis depending on the physiological stimulus (Vita & Henriksson, 2006). Myc interacts with Max, a protein with similar basic helix-loop-helix/leucine –zipper structure (HLH/LZ), and forms a transcriptionally active complex that transcribes several genes such as ODC, eIF4E and CDK4 (Bello-Fernandez

et al., 1993). Myc/Max dimers recognize a specific motif termed an E-box that has a canonical CAYGTG sequence (Bello-Fernandez et al., 1993). Myc recognizes two such highly conserved CACGTG motifs in the ODC promoter (in the first intron) that are required for its transcriptional activity (Fig 1.3) (Bello-Fernandez et al., 1993). Recently an additional CATGTG element was identified in the 5' flanking region of the murine ODC promoter that also responds to Myc (Auvinen et al., 2003). Insight into the mechanism involved in the regulation of ODC synthesis by Myc was provided by the identification of Mnt (Max binding protein) as a transcriptional repressor of ODC. Under resting conditions Mnt complexes with Max (Myc-associated factor X) and competes with the Myc/Max complex to occupy the CAYGTG elements and repress ODC transcription (Fig 1.3) (Nilsson et al., 2004). However, in response to stimuli such as mitogens, Myc is activated and increases transcription of ODC displacing the Mnt/Max complex (Fig 1.3) (Nilsson et al., 2004). Thus, in response to growth activating stimuli, Myc activates transcription of ODC.

Given the oncogenic properties of Myc and the significant role of ODC in carcinogenesis, one study has been carried out so far to directly implicate ODC in Myc induced tumorigenesis. Recent evidence was provided by analyzing the effect of ODC knockdown in the Myc-induced model of Burkitt's lymphoma (Eμ-Myc) (Nilsson et al., 2005). These mice mirror human Burkitt's lymphoma by over-expressing Myc from a heavy chain immunoglobulin enhancer (Eμ). Since ODC -/- mice are not viable, Eμ-Myc mice were crossed with a heterozygous knockout model of ODC +/- and these mice had a delayed formation of lymphomas (Nilsson et al., 2005). More surprisingly, knocking down ODC using DFMO had a greater effect in delaying lymphomagenesis

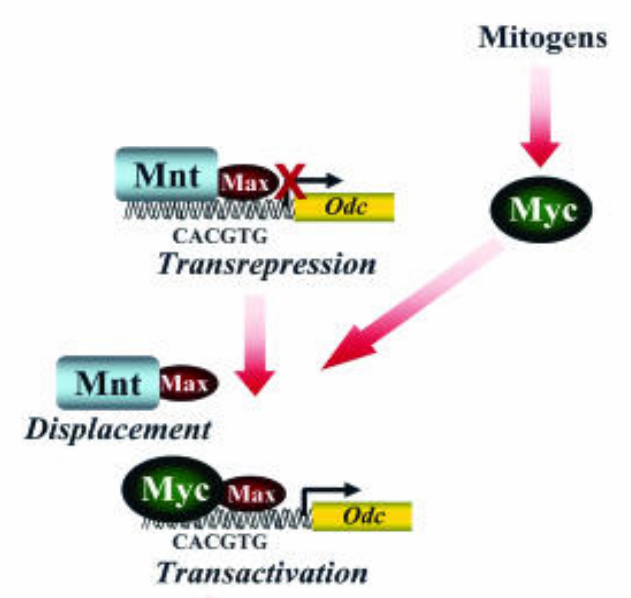

Figure 1.3. Regulation of ODC transcription by Myc (Nilsson et al., 2004)

See text for details

(Nilsson et al., 2005). The effect of ODC knockdown was attributed to the inhibition of Myc-induced proliferation mediated by the relief of suppression of Cyclin dependent kinase inhibitors p21 and p27 (Nilsson et al., 2005).

Further evidence linking transcriptional regulation of ODC to tumorigenesis was provided by the identification of a single nucleotide polymorphism (SNP) in ODC promoter associated with colon cancer risk. In humans, a SNP G315A was found 315 bases from the transcription start site with presence of either one or both alleles of A instead of G (Guo et al., 2000). This SNP is located between the two E-boxes and is recognized by the transcriptional inhibitor Mad1/Max complex (Martinez et al., 2003). Mad1 (Max dimerization protein) was shown to inhibit the expression of luciferase reporter derived from the ODC promoter carrying the A allele much more than the promoter carrying the G allele (Martinez et al., 2003). An encouraging observation was that patients carrying the homozygous A allele were less susceptible to the recurrence of colon polyps and thus exhibited decreased colon cancer risk associated with decreased expression of ODC (Martinez et al., 2003) .

Apart from the correlation of a SNP in the ODC gene with colon cancer, further correlation between ODC activity and colon cancer comes from studies in colon tumors carrying an inactivating mutation in the Adenomatous Polyposis Coli (APC) tumor suppressor gene. Tumors lacking APC expression showed increased levels of ODC and Myc, and expression of wild type APC repressed ODC expression in a Myc dependent manner, suggesting that increased colon tumor formation mediated by loss of APC could be mediated by increased transcription of ODC (Erdman et al., 1999; Fultz & Gerner, 2002). Apart from loss of APC, colonic tumors are also characterized by activating

mutations in the K-Ras oncogene, and activation of Ras has also been shown to activate Myc (Gerner & Meyskens, 2004). Expression of a transcriptionally inactive Myc reversed transformation in Ras transformed NIH/3T3 fibroblasts, which correlated with decreased transcription of ODC (Auvinen et al., 2003). While these studies implicate transcriptional regulation of ODC in carcinogenesis, ODC has been shown to be predominantly regulated translationally under cancerous conditions especially those induced by the Ras oncogene.

Ras signal transduction pathway

Discovery of the Ras oncogene dates back to the 1960's, when retroviruses isolated from a leukemic rat caused tumor formation in new born rats (Malumbres & Barbacid, 2003). These viruses were later identified to contain the Ras oncogene (Malumbres & Barbacid, 2003). The majority of cancers carry activating mutations in one of the three forms of Ras, K-Ras, H-Ras and N-Ras, with mutations in K-Ras being more common than the other two forms (Campbell & Der, 2004). Ras belongs to a family of GTPases that vacillate between a GTP and a GDP bound state (Campbell & Der, 2004) (Fig 1.4). In response to growth factor stimuli that activate receptor tyrosine kinases such as the epidermal growth factor receptor (EGFR), adaptor protein Grb2 exhibits increased association with SOS1 (Campbell & Der, 2004) (Fig 1.4). SOS1 is a guanine nucleotide exchange factor (GEF) that is recruited to the plasma membrane and exchanges GDP for GTP and activates Ras (Campbell & Der, 2004) (Fig 1.4). Ras is inactivated by the activation of its GTP hydrolysis activity with the help of GTPase activating proteins (GAPs) such as p120GAP and NF1-GAP that results in the hydrolysis

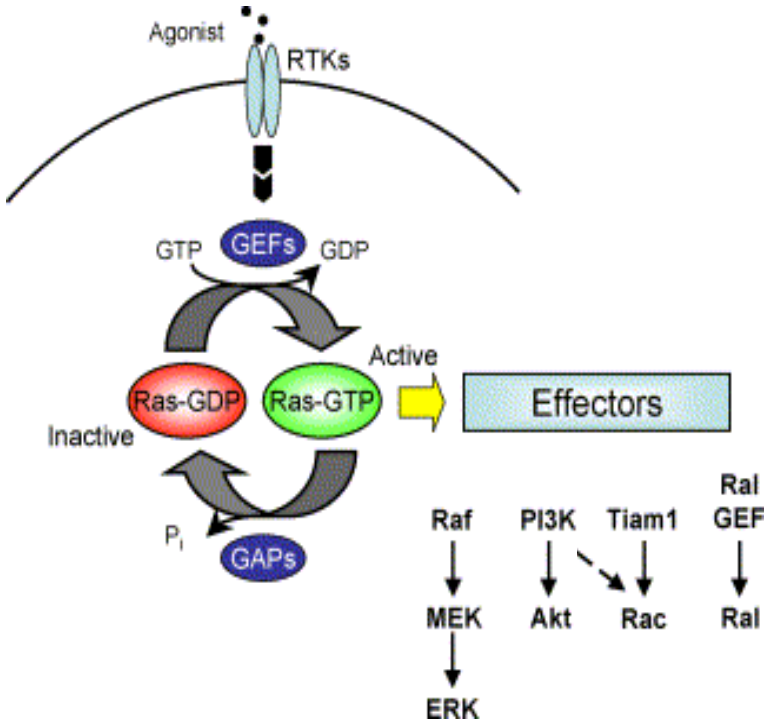

Figure 1.4. Ras signal transduction pathway (Campbell & Der, 2004)

See text for details

of GTP to GDP (Campbell & Der, 2004; Cox & Der, 2002). About 30% of human cancers carry mutations in Ras at codons 12, 13 and 61, which inactivate the GAP activity thus keeping Ras in a constitutively active GTP bound form (Campbell & Der, 2004; Cox & Der, 2002).

Once activated, Ras switches on a complex network of signaling pathways. Four of these pathways are well established as mediators of Ras-induced transformation (Fig 1.4). They are the Raf-kinase, PI3K, Ral GDS and Tiam1-Rac pathways. Ral GDS is a GEF for small GTPases and has been shown to play a role in the anchorage independent growth and metastatic properties of Ras (Campbell & Der, 2004) (Fig 1.4). Tiam1 (T-lymphoma and metastasis invasion protein) is also a GEF but for a small GTPase Rac. In response to Ras, Rac is activated and mediates the invasion and migration properties of Ras transformed cells (Campbell & Der, 2004). There is known to be cross-talk between the Ras activated pathways. For example, PI3K can also activate Rac, and PI3K activated AKT can regulate Raf in specific cell types (Campbell & Der, 2004). Besides these pathways there are other effectors such as the JNK pathway that are activated by Ras, but especially under specific conditions such as stress (Campbell & Der, 2004). Since studies in Ras-transformed NIH/3T3 fibroblasts have established the Raf-kinase and PI3K pathways as critical regulators of ODC synthesis, this introduction will focus on these two pathways.

The Raf-kinase pathway

Raf1 is a serine/threonine kinase activated by Ras. Activated Ras binds to Raf1, recruits it to the plasma membrane and phosphorylates it, although the exact mechanism involved in phosphorylation of Raf is still undefined. There are three well described

family members of Raf, A-, B- and C-Raf (Chong et al., 2003). The different Raf members exhibit a few redundant functions, but their mode of activation varies depending on the type of Ras stimulus (Chong et al., 2003). For example, H-Ras preferably activates C-Raf. Once activated, Raf1 phosphorylates MEK1 and MEK2 (MAPK/ERK: mitogen-activated protein kinase/extracellular signal-regulatory kinase) at serine residues, and MEK1/2 in turn phosphorylates p42 MAPK/ERK1 and p44 MAPK/ERK2 (extracellular signal-regulated kinase) at threonine and tyrosine residues (Chong et al., 2003). Additional regulators of the Raf-kinase pathway include scaffold proteins such as KSR and RKIP. KSR1 (kinase suppressor of Ras) has been shown to associate with Raf and MEK at the plasma membrane and act as a scaffold for ERK, which upon phosphorylation is released from the scaffold to enter the nucleus (Morrison, 2001). Once ERK translocates into the nucleus, it phosphorylates and activates transcription factors such as Elk1 and Myc which in turn increase the transcription of targets such as cFos and ODC (Davis, 1995). Correlation between transcription of ODC and the Raf-kinase pathway comes from observations that the treatment of Ras-transformed NIH/3T3 fibroblasts with the MEK inhibitor PD98059 inhibited the Ras-induced transcription of ODC. In addition, ERK can activate Myc, suggesting that transcription of ODC is activated by the Raf-MEK-ERK pathway in response to Ras (Davis, 1995; Shantz, 2004).

Several cancers carry activating mutations in Raf. For example, about 70% of malignant melanomas carry activating mutations in B-Raf (Chong et al., 2003). Inhibition of the Raf-kinase pathway is sufficient to reverse Ras-induced transformation in NIH/3T3 fibroblasts, and activation of either Raf or MEK alone is sufficient to induce

tumorigenesis in cell-culture and mouse models, strongly implicating the Raf-kinase pathway as a critical transducer of the oncogenic functions of Ras (Gollob et al., 2006). The therapeutic potential of targeting the Raf pathway is currently being tested in phase I clinical trials to treat advance stage cancers using the MEK inhibitor CI-1040 and Raf inhibitor BAY 43-9006 (Cox & Der, 2002). While all these studies are promising, one caveat to the role of Raf-kinase in Ras-activated tumorigenesis is that studies in epithelial cell models suggest that additional pathways such as PI3K are necessary for Ras-induced carcinogenesis, unlike the studies in Ras-transformed NIH/3T3 fibroblasts described above.

PI3K/mTOR pathway

PI3K (phosphatidylinositol 3-Kinase) is a lipid kinase whose catalytic domain p110 subunit is activated by Ras, which upon activation phosphorylates phosphoinositides (PI) to generate PIP3 (PI phosphorylated at positions 3, 4, 5 of the inositol ring) (Campbell & Der, 2004). PIP3 binds to the key effector AKT and recruits it to the plasma membrane, where AKT is activated by phosphorylation by PDK1 (phosphoinositide-dependent protein kinase 1) at threonine 308 and by phosphorylation at serine 273 by the mTOR-Rictor-Lst8/GβL complex (Mamane et al., 2006) (Fig 1.5). Besides PI3K, AKT is also regulated by the phosphatase PTEN (phosphatase and tensin homolog deleted on chromosome ten) but in a negative manner as PTEN dephosphorylates PIP3 and inactivates AKT (Hay, 2005; Mamane et al., 2006) (Fig 1.5).

Regulation of AKT by the tumor suppressor PTEN is important in cancer formation as several cancers carry PTEN inactivating mutations, thus facilitating a constitutive active state of AKT (Mamane et al., 2006). Also, several cancers have shown

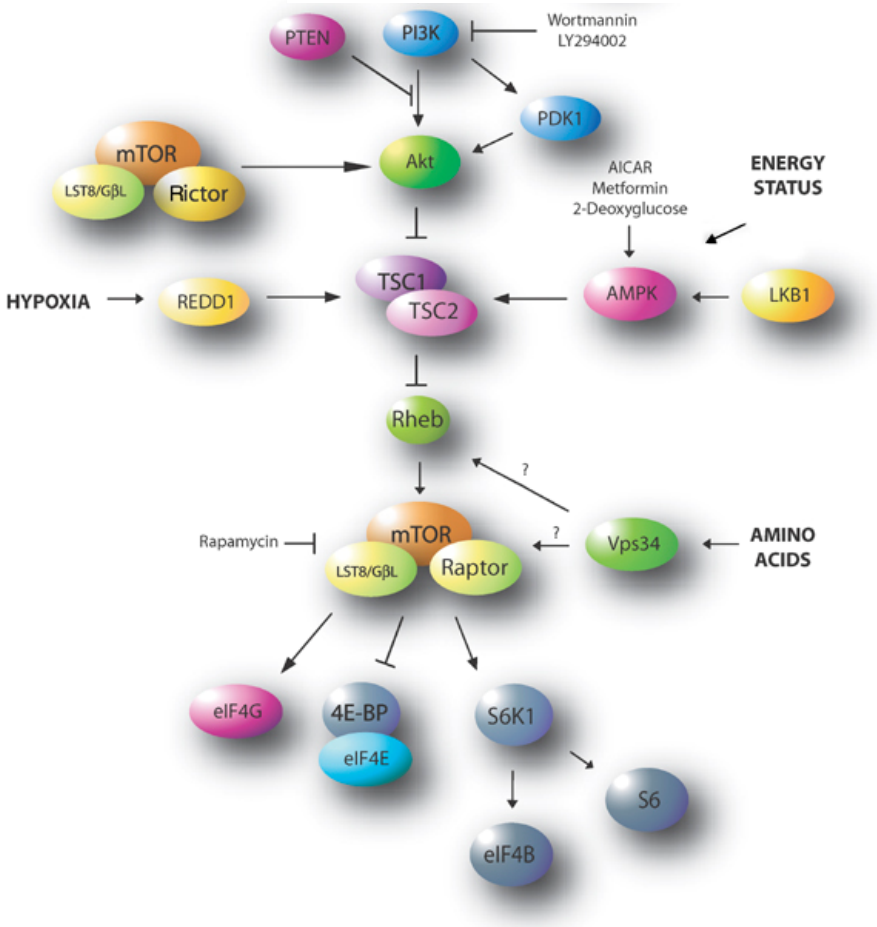

Figure 1.5. Overview of PI3K/mTOR pathway (Mamane et al., 2006)

See text for details

amplification and mutations in the gene that codes for the p110 catalytic subunit of PI3K, potentially resulting in AKT activation (Mamane et al., 2006). The consequence of AKT activation is the inactivation of growth inhibitory transcription factors such as FOXO and activation of growth stimulatory factors such as mTOR (Hay, 2005; Mamane et al., 2006).

Regulation of mTOR

Mammalian target of Rapamycin or mTOR is a kinase that was initially identified as the substrate of the immunosuppressant drug Rapamycin (Brown et al., 1994; Sabatini et al., 1994). Rapamycin forms a complex with the receptor FKBP12 and inhibits the kinase activity of mTOR by binding to a domain in its C-terminus (Chen et al., 1995). While AKT and amino acids activate mTOR, factors such as AMPK (AMP activated protein kinase) and Redd1 negatively regulate it (Hay & Sonenberg, 2004; Kimball & Jefferson, 2004) (Fig 1.5).

Activation of mTOR: AKT activates mTOR by phosphorylating and inactivating the Tuberous Sclerosis Complex 2 (TSC2) (Hay & Sonenberg, 2004; Mamane et al., 2006). TSC1 and TSC2 are considered tumor suppressors and inactivating mutations in them result in a genetic disorder called tuberous sclerosis that is characterized by benign tumors. TSC1 and TSC2 form a complex that inhibits mTOR through inactivation of the GTPase Rheb (Ras homolog enriched in brain) (Hay & Sonenberg, 2004; Mamane et al., 2006). TSC2, when activated, acts as a GTPase inactivating protein (GAP) and promotes hydrolysis of GTP bound to Rheb, thus inhibiting its activity (Fig 1.5). It has been shown that Rheb is essential to activate the kinase activity of mTOR but the exact mechanism involved continues to remain a mystery. Activation of mTOR facilitates the formation of

the mTOR-Raptor-Lst8/GβL complex that recruits mTOR substrates 4EBP1 and p70S6K by interactions with Raptor (Fig 1.5) (Mamane et al., 2006).

Inactivation of mTOR: While phosphorylation of TSC2 by AKT inactivates the TSC complex formation, phosphorylation of TSC2 by AMPK at sites distinct from AKT activates the TSC complex formation, thus inhibiting mTOR (Fig 1.5) (Hardie, 2005). AMPK itself is regulated by its kinase LKB1 and also by the energy status of the cell (AMP/ATP ratio) that can be altered with chemical inhibitors such as AICAR and Metformin (Fig 1.5) (Hardie, 2005). mTOR can also be inactivated by Redd1, a protein that responds to hypoxia and activates the TSC complex by an unidentified mechanism (Fig 1.5) (Brugarolas et al., 2004).

Translation initiation and eIF4E

The primary function of mTOR is to regulate the process of translation initiation. Translation initiation requires the formation of the cap complex eIF4F (eukaryotic translation initiation factor 4F), which helps recruit the ribosomes onto RNA. One of the key components of the eIF4F complex is eIF4E, which recognizes and binds to the cap (m^7GpppN) structure in the 5'UTR of mRNAs (Gingras et al., 1999). Binding of eIF4E to the cap is stabilized by the scaffolding protein eIF4G, which also recruits the helicase eIF4A and initiation factor eIF4B (Fig 1.6). eIF4A is the RNA helicase that helps unwind the secondary structure of RNAs, and its helicase activity is enhanced by eIF4B (Gingras et al., 1999). The eIF4F complex recruits the 43S pre-initiation complex through eIF4G interacting with eIF3 (eukaryotic initiation factor 3). Besides eIF3, the 43S complex consists of the 40S ribosomal subunit, eIF2-GTP-Met-tRNA$_i$ and eIF1A (Fig 1.6) (Gingras et al., 1999). Once the 43S initiation complex is recruited onto the 5'UTR, it

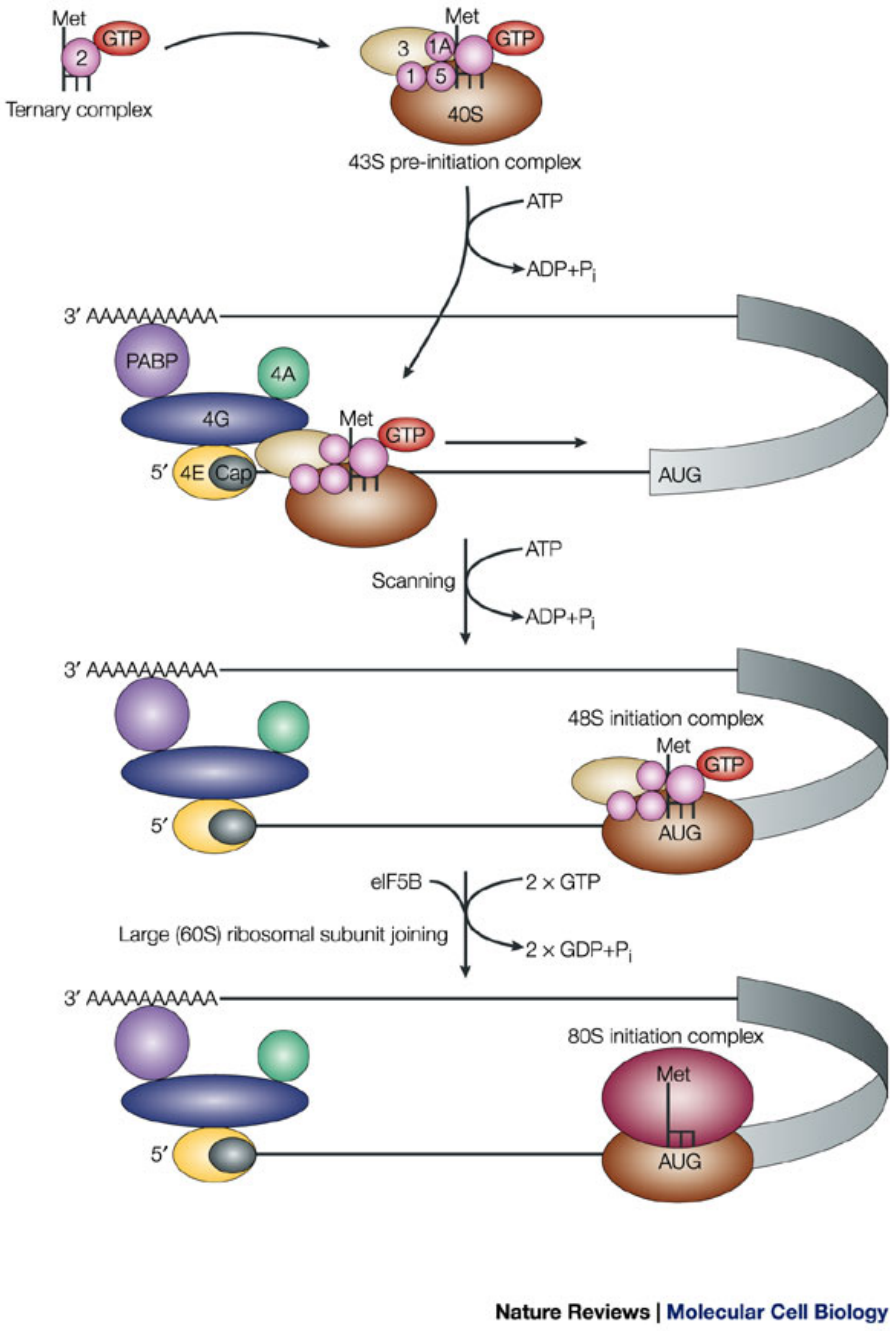

Figure 1.6. Overview of translation initiation (Gebauer & Hentze, 2004)

See text for details

scans the 5'UTR by an undefined mechanism and forms the 48S complex as it reaches the start codon (Fig 1.6). At the start codon, the 40S ribosomal subunit is joined by the 60S ribosomal subunit, and this process is mediated by the action of eIF5 (Gingras et al., 1999). eIF5 releases eIF2 from the 48S complex by its GTPase activating function, which hydrolyzes the GTP of eIF2 (Fig 1.6). Release of factors such as eIF2 and eIF3 then allows the binding of the 60S ribosomal subunit to the 40S subunit, thus commencing the process of translational elongation (Gingras et al., 1999). The entire translation process can take place on circular RNAs, and the circularization process is mediated by interaction of eIF4G and the PABP (Poly A tail binding protein) (Fig 1.6) (Gingras et al., 1999). The critical step in the initiation process is the recognition of the cap by the eIF4F complex and the formation of the cap complex, which is predominantly regulated by the rate-limiting translation initiation factor eIF4E.

eIF4E is a translation factor that can also function as an oncogene. Over-expression of eIF4E is sufficient to transform immortalized fibroblasts, and it cooperates with oncogenes such as Myc to transform primary fibroblasts (Lazaris-Karatzas et al., 1990; Lazaris-Karatzas & Sonenberg, 1992). It was also shown to cooperate with Myc to induce lymphomagenesis in a murine model (Ruggero et al., 2004). Further confirmation of the oncogenic properties of eIF4E comes from observations that eIF4E is over-expressed in several human cancers. Apart from eIF4E, translation factors such as eIF4G have also been found to be critical for transformation. Over-expression of the translation factor eIF4G could transform immortalized fibroblasts, and increased levels of eIF4G were detected in squamous lung carcinomas (Fukuchi-Shimogori et al., 1997). Also, increased levels of eIF4A were detected in specific melanomas and hepatocellular

carcinomas, suggesting that over-expression of the eIF4F complex in general can result in transformation (Eberle et al., 1997).

eIF4E is usually present at very low levels in the cell, and its over-expression increases the translation of RNAs with a complex secondary structure such as factors ODC and Cyclin D1 (Koromilas et al., 1992; Rousseau et al., 1996). These RNAs are inefficiently translated under normal conditions, and one potential explanation for their low basal expression is that under normal conditions factors such as ODC and Myc are simply out-competed by RNAs that are translated efficiently. Thus under normal conditions, levels of growth promoting proteins such as ODC are relatively low. However, elevated eIF4E levels can lead to increased translation of these oncogenic RNAs, thus resulting in transformation (Mamane et al., 2004). Apart from increased translation initiation, recent evidence suggests that the oncogenic properties of eIF4E can also be contributed by its transport functions. eIF4E binds to specific elements in the 3'UTR of RNAs such as Cyclin D1 and ODC, and enhances their transport into the cytoplasm (Culjkovic et al., 2005). The transport functions of eIF4E have also been shown to be up-regulated in specific cancers such as acute myeloid leukemia; however the role of the transport functions of eIF4E in mediating tumorigenesis is a study that is still at its infancy (Topisirovic et al., 2003).

Regulation of eIF4E

Due to its relationship with carcinogenesis, levels of eIF4E are tightly controlled by transcriptional mechanisms, by its phosphorylation status and also by interacting with its repressor 4EBP1 (eIF4E binding protein) (Fig 1.7A). Hypo-phosphorylated 4EBP1 competes with eIF4G to bind to overlapping sites on eIF4E, whereas hyper-

A.

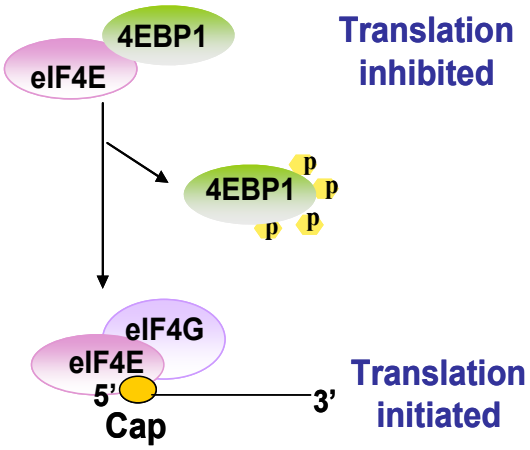

B.

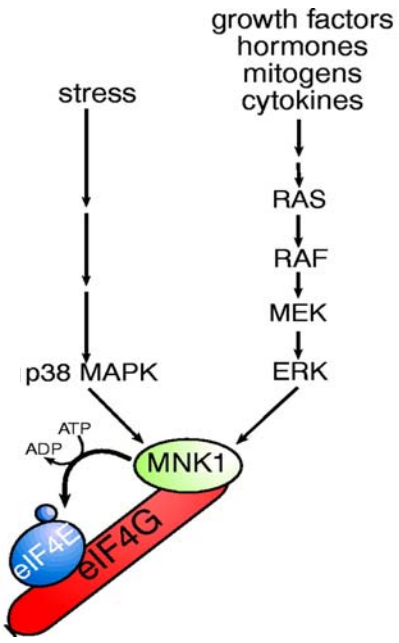

Figure 1.7. (A) Regulation of eIF4E by 4EBP1 (Gebauer & Hentze, 2004) and **(B)** Regulation of eIF4E phosphorylation by Mnk (Gingras et al., 1999)

See text for details

phosphorylated 4EBP1 interacts only weakly with eIF4E thus releasing it to form the cap complex (Fig 1.7A) (Hay & Sonenberg, 2004). So far, seven phosphorylation sites have been identified in 4EBP1. A key regulator of 4EBP1 phosphorylation is mTOR, which through phosphorylating 4EBP1 activates eIF4E (Hay & Sonenberg, 2004). Thus, in response to oncogenic stimuli such as Ras activation, eIF4E is activated primarily through the mTOR pathway.

Additional studies show that eIF4E phosphorylation can also be regulated by the Raf-kinase pathway. eIF4E phosphorylation is elevated in Ras transformed cells, and is increased in response to growth stimuli such as mitogens and hormones (Fig 1.7B) (Waskiewicz et al., 1997). It is also induced in response to stress and this has been shown to be mediated by the p38 MAPK (p38 Mitogen activated protein kinase) pathway, as p38 MAPK and also ERK can activate the eIF4E phosphorylating kinase Mnk (MAPK interacting kinase) (Fig 1.7B) (Buxade et al., 2005; Waskiewicz et al., 1997). Upon activation, Mnk binds to eIF4G and phsophorylates eIF4E at the Ser209 residue (Fig 1.7B). There are two Mnk kinases identified so far, Mnk1 and Mnk2. These kinases differ in that Mnk2 regulates the constitutive basal phosphorylation of eIF4E, whereas Mnk1 regulates phosphorylation induced by growth stimuli (Ueda et al., 2004). In spite of being induced specifically under growth and transformation conditions, disruption of eIF4E phosphorylation by generating a Mnk1 and Mnk2 knockout mouse model did not result in any growth or developmental defect (Ueda et al., 2004). Hence, the role of phosphorylation in mediating eIF4E functions in translation and in regulation of cell growth, are not completely understood.

Regulation of ribosomal protein S6 kinase (S6K) by mTOR

Apart from 4EBP1, mTOR also regulates translation by phosphorylation of p70S6K. S6K is a kinase that phosphorylates the ribosomal protein S6, and there are two isoforms identified so far (S6K1 and S6K2) (Hay & Sonenberg, 2004). The previous belief that S6K functions in translation of TOP (terminal oligo pyrimidine) containing mRNAs was recently invalidated by studies showing that knockdown of both S6K did not affect translation of TOP RNAs (Stolovich et al., 2002). TOP RNAs are a unique set of RNAs that are characterized by a TOP element in their 5'UTR (5' Untranslated region), which starts with a cytidine followed by a stretch of 4-14 pyrimidines (Hamilton et al., 2006). TOP RNAs encode factors that are involved in ribosome biogenesis such as ribosomal proteins S6 S14 and S24 and, factors involved in translation elongation such as elongation factors eEF1 and eEF2 (eukaryotic Elongation Factor1 and 2) (Hamilton et al., 2006). Translation of TOP RNAs though not regulated by S6K were still sensitive to Rapamycin suggesting that their translation is still regulated by the mTOR pathway (Stolovich et al., 2002).

Recent studies show that S6K may have other targets. Studies show that S6K interacts with eIF3, along with the mTOR/Raptor complex and 4EBP1, and is phosphorylated by mTOR at the T389 residue (Shahbazian et al., 2006). Once activated, S6K is released from eIF3 and is phosphorylated at the T229 residue by the kinase PDK1 (Shahbazian et al., 2006). Activated S6K phosphorylates targets such as the ribosomal protein S6. Recent studies show that S6K also phosphorylates the translation factor eIF4B, which can be phosphorylated by both the PI3K/mTOR pathway and also by the Raf-kinase pathway (Shahbazian et al., 2006). However the precise functions of S6K

targets such as eIF4B in translation are not clearly understood.

Thus, through S6K and 4EBP1, the PI3K/mTOR pathway regulates translation and its aberrant activation consequently results in carcinogenesis. Due its causative role in cancers, the therapeutic potential of inhibitors such as Rapamycin is currently being explored. Rapamycin analogs CCI-779 and RAD001 are currently being tested in several clinical trails for treatment of several cancers and show the promise of being developed into a novel chemotherapeutic drug (Mamane et al., 2006).

Translational regulation of ODC

A link between ODC and mTOR was demonstrated by observations that Rapamycin can partially inhibit serum stimulated ODC activity in intestinal epithelial cells (Seidel & Ragan, 1997). Subsequently, studies in cells treated with the growth stimulating ligand gastrin showed that the gastrin-induced ODC activity could be reversed by Rapamycin (Pyronnet et al., 1998). In HeLa cells, Rapamycin inhibited the induction of ODC activity at the G1 phase of the cell-cycle (Pyronnet et al., 2000; Pyronnet et al., 2005). Also in Ras transformed fibroblasts, treatment with Rapamycin partially reversed the induction in ODC activity (Shantz, 2004). Since the mTOR pathway primarily regulates translation initiation, the above mentioned observations suggested that mTOR affects ODC synthesis at the level of translation initiation. In fact, several studies suggest that ODC is regulated predominantly by translation rather than transcription under transformed conditions (Rousseau et al., 1996; Shantz, 2004; Shantz & Pegg, 1994).

Translation of ODC is regulated by its 5'UTR, which is unusually long (about 300bp) and GC rich, especially in the first 150 bases (Shantz & Pegg, 1999). Comparison

of translation efficiencies of RNA with short 5'UTRs and ODC, demonstrated that ODC is translated inefficiently owing to its long and GC rich 5' UTR (Manzella & Blackshear, 1990) (Ito et al., 1990) . Also, *in vitro* and *in vivo* studies showed that the translation mediated by the full length 5'UTR was similar to the translation efficiency of the first 120 bases (GC-rich), suggesting that the inhibitory effect on ODC translation is mediated by its GC rich region and this region was predicted to carry an extensive secondary structure (Manzella & Blackshear, 1990; Van Steeg et al., 1991). Another characteristic of the 5'UTR is an upstream open reading frame (uORF) (Van Steeg et al., 1991). However, the exact role of the uORF in regulating ODC translation is yet to be understood. Besides the 5'UTR, the ODC 3'UTR has also been shown to be involved in translation. *In vivo* studies using reporter plasmids showed that the inhibition of translation caused by the 5'UTR could partially be relieved by the 3'UTR, suggesting that an interaction between the 3' UTR and 5'UTR regulates ODC translation (Grens & Scheffler, 1990). Also, in response to a hypotonic shock, translational induction of ODC was found to be dependent on its 3'UTR (Lovkvist Wallstrom et al., 2001).

While there is no doubt that ODC translation is dictated by its RNA structure, studies also show that its translation is regulated by the availability of the translation factors. ODC translation was found to be increased by insulin and it correlated with the insulin-dependent increase in the phosphorylation of translation factors 4EBP1 and eIF4E (Manzella et al., 1991). Reporter plasmids carrying the ODC 5'UTR could be translated efficiently in response to insulin and in response to over-expression of eIF4E (4E-P2 cells) (Manzella et al., 1991; Rousseau et al., 1996; Shantz & Pegg, 1994). In the 4E-P2 cells translation mediated by the ODC 5'UTR was elevated much more in comparison to

the untransformed parental cells (Rousseau et al., 1996; Shantz & Pegg, 1994). Polysome analysis in these cells revealed a shift in ODC RNA to the heavier polysomal fractions suggesting an increase in the efficiency of ODC translation (Rousseau et al., 1996). Although eIF4E regulates translation of several other RNAs such as Cyclin D1, induction of ODC by eIF4E does have a crucial consequence. Inhibition of ODC in the 4E-P2 cells, either by treatment with DFMO or by over-expression of a dominant negative ODC, reversed their transformed morphology revealing that ODC is a critical mediator of the oncogenic functions of eIF4E (Shantz et al., 1996a; Shantz et al., 1996b). Besides eIF4E, over-expression of translation factor eIF4G also resulted in increased ODC translation (Hayashi et al., 2000). In conclusion, the above reports show increased translation factors could relieve the inhibitions posed by the secondary structure of the ODC 5'UTR possibly by increasing the unwinding (helicase) activity of the eIF4F complex. Consistent with this hypothesis, increased RNA helicase activity was observed in a variant of mouse mammary carcinoma FM3A cells and in FM3A cells over-expressing eIF4G, which correlated with increased ODC translation detected in these cells (Hayashi et al., 2000; Shimogori et al., 1996).

Cap-independent translation

What makes translation of ODC unique is that it can not only be translated by a cap-dependent mechanism, but also by a cap-independent mechanism mediated by an IRES (Internal Ribosome Entry Site). IRES elements were initially identified in picornaviruses that are characterized by very long 5'UTRs that range in length from 500-1500 bases and contain an extensive secondary structure (Hellen & Sarnow, 2001; Stoneley & Willis, 2004). Puzzlingly, their translation did not require the cap binding

protein eIF4E, and both *in vitro* and *in vivo* studies showed that increased sequestration of eIF4E by 4EBP1 or by treatment with Rapamycin did not affect translation of the picornaviruses (Hellen & Sarnow, 2001; Stoneley & Willis, 2004). Later it was identified that the 5'UTR of these viruses contain IRES elements that could recruit ribosomes directly, bypassing the requirement for cap-mediated translation. These IRES elements were identified using the bicistronic plasmid assay (described in Chapter IV), which was also used to identify IRES elements in eukaryotic RNAs (Hellen & Sarnow, 2001; Stoneley & Willis, 2004).

Although the IRES-mediated translation does not require the cap-binding complex, picornaviruses such as EMCV (Encephalomyocarditis virus) exhibited the need for at least some of the factors such as eIF4G and eIF4A. Some of these picornaviruses code for proteases that cleave eIF4G (eIF4G I and II) resulting in the separation of the domain that binds to eIF4E and PABP, from the domain that binds to eIF4A and eIF3 (Hellen & Sarnow, 2001; Stoneley & Willis, 2004). In the model depicted in figure 1.8, viruses such as EMCV recruit to the IRES element the eIF4G fragment bound to eIF4A, which by binding to eIF3, can now recruit the 43S complexes either directly onto the start site or close to the start codon (Hellen & Sarnow, 2001; Stoneley & Willis, 2004). There are exceptions to this model in that viruses such as the cricket paralysis virus have been shown to successfully translate without the need for any translation initiation factors.

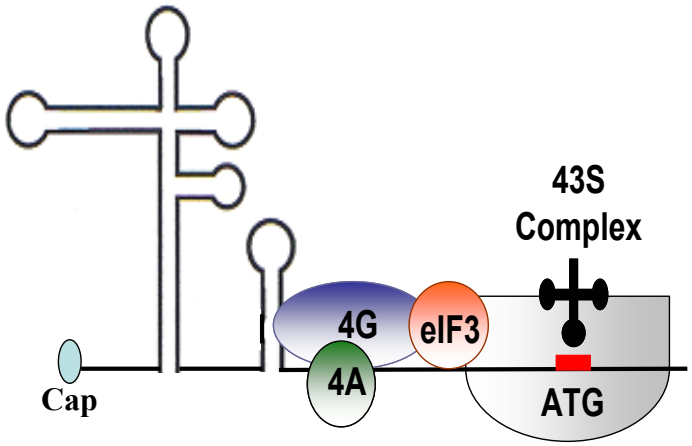

Figure 1.8. Model for IRES-mediated translation (modified from Hellen & Sarnow, 2001)

See text for details

For eukaryotic RNA, the need for translation factors such as eIF4G for IRES-mediated translation is not well documented. However, for eukaryotic RNA and viral RNAs, IRES translation has been shown to be mediated by specific ITAFs (IRES Transacting Factors) such as PTB and HnRNP (Hellen & Sarnow, 2001; Stoneley & Willis, 2004). Interestingly, not all IRES elements are regulated by similar ITAFs and the mode of regulation seems to vary based on the IRES element. For example, PTB (polypyrimdine tract binding protein) positively regulates the Apaf-1 IRES but negatively regulates the Bip IRES (Kim et al., 2000; Mitchell et al., 2001). Regulation by ITAFs can occur without direct interaction between the ITAF and the IRES element. For example, PTB has been shown to positively regulate Apaf-1 by binding only in the presence of the ITAF Unr (Upstream of N-Ras) (Mitchell et al., 2001).

So far IRES elements have been identified in several viral RNAs and eukaryotic RNAs. However, a universal sequence motif that describes all IRESs has not yet been determined. Some clues were provided by a recent study that showed that IRES elements that are regulated by PTB, carry a common structural motif that involves a double stem-loop structure (Mitchell et al., 2005). Based on this observation, it is possible that there is not a universal motif; instead the IRES motif may vary from RNA to RNA based on the type of ITAF that recognizes them. It has been proposed that the stimulation or inhibition of IRES usage is mediated primarily by the availability of the ITAFs under varied physiological conditions, and studies have shown that IRES activities vary vastly between cell-types (Stoneley et al., 2000b).

Physiological context has been shown to play a major role in the regulation of IRES elements. For example the ODC IRES and Myc IRES are stimulated specifically in

the G2-M phase of the cell cycle, when cap-dependent translation is inhibited (Pyronnet et al., 2000). The Myc IRES has also been shown to be induced during apoptosis, where cap-dependent translation is inhibited by the cleavage of eIF4G by caspases and neatly correlates with the constant synthesis of Myc protein (Stoneley et al., 2000a). Interestingly, IRES activity has also been correlated with disease conditions such as cancer and dyskeratosis. A specific defect in ribosomes of patients with X-linked dyskeratosis was found to result in impaired IRES-mediated translation (Yoon et al., 2006). The Myc IRES was found to carry a C to U mutation specifically in patients with multiple myeloma, resulting in increased IRES activity (Chappell et al., 2000).

Given the relevance of IRESs in disease, the detection of an IRES element in ODC 5'UTR may have a significant consequence. Elegant studies by Sonenberg *et.al.*, showed that ODC contains an IRES in the last 150 bases of its 5'UTR. Interestingly, the ODC IRES activity was up-regulated specifically during the G2-M phase of the cell-cycle when cap-dependent translation is inhibited (Pyronnet et al., 2000). It is possible that conditions such as the mitotic phase of the cell-cycle, which require ODC but are not equipped for cap-dependent translation, use the IRES mode of translation to maintain ODC levels.

Some regulation of ODC IRES activity was observed with the identification of ODC splice variants that contained two different intronic sequences in the last 150 bases of the 5'UTR (Pyronnet et al., 1996). These splice variants carried either a 17 bp or a 13 bp intronic sequence and their IRES activity varied not only based on their intronic sequence but also based on the length of their 5'UTR (Pyronnet et al., 2000). The splice variant 303 bp in length containing both 17bp and 13bp intronic sequences exhibited the

strongest IRES activity, while the shortest splice variant about (273 bp) which lacked the intronic sequences (Pyronnet et al., 2000), exhibited the weakest activity. While these reports show that ODC has an IRES element, further studies have to be carried out to identify ITAFs that regulate the IRES activity and to determine the contribution of ODC IRES-mediated translation to disease states such as cancer.

ODC is an important element in Ras-induced carcinogenesis

The linkage between ODC and Ras is complex, with significant consequences in relation to cancer. Ras has been shown to induce ODC in several *in vitro* and *in vivo* models. It has been shown that Ras regulates ODC by several mechanisms in fibroblast models (Holtta et al., 1988; Shantz, 2004). Also, a significant number of studies show a causative role for ODC in Ras mediated carcinogenesis. Over-expression of a dominant negative ODC in Ras transformed fibroblasts resulted in a reversal of transformation (Shantz & Pegg, 1998). Treatment with DFMO blocked Ki-Ras induced tumorigenesis in colon cancer cells (Ignatenko et al., 2004). Also, formation of spontaneous skin papillomas caused by over-expression of MEK could be reversed by treatment with DFMO (Feith et al., 2005). Inhibition of ODC in the same mice by over-expressing its endogenous inhibitor AZ also resulted in a delay and reduction of tumor formation (Feith et al., 2006).

The above mentioned reports emphasize the role of ODC as a causative factor in Ras-induced carcinogenesis. To develop better therapeutic strategies to treat Ras-activated tumors, it is vital to understand in detail the mechanisms involved in regulation of ODC by Ras. The aims of this thesis are designed to understand such Ras-activated regulation of ODC in an epithelial cell system.

Hypothesis and Specific aims

Hypothesis: Ras over-expression in an epithelial cell model (RIE-1 cells) results in induction of ODC by transcriptional and post-transcriptional mechanisms, which is necessary for oncogenic transformation.

I. Biochemical and morphological characterization of Ras-transformed RIE-1 cells

Specific Aim: To characterize the transformation phenotype of RIE-1 cells expressing constitutively active Ras and to identify pathways activated by Ras and their role in regulating ODC synthesis.

II. Post-transcriptional regulation of ODC in response to Ras-activation

Specific Aim: To determine post-transcriptional mechanisms involved in the induction of ODC synthesis in response to constitutive activation of Ras in RIE-1 cells. Regulation by mechanisms such as alterations in stability of ODC RNA or RNA transport or translation will be examined.

III. Effect of Ras activation on cap-independent translation of ODC

Specific Aim: To analyze if Ras activation stimulates cap-independent translation of ODC and to determine which Ras effectors regulate ODC IRES-mediated activity and the mechanism involved.

IV. Identification of genes regulated by AZ to inhibit MEK-induced tumorigenesis

Specific Aim: To use a genomic approach to identify genes that are regulated by AZ (an endogenous inhibitor of ODC), that are important for its tumor suppressor properties in MEK-induced skin tumors.

Chapter II

Biochemical and morphological characterization of Ras-transformed RIE-1 cells

Specific aim: To characterize the transformation phenotype of RIE-1 cells expressing constitutively active Ras and, to identify pathways activated by Ras and their role in regulating ODC synthesis.

Introduction

Ornithine Decarboxylase (ODC) has gained recognition as a critical target for tumorigenesis, especially for cancers triggered by oncogenes such as Myc and Ras (Auvinen et al., 1992; Nilsson et al., 2005; Pendeville et al., 2001). Curtailing ODC activity has been shown to be sufficient to revert the transformation process and to inhibit the genesis of tumors, making it an ideal target for treatment and prevention of certain types of cancers (Casero et al., 2005; Manni et al., 1995a; Pegg et al., 1995). The primary function of ODC is to regulate the intracellular levels of the growth-essential polyamines, by catalyzing the synthesis of the diamine putrescine from its precursor ornithine (Pegg, 1988). Our goal in this study is to understand the intricacies of ODC regulation in response to oncogene-induced tumorigenesis, especially those induced by Ras, using an epithelial cell model. Ras is one of the most commonly mutated oncogenes in human cancers, and previous studies have shown that ODC is a crucial target of Ras (Feith et al., 2005; Ignatenko et al., 2004; Iwata et al., 1999). Ras is a small GTPase factor which, upon growth factor activation exchanges GDP to GTP a process mediated by Guanine nucleotide Exchange Factors (GEFs) (Campbell & Der, 2004; Wennerberg et al., 2005). Ras in its GTP bound form, binds to its effector Raf (a serine/threonine kinase), and translocates it to the membrane (Campbell & Der, 2004; Peyssonnaux & Eychene, 2001). Once activated, Raf phosphorylates MEK, which in turn phosphorylates ERK1/2, and translocates ERK into the nucleus to activate several transcription factors (Campbell & Der, 2004; Peyssonnaux & Eychene, 2001). Although Raf is considered to be the primary target activated by Ras, the other essential downstream effector of Ras that is also a regulator of ODC is PI3K (Li et al., 2004; Morgensztern & McLeod, 2005; Shantz,

2004). PI3K is a lipid kinase that is bound by GTP-Ras and is activated to phosphorylate AKT through PDK1 (Cheng et al., 2005). Phosphorylated AKT, through inhibition of TSC2 (Tuberous Sclerosis Complex), allows Rheb to activate mTOR (Cheng et al., 2005). Activation of mTOR regulates cell growth predominantly through control of translation initiation (Averous & Proud, 2006).

Most of the work characterizing ODC regulation in response to Ras have thus far been carried out using fibroblasts (Auvinen et al., 1997; Holtta et al., 1988; Shantz & Pegg, 1998). However, recent studies using RIE-1 cells have highlighted several differences between epithelial cells and fibroblasts with respect to the Ras effector pathways necessary for the transformation process (Oldham et al., 1996). For example while the up-regulation of Raf is sufficient to transform NIH/3T3 fibroblasts, activation of both Raf and PI3K is required to transform RIE-1 cells (Oldham et al., 1996). Also, in several *in vivo* epithelial models of Ras transformation, ODC has been shown to be an essential target of Ras (Feith et al., 2005; Feith et al., 2006; Hayes et al., 2006; Smith et al., 1998). For example cooperation between ODC and Ras expression in the skin was shown to stimulate spontaneous formation of papillomas (Smith et. al., 1998), and skin tumors formed by over-expressing MEK could be reversed by treating the cells with DFMO, an irreversible inhibitor of ODC (Feith *et.al.*, 2005). Since the Ras activated pathways are well-characterized in RIE-1 cells, they present a good epithelial system to study effects of Ras on ODC synthesis.

In this study we found that RIE-1 cells are transformed by Ras-activation and exhibit induction of the Raf/MEK/ERK and PI3K/mTOR pathways. Cooperation between these pathways contributes to the stimulated ODC activity in the Ras-transformed cells.

The Raf-kinase pathway regulates ODC synthesis at the transcriptional level, whereas PI3K potentially regulates ODC by post-transcriptional mechanisms.

Materials and Methods

Cell culture and stable transfections

RIE-1 cells (kind gift of Dr. K. Brown, Cambridge University, UK) and 4E-P2 cells (kind gift of Dr. N. Sonenberg, McGill University, Montreal) were maintained in Dulbecco's modified essential medium (DMEM) supplemented with 10% (v/v) fetal bovine serum (FBS) and 100 µg/ml penicillin and streptomycin. RIE-1 cells were stably transfected with H-Ras12V mutant plasmid (kind gift of Dr. Michael White, UT Southwestern, Dallas, TX) and empty vector plasmid using lipofectamine plus reagent (Invitrogen). Approximately 3 x 10^5 cells were plated onto each well of a 6-well plate and 48 hrs later were transfected with 2.5µg/µl plasmid DNA mixed with 12µl of plus reagent and 8µl lipofectamine reagent. Stably transfected Ras12V and vector control RIE-1 cells were selected in 400µg/ml Geneticin (G418). More than 50 clones were isolated using cloning cylinders and cultured individually in 24-well plates with continued selection for neomycin resistance. Cell morphology and foci formation on a monolayer was assessed under the light microscope.

β-Galactosidase assay

To optimize transfection efficiency, RIE -1 cells were transiently transfected with a pSV β-Gal plasmid using a range of DNA concentrations (1, 1.5, 2, 2.5, 3 and 4µg). Transfection was carried out as described above and 48 hrs following transfection, β-Galactosidase assay was carried out according to the manufacturer's instructions (Invitrogen), except that instead of using the kit's reagents, fixing and staining solutions were prepared in the lab.

Soft agar experiments

To count foci formed in soft agar, 50,000 cells for both Ras12V cells and control cells were suspended in 0.35% agar media with DMEM and 20% FBS and overlaid on a solidified 0.5% agar layer on a 60 mm plate. Two days after plating, 1ml of DMEM supplemented with 20% FBS was added to the plates. At day 11 and day 18 the number of foci formed were counted and any aggregates of 10 or more cells were counted as a single focus using the light microscope.

Growth curves

To assess the growth rates, both Ras-transformed and control RIE-1 cells were seeded at 2000 cells/cm^2 on a 24-well plate and maintained in DMEM supplemented with 10% FBS and 400µg/ml G418. Number of cells per cm^2 was measured at time 0 h (after allowing the cells to adhere for 16 h), and subsequently at 24, 48, 72, 120, 144, 170 and 194 hrs, until the cells reached a stationary phase. Cells were counted using a coulter counter (Coulter Electronics Inc.). Log of cells per cm^2 (y-axis) was plotted against time in hrs (x-axis) and the generation times in hrs were determined from the plot using an exponential curve fit analysis.

ODC assay and Polyamine measurements

To measure ODC activity in exponentially growing cells and to analyze the effects of inhibitors, 150,000 cells for Ras clones and 40,000 cells for the control cells were plated onto each well of a 6-well plate. The inhibitors PD98059, Rapamycin and LY294002 (Tocris Cookson) were dissolved in DMSO (Dimethyl Sulfoxide) and maintained as 50 mM, 100 µM, 20 mM stocks respectively. DMSO was used at a 1:1000 dilution of media added per plate and for dual inhibitor treatments DMSO was used at a 1:500 dilution. The

cells were allowed to adhere for 16 h, followed by addition of inhibitors and extraction in ODC assay buffer after 24 and 48 hrs. ODC activity was measured by the release of $^{14}CO_2$ from L-[1-^{14}C] Ornithine as described previously (Coleman & Pegg, 1998). Polyamine content was measured using reversed-phase HPLC analysis as described previously and normalized to total protein (Shantz et al., 1992).

Western blots

Cells were plated and treated with inhibitors as described above for the ODC assays and were extracted in a homogenization buffer (4E-HB buffer) containing 20mM HEPES, 2mM EGTA, 50mM NaF, 100mM NaF, 100mM KCl, 0.2mM EDTA, 50mM β-glycerophosphate, 2.5% triton X-100 and 0.25g sodium deoxycholate. Just before use 1mM DTT, 1mM Benzamidine, 0.5mM sodium vanadate and protease cocktail inhibitor (Calbiochem) were added to the buffer. For analysis of ODC protein levels, Ras12V cells and RIE-1 cells were extracted in RIPA buffer (Santa Cruz). Total cellular protein (20μg) was resolved by a 10% SDS PAGE (polyacrylamide gel electrophoresis) analysis and transferred onto PVDF membrane (Micron Separations). Membranes were probed using mouse polyclonal antibodies against Ras (Upstate),GAPDH (Santa Cruz), E-Cadherin (BD Biosciences), and using rabbit polyclonal antibodies against total and phospho AKT (Ser473), total and phospho eIF4E (Ser209), total and phospho ERK1/2 (Thr202 /Tyr204), total and phospho 4EBP1 (Ser65) and phospho p70S6K (Thr389) (Cell-signaling).

Northern blot analysis

For northern blot analysis of ODC RNA, $1.1x10^6$ of Ras12V cells and $0.31x\ 10^6$ of control cells were plated per 100 mm dish. Total cellular RNA was isolated by combining

two 100mm dishes for control cells and from a single 100mm dish for Ras12V cells using the RNAqueous-4PCR kit (Ambion). 20µg of total cellular RNA was separated on a 1.2% (w/v) agarose-formaldehyde gel, transferred to Hybond N+ membrane (Amersham Biosciences) and UV cross-linked using a Stratalinker (Stratagene). A cRNA probe complementary to the full-length ODC transcript was synthesized as described previously (Shantz, 2004).

Promoter activity assay

To assay activity of the ODC promoter, it was cloned into the promoterless Basic-PGL3 vector (Promega) containing Firefly luciferase as the reporter enzyme. The ODC promoter was cloned out of pODC-CAT plasmid (a generous gift of Dr. Ollie Jänne, University of Helsinki, Finland) by digesting with restriction enzymes KpnI and SacI and cloned into the KpnI and SacI sites of Basic-PGL3 plasmid to generate the ODC-pGL3 plasmid. As a transfection control pRL-SV40 vector containing Renilla luciferase as the reporter enzyme was co-transfected with the ODC-pGL3 into both the Ras and RIE-1 cells, and dual luciferase assay was carried out as described in the Methods section of Chapter IV. For inhibitor assays, cells were co-transfected in media with serum and 6 hrs following transfection cells were treated with 50µM PD98059 or 100nM Rapamycin or vehicle control DMSO without replacing the media.

Results

Characterization of the transformed morphology of RIE-1 cells

To determine the effects of Ras over-expression on ODC in an epithelial model, RIE-1 cells were stably transfected with a plasmid encoding Ras12V, a constitutively active Ras mutant (Ras12V cells). Prior to the stable transfection, transfection efficiency of RIE-1 cells was optimized by transiently transfecting the cells with a plasmid encoding β-Galactosidase. Though the transfection efficiency was low (Fig 2.1A), stable clones of RIE-1 cells expressing Ras were successfully obtained (Fig 2.1B). All the clones expressing Ras exhibited characteristics associated with a transformed phenotype. While RIE-1 cells expressing an empty vector were epithelial, with a flat, round morphology, Ras-expressing clones were fibroblastic and refractile (Fig 2.2 A, B). Ras12V cells were able to form foci on a monolayer (Fig 2.2C) and exhibited anchorage-independent growth in soft agar (Table 2.1). These transformed cells displayed about a 7-fold increase in the number of colonies formed in soft agar compared to the control cells (Table 2.1). Ras clones also exhibited a rapid growth rate, with a doubling time of 15-19 hrs compared to the doubling time of 28 hrs in the control cells (Table 2.1). All these morphological characteristics suggested that the Ras-expressing clones were indeed transformed. In the approximately 50 clones screened, the extent of transformation by these measures did not correlate with the levels of Ras expressed. This absence of dose-dependent effect of Ras on the transformation characteristics in the RIE-1 cells suggests the presence of a transformation threshold surpassed by even low levels of Ras.

A clone expressing very high levels of Ras (#35) and another expressing a relatively lower level (#49) were selected for further analysis (Fig 2.1B). Both the

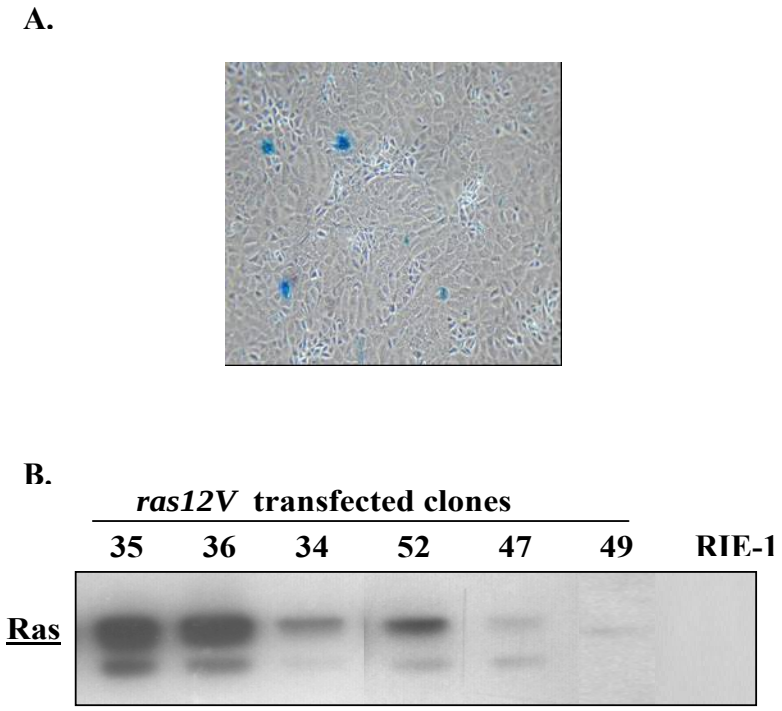

Figure 2.1. Analysis of transfection efficiency of RIE-1 cells and Ras expression in RIE-1 cells stably transfected with Ras12V.

(A) For analysis of transfection efficiency cells were transiently transfected with the pSV β-Gal plasmid as described in Methods. Using light microscopy, transfected cells were visualized as cells stained blue obtained by the activity of β-Galactosidase on the X-Gal substrate.

(B) Over-expression of Ras was analyzed by western blot analysis of cell extracts obtained from six different Ras12V clones and control cells. 20µg of total protein was loaded per lane and the blot was probed with an anti-Ras antibody. Results were confirmed by repeating the experiment twice.

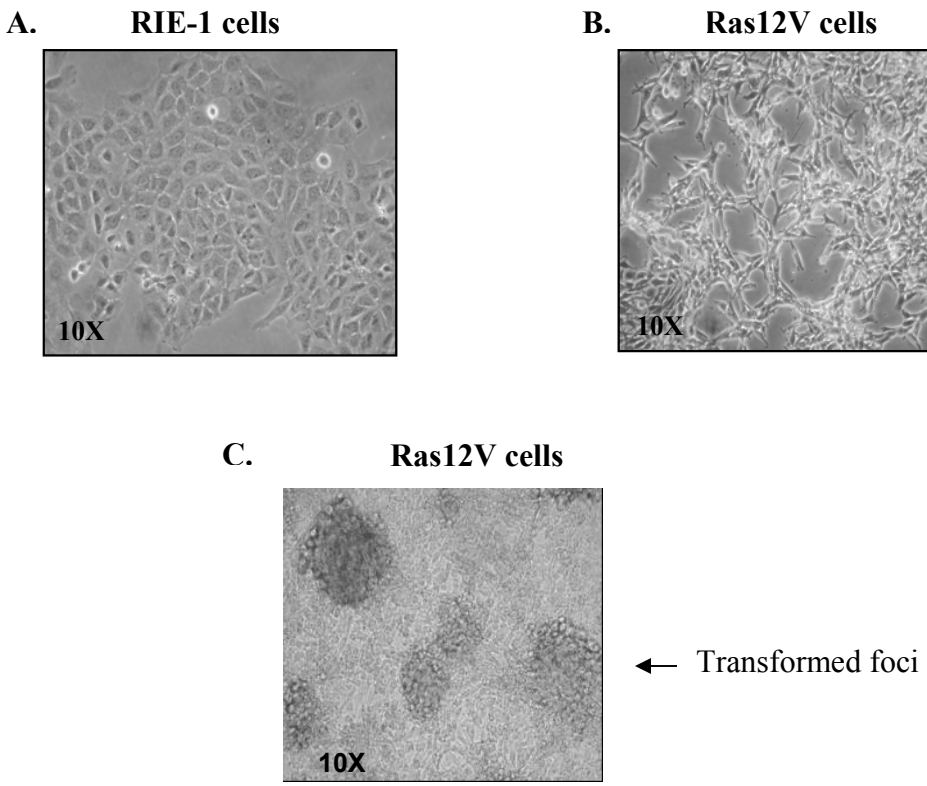

Figure 2.2. Analysis of morphology of RIE cells expressing constitutively active Ras.

Morphology of **(A)** RIE-1 cells stably transfected with empty vector were compared to cells expressing a constitutively active **(B)** *ras12V* plasmid. About 50 clones were screened for Ras expression and all the Ras expressing clones displayed the transformed morphology. Cell morphology and foci formation was analyzed by light microscopy. **(C)** Arrow denotes foci formed by Ras12V cells on a monolayer.

Clones	# of foci Day11	# of foci Day18	Generation time (hrs)
RIE-1	14	18	28.6
#35 High Ras clone	72	138	19.4
#49 Low Ras clone	34	49	15.8

Table 2.1. Changes in anchorage-independent growth and generation time in response to Ras activation.

Measurement of growth in soft agar was performed as described in the Methods. Colonies were counted on day 11 and day 18 after plating. Values represent the average of duplicate samples for all clones. Cell growth rates were measured by estimating the number of cells per cm^2 at 24, 48, 72, 120, 144 and 170 hrs of growth. Generation times were calculated as described in methods. The experiment was performed in duplicate.

high-Ras clone and the low-Ras clone exhibited increased levels of ODC activity at both 24 and 48 hrs of growth compared to the control cells (Fig 2.3A). At 24 hrs of growth ODC activity was increased more than 20-fold in the high-Ras clone and about 10-fold in the low-Ras clone, suggesting a positive correlation with levels of Ras expressed and activity of ODC (Fig 2.3A). To analyze the effects of such high ODC activity, the polyamine content of these cells was measured (Fig 2.3B). Compared to the control cells the Ras12V cells exhibited increased putrescine content, with relatively little change in spermidine and spermine (Fig 2.3B). This pattern is similar to that seen in other cell types (Feith et al., 2005; Manni et al., 1995b).

Ras-activated signaling pathways that regulate ODC activity

The activated Ras oncogene triggers a growth regulating signaling cascade involving the activation of several downstream effector pathways (Campbell & Der, 2004). Two pathways that have been established as critical to Ras-mediated transformation in RIE-1 cells are those downstream of Raf and PI3K (Campbell & Der, 2004) (Fig 2.4). In order to characterize the up-regulation of the Raf-kinase pathway in our system, western blot analyses using antibodies targeted against both phosphorylated and total ERK1/2 (p44/42 MAPK) were carried out. At 24 hrs of growth there was an increase in total and phosphorylated levels of ERK1/2 in both Ras clones compared to parental controls (Fig 2.5A). Activation of the other principal pathway controlled by PI3K was confirmed by an increase in the phosphorylated and total levels of AKT in the Ras12V cells in comparison to the controls (Fig 2.5B). One of the crucial targets of AKT is mTOR, which when activated, phosphorylates factors such as 4EBP1 and p70S6K. 4EBP1 upon phosphorylation releases the RNA binding translation initiation factor

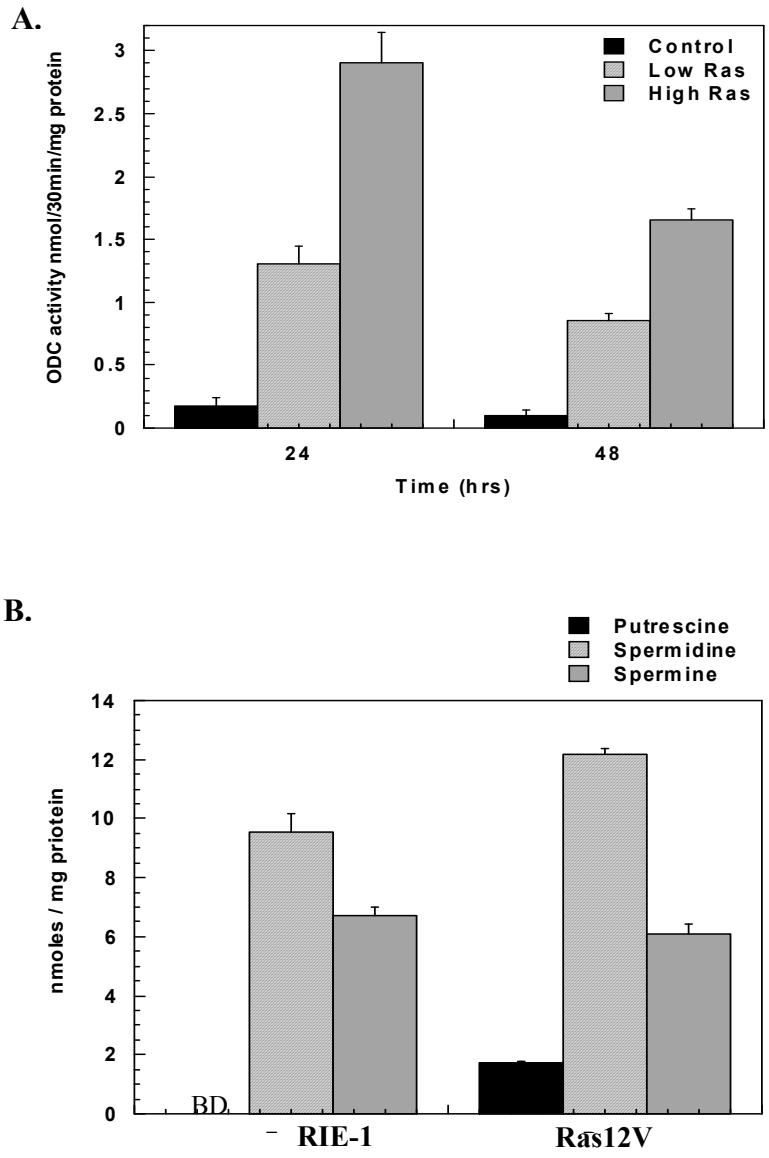

Figure 2.3. ODC activity and polyamine content in Ras12V cells compared to parental control. (See next page for figure legend)

Figure 2.3. ODC activity **(A)** and polyamine content **(B)** in Ras12V cells compared to parental control.

(A) ODC activity for each clone was measured at both 24 and 48 hrs of growth. Graph represents the average of two experiments with triplicate samples measured per experiment for Ras12V cells and duplicate samples for control cells. Both the Ras clones at 24 and 48 hrs of growth were significantly different from control cells with a $p<0.0001$ as calculated by a two-tailed T test.

(B) Putrescine, spermidine and spermine content was measured as described in the Methods and normalized to total protein. Putrescine levels were below the limits of detection (BD) in RIE-1 cells. Graph represents the average of triplicate sample estimations per cell line measured at 24 hrs of growth. Spermidine levels were significantly different between both the cell lines with a $p=0.015$ and the difference in spermine levels were not found to be significant as measured by a two-tailed T test.

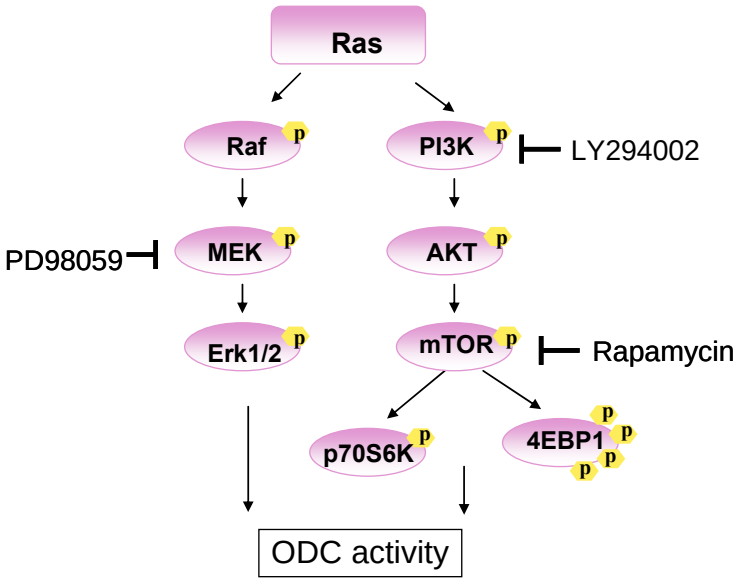

Figure 2.4. Schematic of the Ras-activated Raf-kinase and PI3K pathways

Activated Ras binds to and activates effectors such as Raf and PI3K. Raf-kinase upon activation phosphorylates MEK, which in turn phosphorylates ERK 1/2-kinase.The other primary Ras effector is PI3K, which upon activation phosphorylates AKT, which in turn activates mTOR, a kinase that phosphorylates p70S6K and 4EBP1 resulting in enhanced protein-synthesis. Our study aims to determine the role of either of these pathways in regulating ODC activity by inhibiting MEK-activation with PD98059 and inhibiting activation of PI3K and mTOR with LY294002 and Rapamycin, respectively.

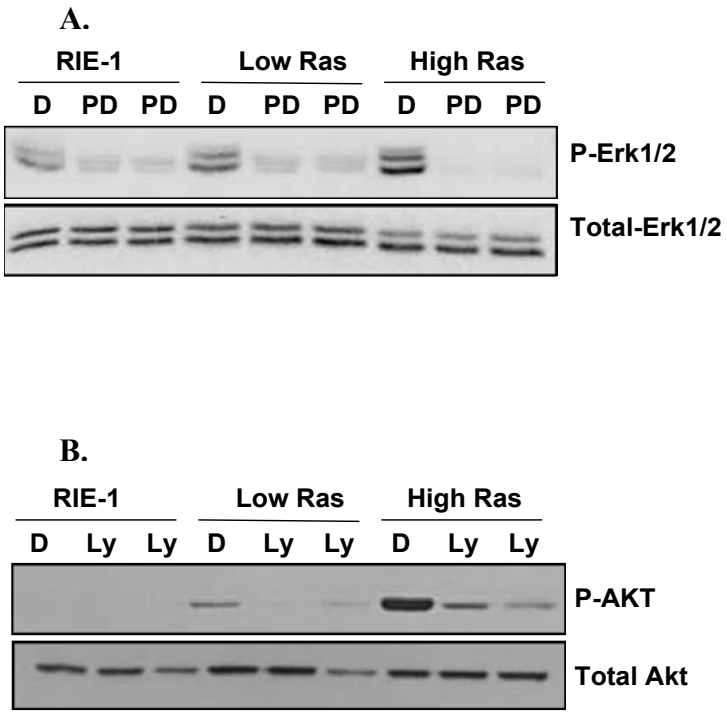

Figure 2.5. Biochemical characterization of the Raf/MEK/ERK and PI3K pathways in Ras12V cells

Western blot analysis of cell extracts from Ras12V and vector control clones. Cells were grown in the presence of media containing 10% serum for 24 h, and then treated with either the vehicle D-DMSO or 50 μM PD-PD98059, 20 μM LY-LY294002 in serum-free media for 2 hrs. 20μg of total protein was loaded for each sample. Experiment was performed in duplicate.

(A) Levels of phosphorylated ERK1/2 (above) and total ERK1/2 (below) in both low and high-expressing Ras12V clones and control cells in the presence and absence of the MEK inhibitor PD98059 (PD) were analyzed in duplicate for each clone.

(B) Levels of phosphorylated AKT (above) and total AKT (below) in both low and high-expressing Ras12V clones were compared to the vector control, and the effect of the PI3K inhibitor LY294002 (LY) was analyzed in duplicate for each clone.

eIF4E, thus enhancing cap-dependent translation (Richter & Sonenberg, 2005) and phosphorylation of p70S6K activates translation of the TOP (Terminal Oligopyrimidine) mRNAs that encode several ribosomal proteins and translation elongation factors eEF1α, eEF2 (Ruvinsky & Meyuhas, 2006). The phosphorylated levels of both p70S6K and 4EBP1 were found to be increased in the Ras12V cells along with the total levels of 4EBP1, suggesting a possible increase in overall protein synthesis in response to Ras (Fig 2.6 A,B). Another pathway that is activated by Ras and plays a significant role under stress conditions is the p38 MAPK pathway (Martin-Blanco, 2000). Analysis of p38 levels revealed that the total p38 MAPK levels were similar between the Ras and control cells (Fig 2.8C) and the phosphorylated p38 levels were below the limits of detection in both the cell lines, suggesting that the p38 MAPK pathway is not a significant Ras effector in the Ras12V cells.

Following establishment of the activation of the Raf-kinase and the PI3K pathways, the effect of these pathways in regulating ODC activity was determined by treating the Ras-transformed cells with LY294002 and Rapamycin, which inhibit PI3K and mTOR respectively, and PD98059, which inhibits MEK (Fig 2.4). MEK inhibition was effective in inhibiting phosphorylation of ERK1/2 within 90 min, without affecting total levels of ERK1/2 (Fig 2.5A).The effect of LY294002 was confirmed by a decrease in the phosphorylated levels of AKT (Fig 2.5B), and in the presence of Rapamycin a decrease was observed in the phosphorylated levels of p70S6K and 4EBP1 (Fig 2.6A, B). When Ras12V cells were grown in the presence of these inhibitors for 24 h (Fig 2.7A), a 50-60% decrease in ODC activity was observed in both the high Ras clone and low Ras clone compared to the vehicle treated controls. However, none of these inhibitors

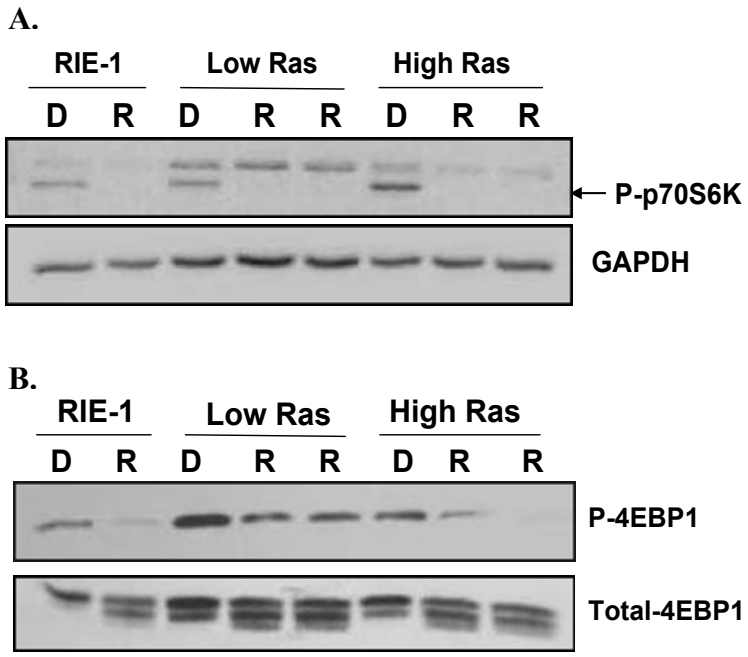

Figure 2.6. Characterization of the PI3K/mTOR pathway in Ras12V cells

To measure levels of the mTOR effectors 4EBP1 and p70S6K and to analyze the effects of Rapamycin, western blot analysis on RIE and Ras12V cells was carried out as described in Figure 2.4, except that the cells were treated with either DMSO or 100nM Rapamycin (R). **(A)** Levels of phosphorylated p70S6K (above) and GAPDH (below) as a loading control and **(B)** levels of phosphorylated 4EBP1 (above) and total 4EBP1 (below) were analyzed in both low and high-expressing Ras12V clones and compared to the vector control. The effect of Rapamycin was analyzed in duplicate for each Ras clone.

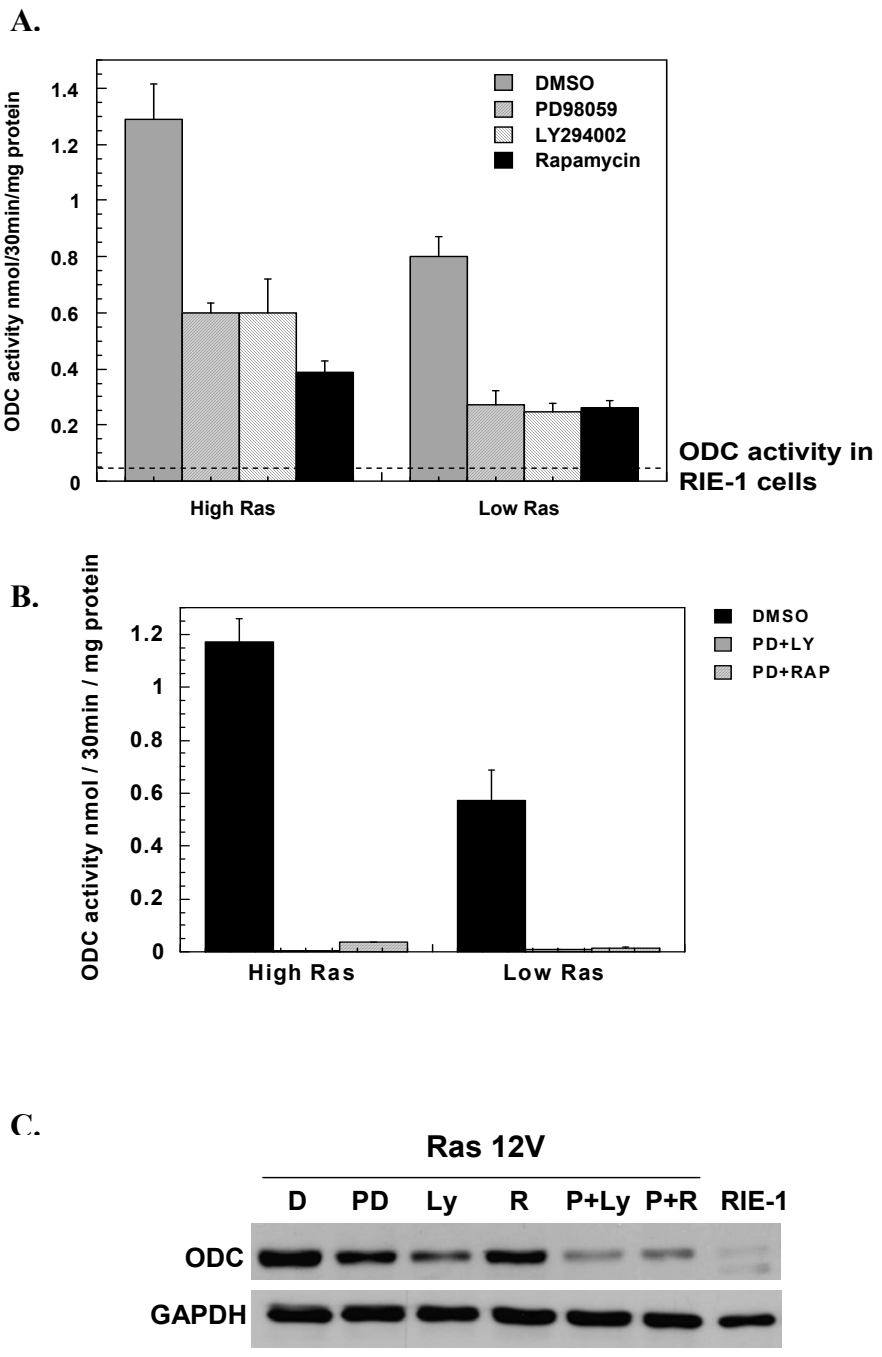

Figure 2.7. Effect of MEK and PI3K/mTOR inhibition on ODC activity in Ras12V cells

(See next page for figure legend)

Figure 2.7. Effect of MEK and PI3K/mTOR inhibition on ODC activity in Ras12V cells

ODC activity and protein levels for each clone was measured by treating the cells with either the vehicle **(A)** DMSO, 50 μM PD98059 (PD), 20 μM LY294002 (LY) or 100nM Rapamycin (R) or **(B)** by using a combination of either 50 μM PD98059 and 20 μM LY294002, or 50 μM PD98059 and 100nM Rapamycin for 24 hrs of growth. Graphs represent the average of triplicates per experiment and the experiment was performed in duplicate. ODC activity in the presence of inhibitors was found to be significantly different from the vehicle controls with a $p<0.01$ as measured by a one-way ANOVA test. **(C)** To analyze effect of inhibitors on ODC protein levels 30μg of total protein was loaded per lane and probed with mouse polyclonal antibody against ODC. Results were also confirmed by western blot analysis of Ras and RIE-1 cells extracted in ODC assay buffer.

individually was sufficient to reduce ODC activity to levels comparable to those found in parental control cells. Such a drastic inhibition in ODC activity was only observed when both pathways were inhibited (Fig 2.7B). These results suggest that both the Raf and PI3K pathways together are necessary for maintaining the Ras-induced ODC activity in this epithelial model. Effects of inhibitors on ODC activity were also confirmed by analysis of protein levels using an immunoblot (Fig 2.7C). Effect of the inhibitors on ODC activity in the parental RIE-1 cells could not be determined as these cells have very low basal levels of ODC activity and treatment with the inhibitors reduced the ODC activity below the limit of detection of our assay.

It is possible that the effects of PI3K and the Raf/MEK/ERK pathways in the Ras12V cells are not exclusive and their effects could be mediated by a significant cross-talk between the two pathways. Zimmermann et. al., showed that AKT physically associates and phosphorylates Raf to inhibit activation of the Raf-kinase pathway in a cell-specific manner (Rommel et al., 1999; Zimmermann & Moelling, 1999). Also, inhibition of the ERK pathway in human leukemic U937 cells induced apoptosis by down regulating activation of AKT (Moon et al., 2007). Therefore, to examine the effect of inhibiting MEK on the PI3K pathway, cells were treated with PD98059 and levels of 4EBP1 phosphorylation were measured. Treatment of both the high Ras and low Ras clone with PD98059 had no effect on either the phosphorylation or total levels of 4EBP1, suggesting that inhibition of MEK did not affect the PI3K/mTOR pathway (Fig 2.8A). Alternately, in the presence of LY294002 no effect on the total levels of ERK1/2 was observed in the low Ras and high Ras clone (Fig 2.8B). However, phosphorylation of ERK1/2 was induced by LY294002 in the low Ras clone and a slight induction was also

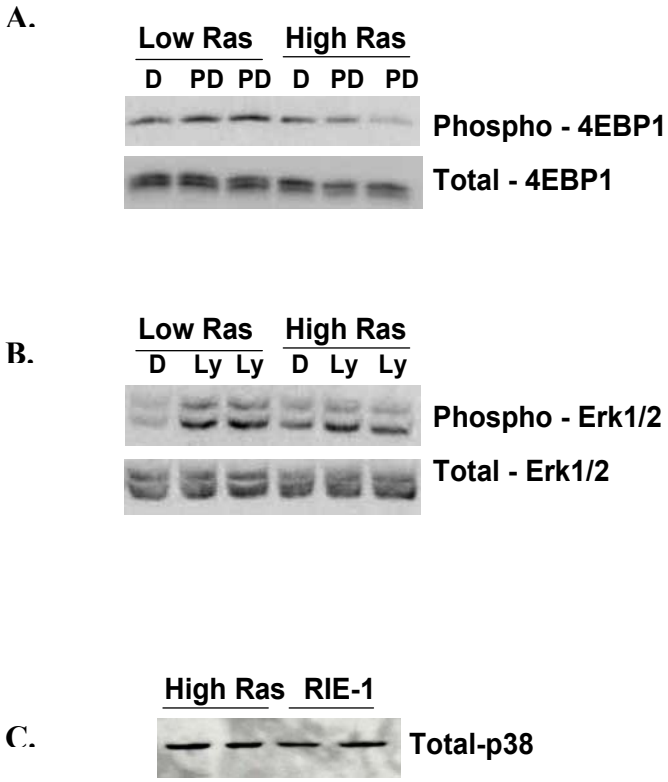

Figure 2.8. Determination of cross-talk between the Raf-kinase and PI3K pathway

Cross-talk between the Raf-kinase and PI3K pathway was analyzed by western blot analysis of Ras cell extracts treated with DMSO (D), 50μM PD98059 (PD) or 20μM LY294002 (LY) as described in figure 2.5. **(A)** Cells treated with PD98059 were assayed for changes in 4EBP1 phosphorylation levels and **(B)** cells treated with LY294002 were assayed for changes in ERK1/2 activation. **(C)** Activation of additional pathways was examined by measuring total levels of p38 MAPK by western blot analysis of Ras12V cells in comparison to the controls.

observed in the high Ras clone, suggesting that inhibition of AKT may result in a mild activation of the Raf-kinase pathway (Fig 2.8B). Up-regulation of the Raf-kinase pathway could contribute to the lack of complete inhibition of ODC activity observed with LY294002 treatment.

An interesting phenotype observed with the inhibition of MEK is the reversal of the transformed phenotype in Ras12V cells from fibroblastic to a more epithelial-like morphology (Fig 2.9A). This reversal was further confirmed by the enhanced expression of E-Cadherin, an epithelial cell marker, which re-expresses when Ras-transformed cells are treated with PD98059 for about 72 hrs (Fig 2.9B). EMT (Epithelial to Mesenchymal Transition) has been implicated in enabling cells to dislodge from a primary tumor site to undergo metastases. Changes in phenotype of the RIE-1 cells upon Ras expression suggests that the Ras12V cells have undergone an EMT and the effects of PD98059 suggest that their epithelial nature could be restored by inhibition of MEK (Fig 2.9A). No such morphological change was observed in the presence of either LY294002 or Rapamycin under similar experimental conditions further suggesting that only the MEK pathway is necessary for the phenotypic variation associated with Ras transformation.

Regulation of ODC synthesis

Synthesis of ODC can be regulated by multiple mechanisms involving transcriptional and post-transcriptional modifications. To explain the enhanced ODC activity in response to Ras, transcriptional activation was analyzed by northern blot analysis and revealed a 2-fold increase in ODC mRNA levels in the Ras12V cells compared to the controls (Fig 2.10). This increase in ODC RNA levels was confirmed to be transcriptional regulation using an ODC promoter activity assay. In this assay,

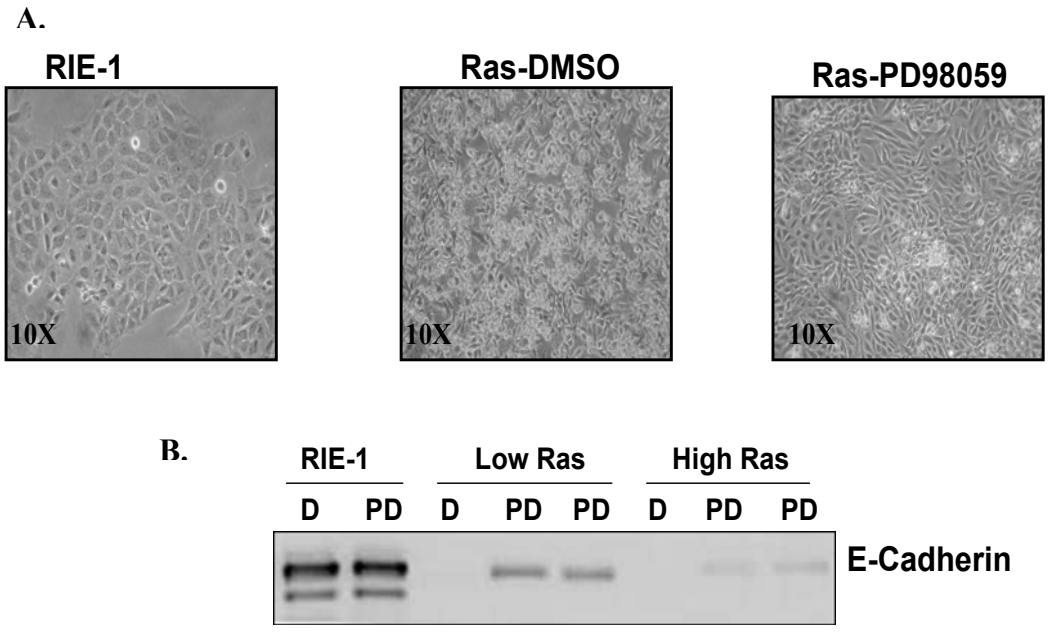

Figure 2.9. Morphology of Ras12V cells in response to prolonged inhibition of MEK

(A) Images represent the cell morphology of vector control cells (left), Ras12V cells treated with vehicle DMSO (center) and Ras12V cells treated with 50 μM PD98059 (right) for 72 hrs. **(B)** Levels of the epithelial cell marker E-Cadherin were determined by western blot analysis of control, low expressing Ras12V clone and high expressing Ras12V cell extracts. Cells were treated with either D-DMSO or 50 μM PD98059 (PD) for 72 hrs. 20 μg of total protein was loaded per lane. For both the Ras clones, samples were treated in duplicate with PD98059 and the experiment was repeated twice.

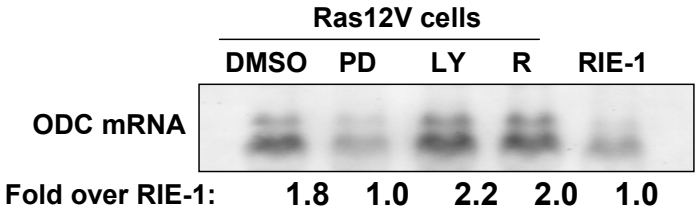

Figure 2.10. ODC RNA levels in response to Ras-activation

ODC RNA levels in both control and Ras12V cells were analyzed by northern blot analysis. Cells were treated with the vehicle DMSO or inhibitors 50 μM PD98059 (PD), 20 μM LY294002 (LY) or 100nM Rapamycin (R) for 24 hrs. 20μg of total RNA was loaded per lane. Blots were probed with a fluorescent probe complementary to the full length ODC transcript. Levels of ODC RNA in Ras12V cells and with the inhibitor treatments was measured as a fold change over the parental RIE-1 cells and the experiment was repeated twice.

transcriptional ability of ODC promoter in Ras12V and RIE-1 cells was assayed by measuring expression of Firefly luciferase derived from the promoter of ODC (Fig 2.11A). A 2-fold increase in ODC promoter activity was observed in the Ras12V cells in comparison to the controls (Fig 2.11B), which was reduced to the control levels by treatment with the MEK inhibitor PD98059 (Fig 2.12). ODC RNA levels were also reduced 2-fold by PD98059, suggesting that Ras-activated transcription of ODC is regulated by the MEK pathway (Fig 2.10). However, no effect on ODC RNA levels or promoter activity was observed in the presence of Rapamycin or LY294002, suggesting that the PI3K/mTOR pathway does not regulate ODC activity by transcriptional mechanisms (Fig 2.10 and 2.12).

These results suggest that the 2-fold up-regulation of ODC transcription, though important is not sufficient to explain the 20-fold increase in ODC activity in Ras12V cells. Therefore additional post transcriptional mechanisms must exist to regulate ODC synthesis. One such post-transcriptional mechanism is an alteration in protein stability, which was analyzed by treating the cells with cycloheximide to halt protein synthesis, and the remaining ODC activity was measured at 0, 30, 60 and 90 min following cycloheximide treatment. The half-life of ODC activity was estimated to be 30-35 min control cells; however the half-life was almost doubled to 60-65 min in both the high Ras and low Ras clone (Fig 2.13), suggesting that stability of ODC protein is also increased about 2-fold in response Ras.

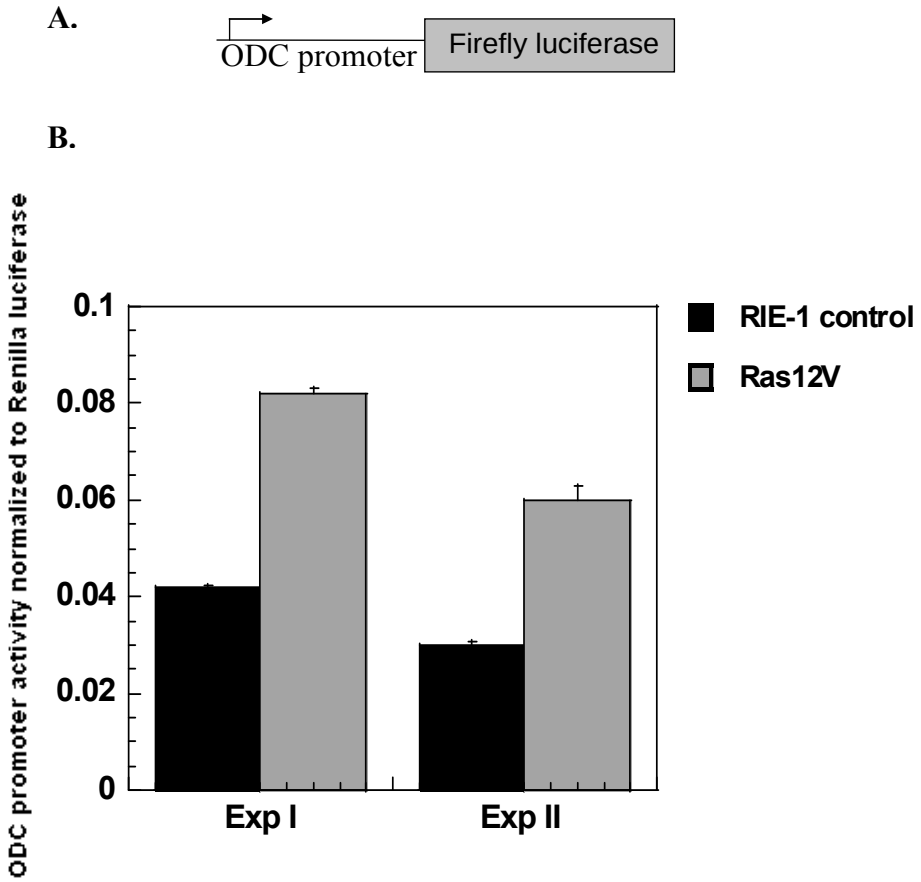

Figure 2.11. Regulation of ODC promoter activity in control RIE-1 and Ras12V cells

Schematic shows ODC promoter linked to Firefly luciferase observed in the ODC-pGL3 plasmid used for transfection and arrow indicates the direction of transcription. Graph shows ODC promoter activity measured in RIE-1 and Ras12V cells in two different experiments (Exp I and II). ODC-pGL3 vector was co-transfected with pRL-SV40 (transfection control) and 24 hrs following transfection ODC promoter activity was measured as Firefly luciferase activity normalized to Renilla luciferase activity (transfection control).

Figure 2.12. Effect of Ras effectors on ODC promoter activity

Graph shows ODC promoter activity measured in Ras12V cells in response to treatment with DMSO, inhibitors 50 μM PD98059 or100nM Rapamycin. ODC-pGL3 and pRL-SV40 (transfection control) plasmids were co-transfected and ODC promoter activity was measured as described in figure 2.11 and Methods.

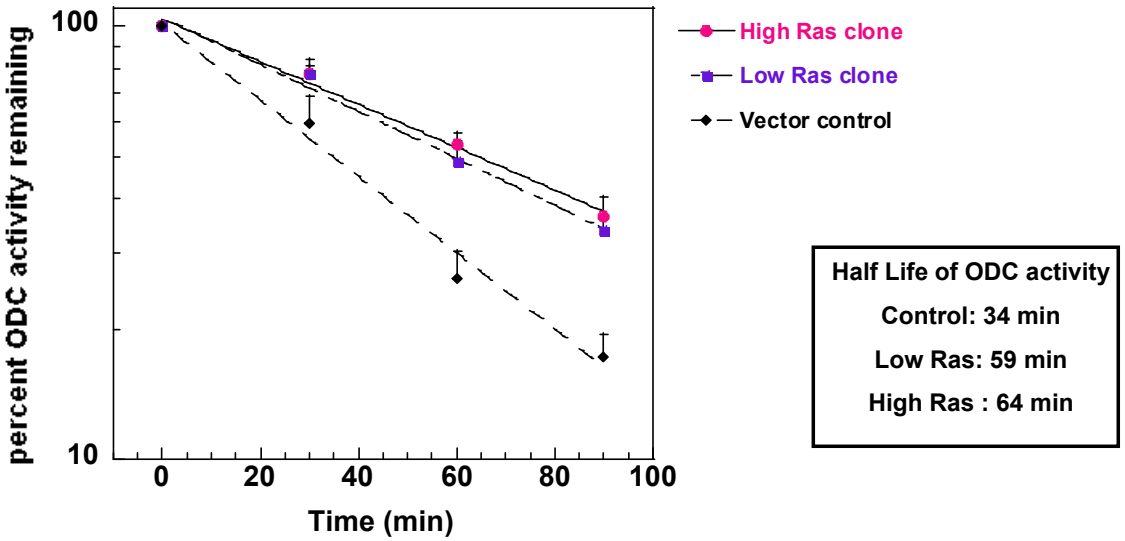

Figure 2.13. Stability of ODC protein as measured by activity

Cycloheximide (1mM) was added to Ras12V and RIE-1 cells after 40 hrs of growth. Immediately after addition, cells were extracted in ODC assay buffer and assayed at time 0 min and extracted thereafter at 30, 60 and 90 min. ODC activity at time 0 min was plotted as 100% and residual ODC activity at the time points tested was plotted as a percent change relative to the 0 time point . Triplicate samples were assayed for each time point and half-lives of ODC activity were measured using a linear regression fit. Results were confirmed by performing the experiment in duplicate.

Discussion

ODC is necessary for transformation induced either by the direct activation of the Ras oncogene or by activation of one of its crucial targets such as MEK (Feith et al., 2005; Graff et al., 1997). While studies in Ras transformed NIH/3T3 fibroblast cells have advanced the understanding of ODC regulation in response to Ras, the present study delves into the regulation of ODC in a pathologically relevant epithelial cell-line model transformed by Ras. Studies in these Ras-transformed RIE-1 cells show that similar to the NIH/3T3 fibroblasts, both the Raf/MEK and PI3K/mTOR pathways regulate ODC activity at the levels of both transcription and translation respectively.

Stable activation of Ras in the RIE-1 cells resulted in about a 20-fold increase in ODC activity and this increased ODC activity correlated with increased polyamine content, especially in levels of putrescine. Increased polyamine content under typical conditions results in a feedback inhibition of ODC. However Ras transformation as reported previously resulted in an absence of such feedback inhibition thus ensuring elevated levels of polyamines needed to maintain the transformed state of the cells (Shantz, 2004)

Inhibition of either MEK or PI3K reduced ODC activity in Ras12V cells to about 50-60% of control cells. However, the greatest effect especially in the high Ras clone was observed by using Rapamycin, an inhibitor of mTOR. As targets of mTOR primarily regulate translation, these results suggest a substantial regulation of ODC by translation in these cells. Supporting evidence for translational regulation of ODC is twofold. First, ODC promoter activity and as a result ODC RNA levels is increased

about two-fold, however ODC activity is increased about 20-fold with only a two-fold increase in protein stability, suggesting that apart from transcriptional regulation, ODC is regulated by translational mechanisms. Second, inhibition of the PI3K/mTOR pathway did not affect ODC promoter activity or ODC RNA levels, but it did inhibit ODC activity, further suggesting post-transcriptional regulation of ODC. Post-transcriptional regulation could involve multiple mechanisms such as changes in ODC RNA stability, RNA transport, translation, and contributions of each of these mechanisms to the overall synthesis of ODC is analyzed in detail in chapter III. Bias towards translational regulation of ODC comes from results in the Ras-transformed RIE-1 cells that show increased activation of translation factors such as p70S6K and increased phosphorylation of 4EBP1, which upon phosphorylation binds the translation initiation factor eIF4E less efficiently, thus enhancing cap-dependent translation (Gebauer & Hentze, 2004). Also, an increased level of this rate-limiting factor eIF4E has been correlated with efficient translation of ODC, as NIH/3T3 cells transformed by over-expressing eIF4E exhibit a shift of ODC RNA to the heavier polysomal fractions (Rousseau et al., 1996).

While all these studies support translational regulation of ODC, it does not negate the role of transcriptional regulation, especially since the inhibition of the MEK pathway inhibited ODC activity to a similar extent as the PI3K inhibitor LY294002. Inhibition of MEK was sufficient to reverse the 2-fold increase in ODC promoter activity and ODC RNA levels, suggesting that the MEK pathway regulates transcription of ODC in response to Ras. A diverse set of transcriptional factors are activated by the MEK effector ERK1/2 and one such transcriptional factor is Myc

which has been established as an important regulator of ODC transcription (Bello-Fernandez et al., 1993; Chang et al., 2003; Lee & McCubrey, 2002) . Myc in complex with its co-activator Max has been reported to recognize three binding sites in the ODC promoter and induce synthesis of ODC RNA (Auvinen et al., 2003; Fultz & Gerner, 2002; Nilsson et al., 2004; Tobias et al., 1995; Walhout et al., 1997).

A previous report using a dominant negative Myc showed that repression of Myc in Ras12V transformed NIH/3T3 fibroblasts reversed the transformed cell morphology and also repressed transcriptional activity of ODC as assayed by ODC-CAT reporter activity (Auvinen et al., 2003). It has been demonstrated in the Ras-transformed NIH/3T3 cells and RIE-1 cells used in this study that inhibition of ODC transcription by inhibiting the MEK pathway does significantly reduce ODC activity (Shantz, 2004). It would therefore be interesting to analyze if reversal of transformation induced by dominant negative Myc in Ras transformed cells was due to its effects on ODC synthesis and as a result down-regulation of polyamine levels. Also, it may be informative to analyze if Myc is a Ras effector in the Ras transformed RIE-1 cells. Not only would these cells serve as an epithelial model, but also as a model to study Ras activated intestinal cancers, since about 40% of colon cancers carry Ras-activating mutations in them and the mutations in some cases arise early and are observed even in small adenomas (Grady & Markowitz, 2002; Vogelstein et al., 1988). Recent studies have shown Myc as an activator of ODC transcription in tumor suppressor APC (Adenomatous Polyposis Coli)- mutated colon carcinomas (Fultz & Gerner, 2002; Gerner et al., 2005). It would be interesting to further establish the role of Ras activating mutations in APC-mutated colon carcinomas and

their effect on Myc transcription of ODC.

The effects of the MEK and PI3K pathways in this study suggest that ODC is regulated both by transcription and by post-transcriptional mechanisms in response to Ras transformation in an epithelial model. It also suggests cooperativity between the MEK and PI3K/mTOR pathway in regulating ODC activity, as inhibition of either of these pathways individually did not completely inhibit ODC activity. However, inhibition of both these pathways together reduced ODC activity to the control levels.

Chapter III

Post-transcriptional regulation of ODC in response to Ras activation

Specific aim: To determine post-transcriptional mechanisms involved in the induction of ODC synthesis in response to constitutive activation of Ras in RIE-1 cells. Regulation by mechanisms such as alterations in stability of ODC RNA or RNA transport or translation will be examined.

Introduction

Most human cancers carrying Ras activating mutations are predominantly of an epithelial cell origin (Burns et al., 1993; Harris et al., 1991; Kopnin, 1993; Paraskeva et al., 1990; Wynford-Thomas, 1997; Yee et al., 1989) . One of the essential mediators of Ras-activated carcinogenesis is ODC (Feith et al., 2005; Hayes et al., 2006; Ignatenko et al., 2004; Iwata et al., 1999; Pegg, 2006). Knocking down ODC using the irreversible inhibitor DFMO has been shown to reverse formation of skin papillomas induced by activation of the Ras effector MEK, and inhibit carcinogenesis in several cell culture models over-expressing Ras (Feith et al., 2005; Holtta et al., 1988; Hurta, 2000; Ignatenko et al., 2004; Iwata et al., 1999; Shantz & Pegg, 1998). Our study aims to determine the mechanism involved in up-regulation of ODC in response to Ras activation using an epithelial cell line as a model.

Our results in the previous chapter show that ODC activity is induced by about 20 fold in response to Ras activation in RIE-1 cells and both the Ras effector pathways PI3K/mTOR and Raf-MEK-ERK act in cooperation to maintain the induction of ODC synthesis. Inhibition of the Raf-MEK-ERK pathway reduced the 2-fold induction of ODC transcription seen in the Ras transformed cells. However, the PI3K/mTOR pathway did not have any effect on ODC transcription, suggesting that it must regulate ODC by post-transcriptional mechanisms such as enhanced translation initiation or by stabilizing RNA. PI3K/mTOR pathway when activated in response to Ras or stimuli such as insulin signaling, initiates translation by phosphorylating the translation regulatory factors 4EBP1 and p70S6K (Brunn et al., 1997; Gingras et al., 2001; Jefferies et al., 1997). 4EBP1 upon phosphorylation has decreased affinity for the cap binding factor eIF4E and

is replaced by the initiation factor eIF4G, which in turn assembles the eIF4F cap complex to initiate translation (Averous & Proud, 2006; Gingras et al., 1998). While regulation of translation initiation is the more commonly described mTOR function, few studies also show that the PI3K/mTOR pathway is involved in RNA degradation. In *S.cerevisiae,* inhibition of mTOR using Rapamycin induced destabilization of multiple mRNAs suggesting that mTOR functions also involve regulation of mRNA turnover (Albig & Decker, 2001; Foat et al., 2005). In mammalian systems, Rapamycin treatment increased the degradation of RNAs such as Cyclin D1, Myc and IL-3 by recruiting RNA destabilizing factors that recognize AU rich elements in their 3'UTRs (Banholzer et al., 1997; Hashemolhosseini et al., 1998; Marderosian et al., 2006). The ODC 3'UTR also contains similar AU rich elements, suggesting that it could be regulated by mTOR via alterations in RNA stability (Lovkvist Wallstrom et al., 2001). Since inhibition of the PI3K/mTOR pathway did not affect ODC transcription but did inhibit ODC activity, it suggests that ODC must be regulated at the level of translation. Additionally, ODC activity was induced in the Ras cells by 20-fold without much effect on transcription or protein stability, further suggesting that Ras must activate ODC primarily by a translational mechanism.

Previous studies in NIH/3T3 fibroblasts have correlated the Ras-induced levels of the translation initiation factor eIF4E with ODC synthesis (Shantz, 2004). Over-expression of eIF4E is believed to relieve the inhibitions imposed by the long and secondary structure rich ODC 5'UTR (Rousseau et al., 1996; Shantz et al., 1996b). It is proposed that under conditions where the rate limiting factor eIF4E is low, ODC is poorly translated. However, when more eIF4E is available there is less competition from

RNAs that are efficiently translated which allows cap complex formation and enhances translation of oncogenic RNAs such as ODC and Cyclin D1 (Mamane et al., 2004; Rousseau et al., 1996). Thus, under conditions that elevate eIF4E levels such as Ras transformation, ODC synthesis is also upregulated.

Interestingly, Ras transformation of NIH/3T3 fibroblasts not only induces total levels of eIF4E but also its phosphorylation levels (Shantz, 2004). The exact role of eIF4E phosphorylation in mediating protein synthesis is an unsolved puzzle, but a recent study showed that phosphorylation of eIF4E facilitates its transformation potential (Topisirovic et al., 2004). However, knocking out the eIF4E phosphorylating kinases Mnk1 and Mnk2 did not generate any growth or developmental defect and did not affect global protein synthesis (Ueda et al., 2004). Since eIF4E phosphorylation is elevated under specific conditions such as Ras transformation and is essential for the transformation properties of eIF4E, it is possible that eIF4E may not be required for normal growth and development but instead regulates synthesis of specific RNA under physiological conditions such as transformation. Regulation of specific RNAs was observed in fibroblasts over-expressing a non-phosphorylatable eIF4E Ser-209 mutant, which resulted in decreased foci formation compared to its wild-type counterpart (Topisirovic et al., 2004). The abrogation of eIF4E transformation capabilities was attributed to the decreased synthesis of Cyclin D1 caused by the impeded transport of Cyclin D1 RNA into the cytoplasm (Topisirovic et al., 2004). Since Cyclin D1 and ODC face similar translational obstructions caused by their complex 5'UTRs, it is possible that eIF4E phosphorylation may not affect global protein synthesis but affects synthesis of sensitive RNAs such as ODC and Cyclin D1 under specific conditions such as

transformation. Since inhibition of ODC by expressing a dominant negative ODC mutant reverses eIF4E-induced transformation (Shantz et al., 1996a), we aimed to determine the relationship between eIF4E phosphorylation and ODC translation in the context of Ras transformation.

In this study we used polysome analysis and observed that in response to Ras activation in RIE-1 cells translation efficiency of ODC is not altered, but the levels of ODC RNA recruited to polysomes is increased. This was found to be predominantly contributed by the Ras induced stabilization of ODC RNA. Rapamycin abrogated the effect of Ras by decreasing RNA stability without affecting translation efficiency of ODC suggesting that the PI3K/mTOR pathway regulates ODC synthesis in response to Ras at the level of RNA stability. Interestingly, the factor that did affect translational efficiency of ODC was eIF4E phosphorylation as determined using the Mnk1/2 inhibitor CGP57380. Also, dephosphorylation of eIF4E in the Ras12V cells did not affect global protein synthesis or the cap complex formation, yet inhibited ODC activity suggesting that under Ras transformed conditions eIF4E phosphorylation can regulate translation of specific RNAs such as ODC.

Materials and Methods

Culture of Ras12V, RIE-1 and 4E-P2 cells was carried out as described in chapter II.

Western blot analysis

For analysis of eIF4E levels, Ras and RIE-1 cells at 24 and 48 hrs of growth were extracted in 4E-HB buffer (buffer components described in the Methods of chapter II) and just before use 1mM DTT, 1mM benzamidine, 0.5mM sodium vanadate and protease cocktail inhibitor (Calbiochem) were added to the buffer. For analysis of TTP levels, both Ras and RIE-1 cells were extracted in RIPA buffer (Santa Cruz). Western blot analysis was carried out as described in chapter II except 30 μg of total protein was loaded per lane and membranes were probed with rabbit polyclonal antibodies targeting total and phosphorylated eIF4E (Ser209) (Cell-Signaling Technology) and total TTP (Santa Cruz).

Immunoprecipitation (IP) analysis

Ras12V cells ($0.7x10^6$) and RIE-1 cells ($0.9x10^6$) were plated on 10-cm plates and allowed to adhere overnight, and extracted 24 hrs later. For inhibitor treatments, Ras12V cells were treated for 2 hrs with either DMSO, or 100nM Rapamycin or 20 μM CGP57380 after 24 hrs of growth. Cells were extracted in 600μl of 4E-HB buffer prepared as described for western blot analysis and centrifuged at 3000 rpm for 3min. About 500μl of supernatant containing 1000μg of total protein was incubated overnight with 75μl of eIF4E mouse monoclonal antibody (Kind gift of Dr. Jim Jefferson and Scot Kimball, PSU), 175μl of phosphate buffered saline and 12.5μl Triton X-100 by rotating the tubes at 4°C. For each sample, 1ml of Biomag magnetic beads coated with anti-mouse polyclonal IgG (Qiagen) were washed 3X in Low Salt buffer (LSB) containing 20mM Tris-Cl and 150mM NaCl, 5mM EDTA, 0.5% Triton X-100, 0.1% β-

Mercaptoethanol (pH 7.4 at 4°C). Beads for each sample were resuspendend in 0.5ml LSB with 0.1% non-fat dry milk and rocked with the samples with primary antibody at 4°C for 1 hr. Beads were cleared of supernatant by capturing them on a magnetic base and washed 2X in LSB and 1X in High Salt buffer containing 50mM Tris-HCl, 500mM NaCl, 5mM EDTA, 1% Triton X-100, 0.5% Sodium deoxycholate, 0.1% SDS, 0.04% β-Mercaptoethanol (pH 7.4 at 4°C). Beads were resuspendend in100ul of 1X SDS sample buffer (5X SDS buffer contains 250mM Tris-HCl pH 6.8, 10% SDS, 50% glycerol, 0.02% Bromophenol blue ,1% β-Mercaptoethanol). Beads were boiled for 5min to separate immunoprecipitated eIF4E bound to beads. 15µl of sample in sample buffer was loaded per lane and subjected to immunoblot analysis as described above. Western blots were probed with rabbit polyclonal antibodies that bind total eIF4E, eIF4G or 4EBP1 (Cell-Signaling Technology).

Methyl-7-GTP Sepharose chromatography

Methyl-7-GTP Sepharose chromatography was performed as described previously with the following modifications (Pyronnet et al., 2001). To isolate eIF4E and proteins bound to eIF4E, about 1x 10^6 Ras12V cells were plated per 10-cm dish and allowed to adhere overnight. 24 hrs later cells were treated for 2 hrs with DMSO,100 nM Rapamycin or 20 µM CGP57380 and extracted in 1ml lysis buffer (50mM Tris-HCl pH 7.4, 50mM KCl, 1 mM EDTA, 0.5% Nonidet P-40, protease inhibitor cocktail from Calbiochem). Lysis was carried out on ice for 30 min and samples were centrifuged at 10000 rpm for 10min. Before use, m^7-GTP Sepharose-4B resin (Amersham) was briefly centrifuged at 2500 rpm for 2min and resuspendend in 25µl of lysis buffer. Supernatant containing 750µg of total protein was added to 25µl of m^7-GTP Sepharose-4B resin and rocked at 4°C

overnight. Unbound sample was removed by centrifugation at 1500 rpm for 10 min and washed 3X in 1ml lysis buffer followed by centrifugation at 1500 rpm for 10min. Sample was finally resuspendend in 50 µl of 2X SDS sample buffer and briefly spun at 1500 rpm for 30sec and proteins bound to m^7GTP sepharose were separated from resin by boiling for 3 min. 12µl of sample was loaded per lane and subjected to western blot analysis as described for IP analysis.

Cell fractionation and RNA extraction

Cell fractionation to separate nuclear and cytoplasmic RNA was carried out as described previously (Rousseau et al., 1996). 0.9 x 10^6 RIE-1 and 0.7 x 10^6 Ras12V cells were plated per 10 cm plate and allowed to adhere overnight. After 24 hrs of growth about 3-10 cm plates were trypsinized and combined to obtain 10 million cells per fractionation sample. Cells were washed in 1ml ice-cold PBS and centrifuged at 1000 rpm for 3 min. Cells were resuspendend in 300 µl of cell fractionation buffer (10mM Tris pH 8.4, 140 mM NaCl, 1.5mM $MgCl_2$, 0.5% NP-40, 1mM DTT and Superasin (100U/ml), Ambion) carefully with slow vortexing for 3min. The cytoplasmic fraction was isolated as the supernatant obtained by centrifuging samples at 2500 rpm for 3min at 4°C. Nuclear pellets were resuspended by slow vortexing for 3 min in 300µl of fractionation buffer containing 1/10^{th} volume of DOC/Tween solution (3.3% Sodium deoxycholate and 6.6% Tween-40) and incubated on ice for 5 min. Samples were centrifuged at 2500 rpm for 3min at 4°C and the supernatant (post-nuclear fraction) was combined with the cytoplasmic fraction. Nuclei were washed 1X in fractionation buffer, resuspended in fractionation buffer and RNA was extracted using the Trizol isolation method as per the manufacturer's instructions (Invitrogen). Northern analysis was carried out as described

in chapter II and radiolabeled cDNA probes were synthesized as described below.

Polysome analysis

Polysome analysis was carried out as described previously (Johannes & Sarnow, 1998). 0.9 x10^6 RIE-1 and 0.7 x 10^6 Ras12V cells were plated per 10 cm plate and allowed to adhere overnight. After 24 hrs of growth cells were incubated with 0.1 mg/ml cycloheximide for 4min at 37°C. Cells were washed 2X in ice cold PBS containing 0.1 mg/ml cycloheximide and harvested on ice by scraping cells in polysome lysis buffer (15mM Tris-HCl pH 7.6, 15mM $Mgcl_2$, 0.3M NaCl, 1% Triton X-100, 0.1 mg/ml cycloheximide and 1mg/ml heparin). 200µl of polysome lysis buffer was added per 10 cm plate and three 10 cm plates were combined together into one eppendorf tube such that 10 million cells were suspended in 600µl of polysomes lysis buffer. Samples were rocked for 10min at 4°C and cell extracts were centrifuged at 10000 rpm for 10min at 4°C to clear the lysate of nuclei and debris. 600µl of the supernatant was loaded on top of the sucrose gradient containing 9 layers of polysome lysis buffer prepared with varying concentrations of sucrose ranging from 20% on top to 47% at the bottom. Gradients were centrifuged at 34000 rpm for 5 hrs using a SW41 rotor (Beckman). Gradients were read at absorbance UV 254 nM as they were pumped by passing Flourinert (Isco) through the bottom of the tube. Fractions were collected every 30 sec and a total of 11 fractions were collected from the top directly into 50 ml Rnase-free falcon tubes (VWR) containing 3ml of 8M Guanidine HCl and 0.5 ml nuclease-free water. Fractions were then vortexed for 1 min and equal volumes of 100% ethanol were added per tube, mixed and RNA was precipitated overnight at -20°C. Fractions were centrifuged at 8500 rpm for 20min at 4°C, washed in 75% ethanol made with nuclease-free water and the RNA pellet was dissolved

in 400µl nuclease free Tris-EDTA pH 8.0. RNA was reprecipitated overnight at -20°C by addition of 1/10th volume of 3M Sodium acetate pH 5.2 and 2.5X volume of 100% ethanol. RNA was pelleted by centrifugation at 10000 rpm for 20min and washed in 75% ethanol. 20µl of nuclease free water was added to the RNA pellet and incubated at 4°C for 30min, then resuspendend by pipetting. For each fraction equal volumes of RNA were analyzed by northern hybridization as described in Chapter IV. Integrity of RNA was ensured by staining the formaldehyde agarose gels with Ethidium bromide.

Synthesis of radiolabeled cDNA probes

cDNA probes were prepared by radiolabeling 100ng DNA with P32 dCTP using the Rad prime DNA kit (Invitrogen) as per the manufacturer's instructions. To prepare full length ODC probe, pGEM ODC vector (Shantz, 2004) was digested at restriction sites BamHI and EcoRI and the expected 1.8kb fragment was isolated by gel purification. To prepare probes complementary to CyclinD1, EF1A, Cyclophilin, Lys t-RNA and U1SnRNA, RNA from Ras12V cells was reverse transcribed as described in Chapter IV and the following primers were used for PCR amplification reactions:

U1 SnRNA Forward - 5' GATACCATGATCACGAAGGTGTTTTC 3'

U1 SnRNA Reverse - 5' CAGTCCCCCGCACTACCACAAATTATGC 3'

Lys tRNA Forward - 5' GCCCGGCTAGCTCAGTCGG 3'

Lys tRNA Reverse - 5' TGGCGCCCAACGTGGGGCTC 3'

Cyclin D1 Forward - 5' GCTCCTGTGCTGCGAAGTG 3'

Cyclin D1 Reverse - 5' GATGCCACTACTTGGTGACTC 3'

Cyclophilin A Forward - 5' CGCTGTCTCTTTTCGCCGC 3'

Cyclophilin A Reverse - 5' GCAATCCTGCTAGACTTGAAG 3'

EF1A Forward - 5’ GGTATGGTGGTTACCTTTGC 3’

EF1A Reverse - 5’ CGATGCATTGTTATCATTAACCAG 3’

The following PCR conditions were used for U1SnRNA, Cyclin D1, EF1A, and Cyclophilin: initial denaturation- 98°C 1min 30sec, denaturation 95°C 1min, annealing 57°C 1min, elongation 72°C 1min 30sec, 30 cycles and final elongation 72°C 10min. For Lys tRNA exactly the same PCR conditions were used except 65°C was used as the annealing temperature.

RNA stability assay

To analyze stability of ODC RNA, cells were cultured on 10 cm plates similar to polysome analysis and after 24 hrs of growth, cells were treated with 5 μg/ml Actinomycin D (1mg/ml stock in DMSO) (Sigma) added in fresh media. RNA was isolated using the RNAqueous kit as per the manufacturer’s instructions (Ambion). Northern analysis was carried out using radiolabeled cDNA probes synthesized for ODC and Cyclophilin as described above. Half-life of ODC RNA for both Ras and control cells was determined using a linear curve fit analysis. For Ras cells the analysis was extended out to 20 hours and the approximate half-life was derived by extrapolating the fit to axis.

Results

Translation initiation in Ras12V cells

eIF4E is the least abundant translation initiation factor in the cell, hence over-expressing eIF4E can result in changes in global protein synthesis (Mamane et al., 2004). Over-expression of eIF4E has been shown to increase translation of RNAs such as ODC that are in general inefficiently translated (Rousseau et al., 1996; Shantz et al., 1996b). To determine if increased ODC synthesis correlates with increased levels of eIF4E, both total and phosphorylated levels of eIF4E were measured in Ras12V cells compared to RIE-1 controls and were found to be increased in Ras12V cells at 24 hrs and more so at 48 hrs of growth (Fig 3.1A). While levels of eIF4E correlate with the increase in ODC synthesis, it is more informative to analyze how the increased levels of eIF4E affect cap complex formation. eIF4E associates with eIF4G, which in turn recruits the helicase eIF4A to facilitate eIF4F cap complex formation to initiate translation (Gebauer & Hentze, 2004). The cap complex formation is limited by the levels of 4EBP1 bound to eIF4E, as hypophosphorylated 4EBP1 competes with eIF4G to bind to eIF4E, resulting in inhibition of translation (Gingras et al., 2001). Though the overall levels of 4EBP1 were increased in Ras12V cells, phosphorylation levels of 4EBP1 were also enhanced (Chapter II Fig 2.6B), suggesting that increased levels of eIF4E could result in increased cap-complex formation.

Immunoprecipitation of eIF4E revealed the expected increase in eIF4E levels in Ras12V cells compared to controls, as observed with immunoblot analysis of whole cell extracts at 24 hrs of growth (Fig 3.1 A, B). Ras12V cells exhibited an increase in the

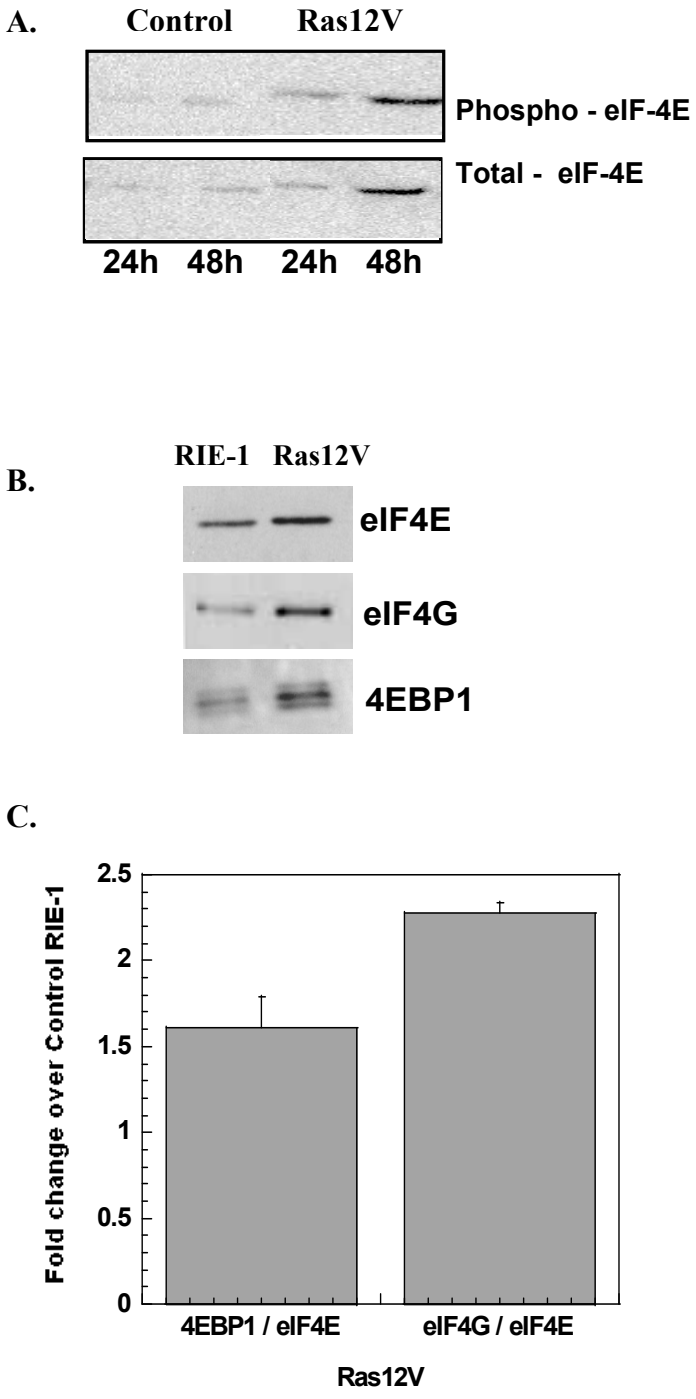

Figure 3.1. Translation initiation in response to activated Ras

See next page for figure legend

Figure 3.1. Translation initiation in response to activated Ras

(A) Increase in translation initiation was determined by measuring total and phosphorylated levels of eIF4E. Western blot analysis on cells extracted at 24 and 48 hrs of growth was carried out as described in Methods. 20ug of total protein was loaded per lane and the experiment was repeated twice.

Immunoprecipitation (IP) of total eIF4E protein was performed as described in Methods. **(B)** On cells grown for 24 hrs, the levels of eIF4G bound to eIF4E and 4EBP1 bound to eIF4E were analyzed by immunoblot analysis. IP analysis using mouse IgG antibody was used as negative control (Results shown in Figure 3.17). **(C)** For graphical representation of IP results, ratio of levels of 4EBP1 to eIF4E and eIF4G to eIF4E was determined for both RIE-1 and Ras12V cells and the ratios calculated for Ras12V cells were expressed as a fold change over ratios calculated for RIE-1 cells**.**

association of 4EBP1 with eIF4E compared to controls. However this could partially be explained by the increased levels of 4EBP1 in these cells. There was a greater increase (2.3 fold) in the levels of eIF4G associated with eIF4E, suggesting an increase in the formation of cap complex in response to Ras activation (Fig 3.1 B, C). These results suggest that increased cap complex formation in Ras12V cells could contribute to the increase in ODC synthesis by stimulating the rate of translation initiation.

Polysome profiles of ODC RNA

To determine if the efficiency of ODC translation was increased in response to Ras activation, analysis of ODC polysome profiles was carried out using the sucrose gradient centrifugation technique (Fig 3.2 A, B). Ethidium bromide staining of formaldehyde-agarose gels showed that the RNA was intact and analysis of the 18S and 28S rRNA profile confirmed the efficient separation of individual ribosomal subunits 40S and 60S into fractions 3 and 4 and sedimentation of monosome and polysomes into fractions 5 through to 11 (Fig 3.3). Interestingly, polysome profiles revealed that rather than a shift in ODC RNA from lighter to heavier polysome fractions, an increase in the amount of RNA in the Ras12V cells was observed in comparison to the control RIE-1 cells (Fig 3.4 A, B). By normalizing the amount of ODC RNA in each fraction to the relatively stable levels of Cyclophilin RNA associated with polysomes in both Ras and RIE-1 cells, we observed a 5-fold increase in the levels of ODC RNA associated with the heavier polysomal fractions, especially fractions 9 through 11, in the Ras12V cells. These results suggest that rather than an increase in the rates of translation initiation, increased synthesis of ODC protein is contributed by the increase in the amount of RNA associated with the polysomes.

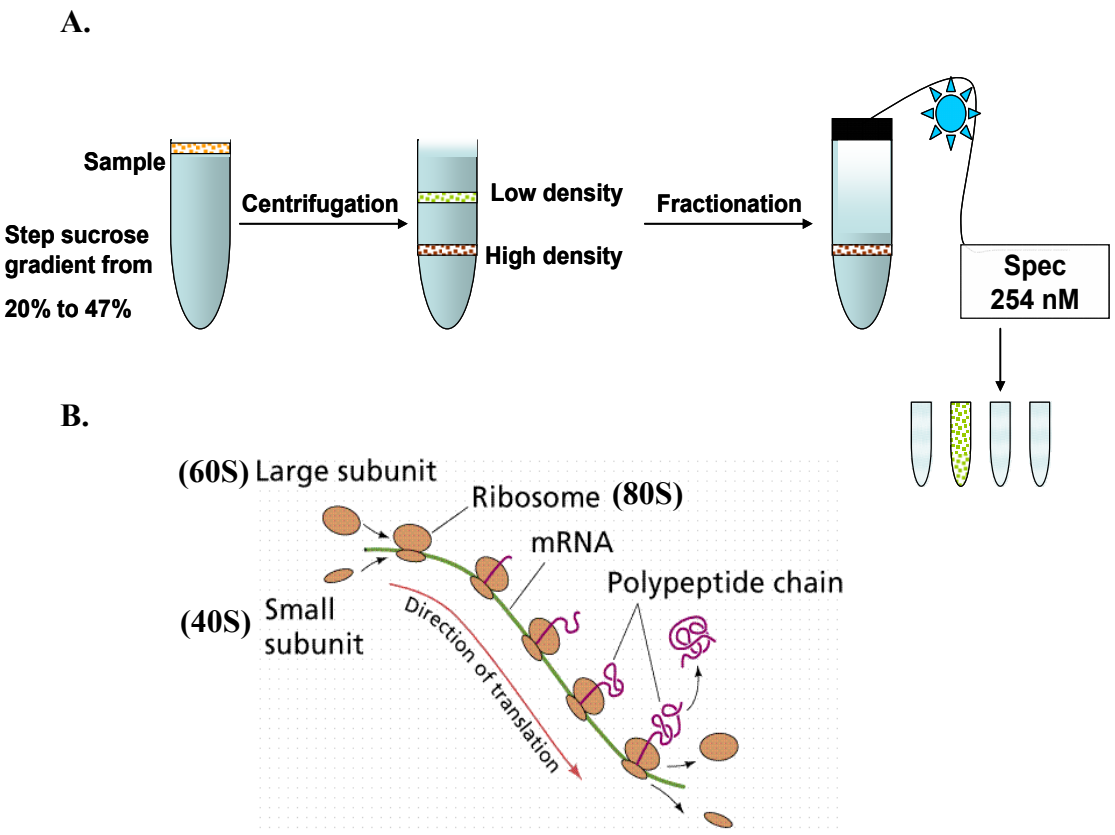

Figure 3.2. Schematic of sucrose gradient centrifugation technique to analyze polysomal association of RNA (**A.** Modified from - The cell: A molecular approach, 2nd edition, Geoffrey M.Cooper, **B.** Adpated from - Life: The science of biology, 4th edition, Sinauer associates).

(See next page for figure legend)

Figure 3.2. Schematic of sucrose gradient centrifugation technique to analyze polysomal association of RNA

(A) To sediment ribosomes based on density, samples are loaded onto sucrose gradients and centrifuged at high speeds such that the heavier density polysomes would sediment at the base of the gradient and individual ribosomal subunits of lighter density would sediment close to the top. Fractions are then collected, as the gradient profile is read at UV absorbance (254nM) and total RNA is extracted from each fraction.
(B) The number of ribosomes that associate with the RNA depends on the rates of initiation and elongation and also on the length of the RNA. If the RNA of interest is associated with fractions containing individual ribosomal subunits (40S and 60S) or a monosome (80S) it suggests it is translated less efficiently as opposed to when the RNA is associated with the polysomal fraction.

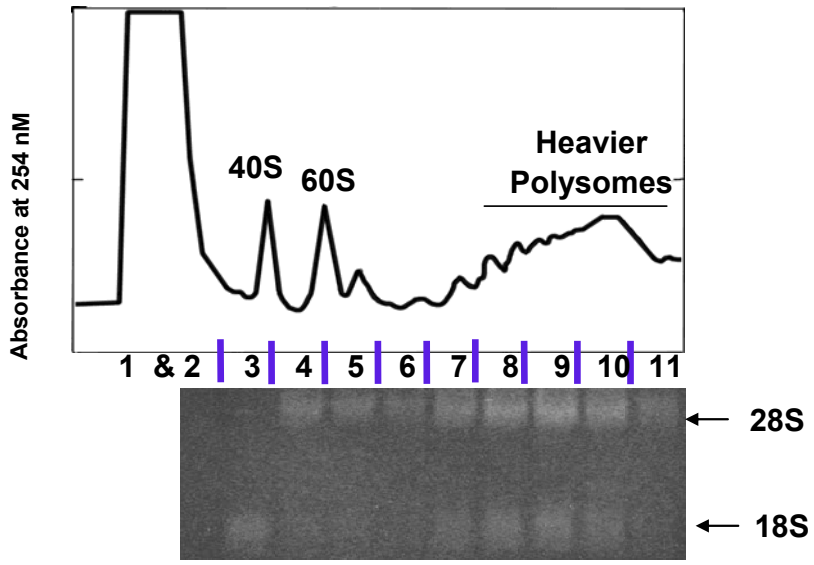

Figure 3.3. Analysis of separation of ribosomal subunits and integrity of polysomal RNA

Sucrose gradient centrifugation and polysome analysis of Ras12V cells was carried out as described in Methods. Eleven gradient fractions were collected and RNA was isolated from each fraction and analyzed on a 1.2% formaldehyde-MOPS agarose gel stained with Ethidium bromide. Equal volumes of total RNA were loaded for each fraction and the gel image shows total RNA corresponding to each fraction. Arrows indicate the position of the18S rRNA and 28S rRNA. Fraction 1 and 2 do not show any detectable levels of RNA as they represent the non-polysomal fraction. Only 18S rRNA is visible for fraction 3, suggesting that it consists predominantly of the 40S ribosomal subunit. Fraction 4 represents the 60S ribosomal subunit that consists mostly of 28S rRNA. Fractions 5 and 6 represent the 80S and disome fractions showing mostly 28S rRNA and faint levels of 18S rRNA. Fractions 7 through 11 represent the polysomal peak displaying similar levels of 18S rRNA in comparison to 28S rRNA.

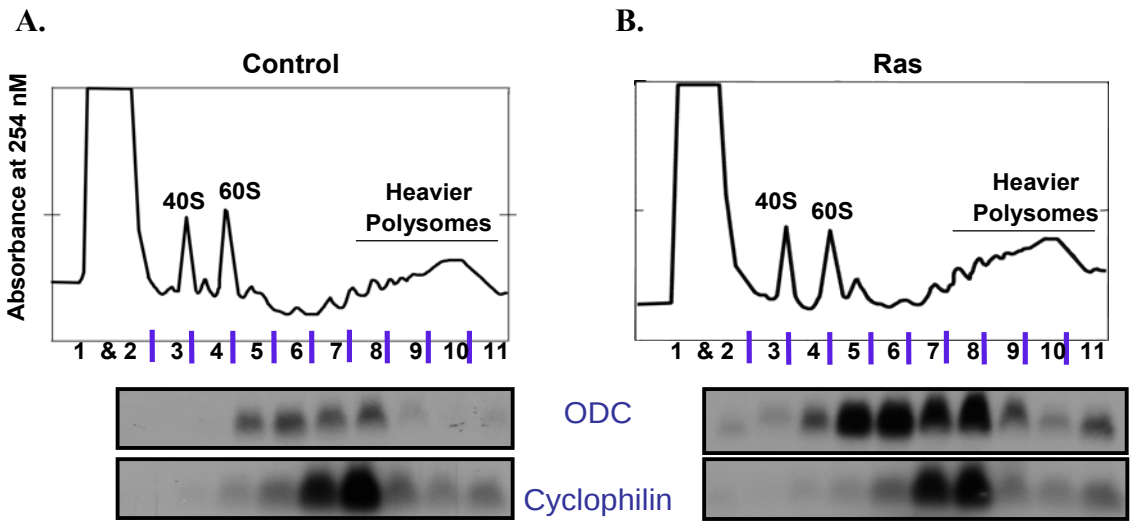

Figure 3.4. Analysis of polysomal association of ODC RNA

Polysomal analysis of ODC RNA was carried out in both **(A)** RIE-1 and **(B)** Ras12V cells as described in Methods. Equal volumes of RNA were loaded per lane and northern blots were probed with radiolabeled cDNA complementary to full length ODC and stripped and reprobed with cDNA complementary to Cyclophilin. Experiment was performed in duplicate and the results were consistent.

The observed increase in ODC RNA associated with polysomes could be explained by mechanisms such as increased transcription or nuclear export of ODC RNA, and increase in RNA stability or a combination of these mechanisms. ODC transcription rates as determined previously were only increased by 2-fold in Ras12V cells in comparison to the controls (Chapter II Fig 2.11). This 2-fold increase is probably not sufficient to explain the greater than 5-fold increase in ODC polysomal RNA, suggesting that additional regulatory mechanisms should exist. Next we compared levels of ODC RNA in the nucleus and cytoplasm. This revealed a mild increase in cytoplasmic levels of ODC RNA and a slight decrease in the nucleus of Ras12V cells in comparison to the controls (Fig 3.5). While the increase in cytoplasmic levels of ODC RNA can not be ignored, the mild increase likely represents only a minor contribution to the increase in polysomal levels of ODC RNA.

Regulation of ODC RNA stability by Ras

Next, we probed for any alterations in stability of ODC RNA induced by activated Ras. To measure stability of RNA, cells were treated with Actinomycin D (ActD) to inhibit transcription and RNA levels were measured every 2 hrs upto 8 hrs following ActD treatment. Interestingly, ODC RNA stability was dramatically different between Ras12Vand RIE-1 cells. After 4 hrs of ActD treatment, ODC RNA levels were reduced by 50% in RIE-1 cells with close to complete degradation by 8 hrs. In contrast in Ras12V cells the levels remained stable and were reduced only by about 15-20% even after 8 hrs (Fig 3.6 A, B, C). Such a drastic difference in ODC RNA stability between Ras and RIE-1 cells suggests that alterations in RNA stability play a key role in determining the increased levels of ODC RNA associated with polysomes in Ras12V cells. To further

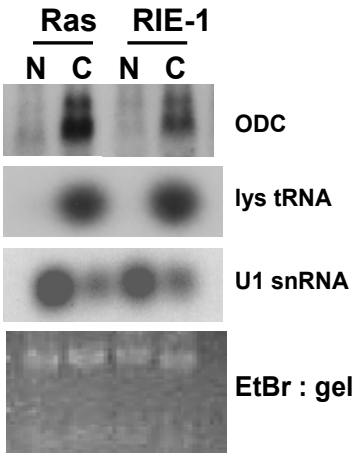

Figure 3.5. Analysis of localization of ODC RNA

Isolation of nuclear and cytoplasmic RNA from both Ras12V and RIE-1 control cells was performed as described in Methods. 20μg of total RNA was loaded per lane and the northern blot was probed with radiolabeled cDNA complementary to full-length ODC and lys-tRNA transcript (cytoplasmic marker). The same blots were stripped and reprobed for nuclear marker U1snRNA (enriched in nucleus). The ethidium bromide stained agarose gel (EtBr) used for northern analysis was also analyzed to ensure equal loading of RNA.

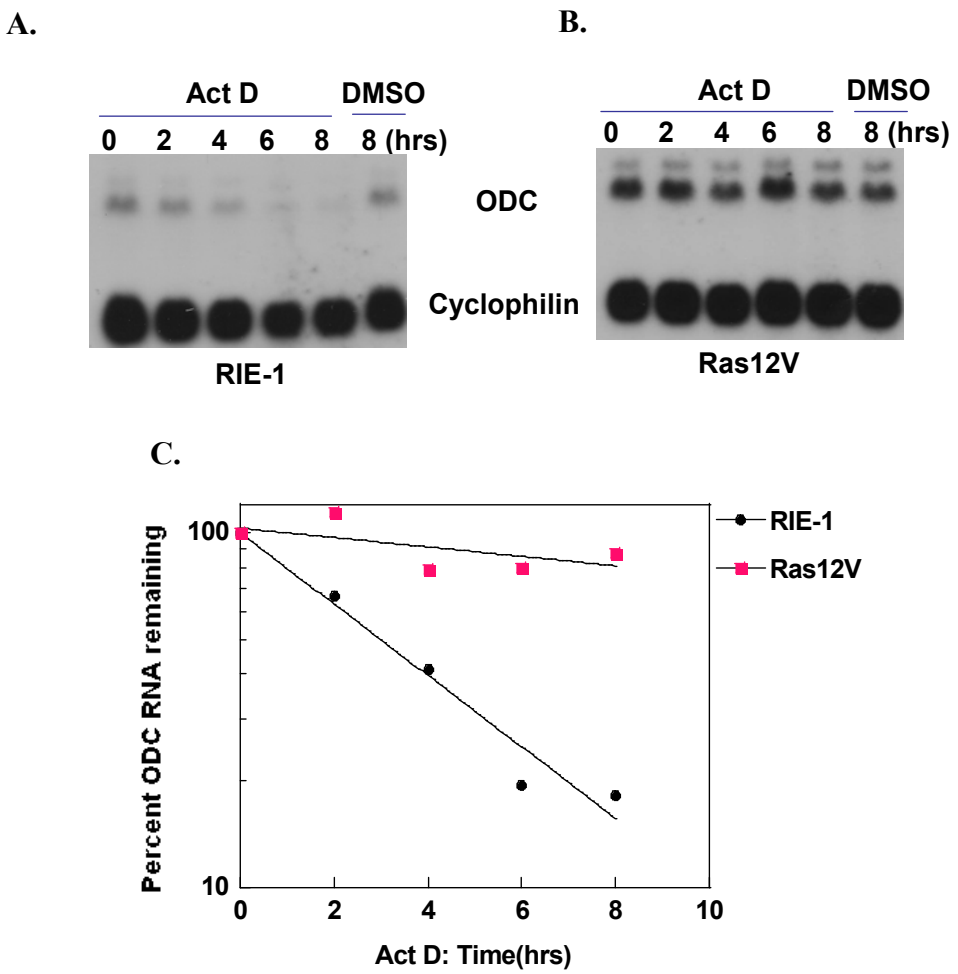

Figure 3.6. Stability of ODC RNA in RIE-1 and Ras12V cells

(A, B) To analyze stability of ODC RNA, cells were treated with either 5ug/ml Actinomycin D (ActD) or vehicle DMSO and, RNA was isolated immediately after addition of ActD at 0hrs and thereafter at 2, 4, 6 and 8 hrs and at 8hrs for DMSO treated cells. For northern analysis, 20µg of total RNA was loaded per lane and probed for ODC and Cyclophilin simultaneously. **(C)** Graph represents the percent of ODC RNA remaining at each time point of ActD treatment calculated with the amount of RNA at 0 hrs taken as 100%.

understand the role of Ras activated pathways in regulating ODC RNA stability, Ras12V cells were treated either with Rapamycin, an inhibitor of mTOR, or with PD98059, an inhibitor of MEK. Relative to the DMSO (vehicle) and PD98059 treated cells, Rapamycin had the greatest effect on ODC RNA stability reducing the RNA levels to 35-40% following 8 hrs of ActD treatment (3.7 A, B). However, Rapamycin treatment did not affect ODC RNA turnover to levels observed in RIE-1 cells suggesting that apart from mTOR other undetermined factors or pathways contribute to the regulation of ODC RNA stability.

A previous report has shown that in serum deprived cells ActD can increase the activity of p70S6K, which was associated with increased translation of TOP mRNAs such as translation elongation factors and ribosomal proteins (Loreni et al., 2000). It is therefore possible that the effects of Rapamycin on ODC RNA stability are in fact an experimental artifact resulting from inhibition of p70S6K activation induced by ActD treatment. To address this possibility we analyzed the phosphorylated levels of p70S6K in Ras12V cells treated with ActD for 4 and 8 hrs and found no increase in activation p70S6K. This suggests that destabilization of ODC RNA by Rapamycin is not an experimental artifact (Fig 3.7 C).

Further confirmation of regulation of ODC RNA turnover by the PI3K/mTOR pathway was obtained by polysome analysis of Ras12V cells treated with Rapamycin for 24 hrs (Fig 3.8 A, B). Total levels of ODC RNA associated with polysomes were greatly reduced in response to 24h of treatment with Rapamycin compared to the DMSO treated controls (Fig 3.8 A, B). This prolonged treatment of Ras12V cells with Rapamycin also caused an overall decrease in the levels of 40S, 60S, and 80S ribosomal subunits and in

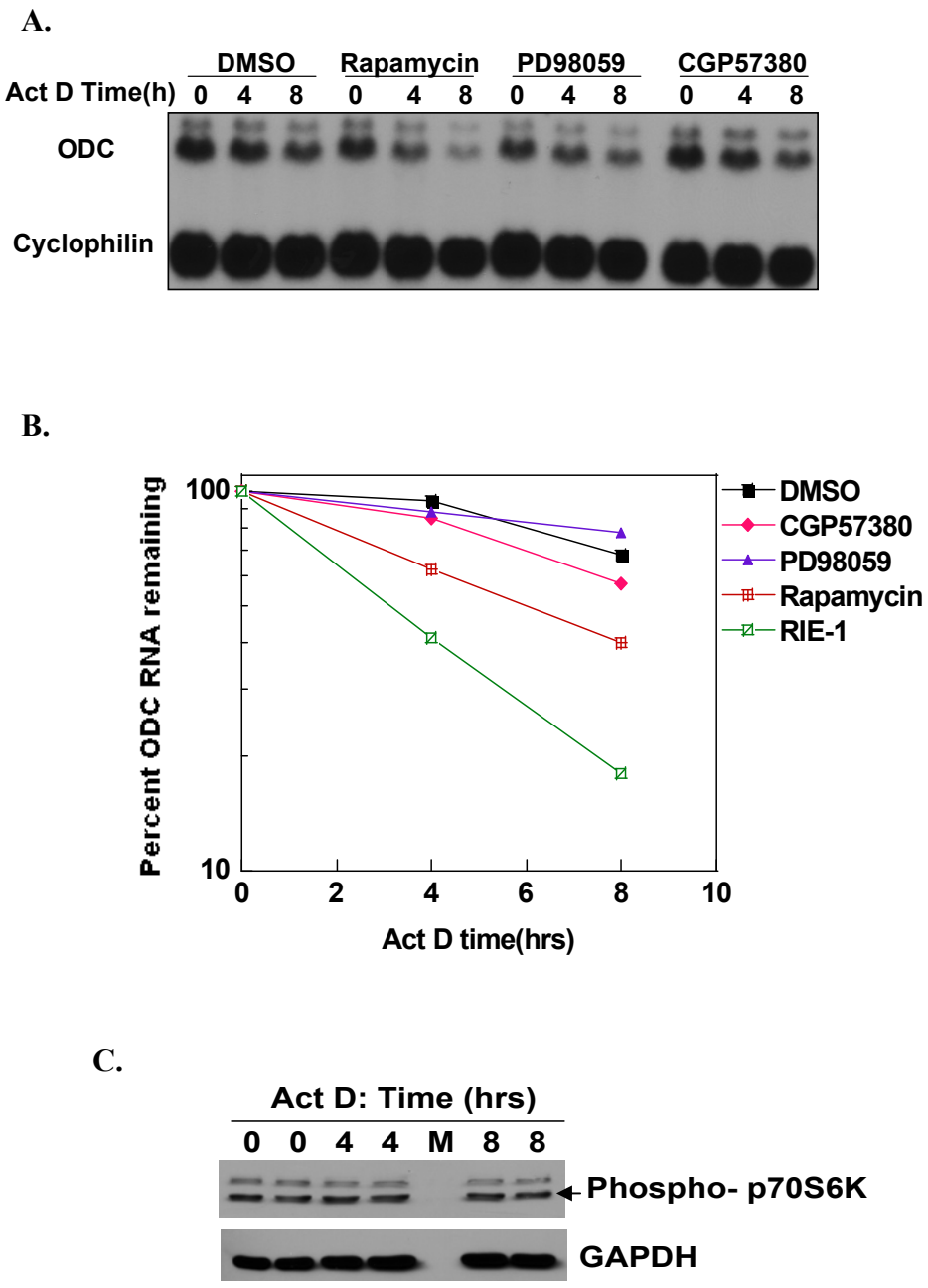

Figure 3.7. Regulation of ODC RNA stability by Raf-MEK-ERK and PI3K/mTOR pathways (see next page for figure legend)

Figure 3.7. Regulation of ODC RNA stability by Raf-MEK-ERK and PI3K/mTOR pathways

(A) Stability of ODC RNA was analyzed as described in figure 3.6, except inhibitors 100nM Rapamycin, 50uM PD98059, 20uM CGP57380 and vehicle DMSO were added directly to the plates 24 hrs before the addition of ActD, and RNA was collected immediately after addition of ActD at 0hrs and 4 and 8 hrs later. **(B)** Graph represents the quantitation of ODC RNA band and represents the average of two experiments.

(C) At 0, 4 and 8hrs of ActD treatment, cells were extracted and analyzed for phosphorylated p70S6K expression and GAPDH (loading control) using western blot analysis as described in Methods. M represents the lane containing a pre-stained protein marker. The experiment was performed in duplicate.

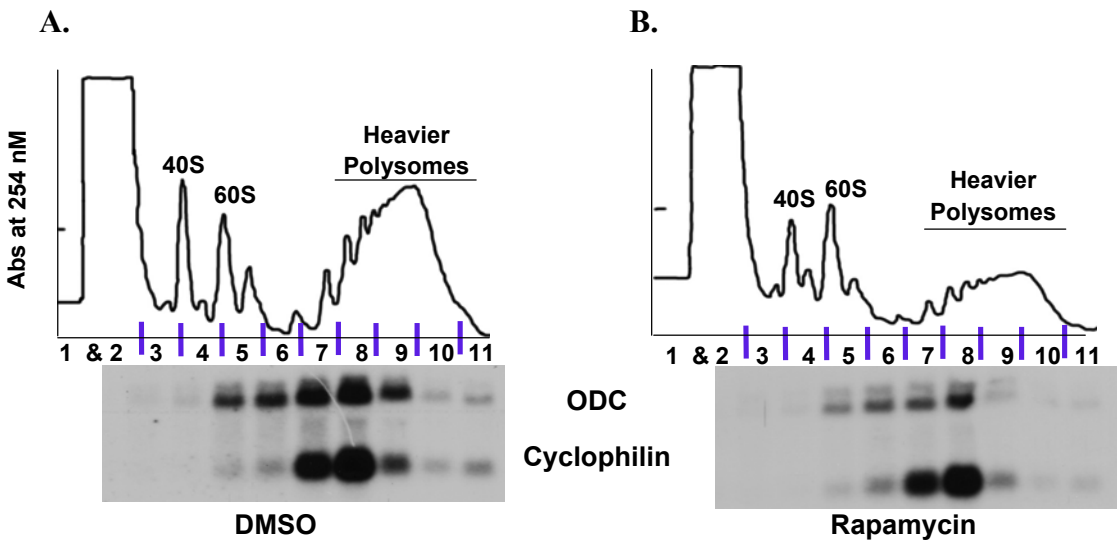

Figure 3.8. Regulation of polysomal association of ODC RNA by PI3K/mTOR pathway

Polysome analysis was performed as described in Methods except Ras12V cells were treated for 24 hrs with either vehicle **(A)** DMSO or (**B)** 100nM Rapamycin (added directly to the plates). Northern blots were probed for ODC and Cyclophilin RNA simultaneously and the experiment was repeated twice.

the polysome peak as determined analytically from polysome profiles (Fig 3.8 A, B). This is consistent with previous reports that inhibition of mTOR inhibits translation of ribosomal proteins themselves such as ribosomal proteins S6, S4, S14, S24 (Terada et al., 1994) and that mTOR when activated regulates ribosome biogenesis by activating the Forkhead like transcription factor (Martin et al., 2004). This could also possibly explain the slight decrease in the levels of Cyclophilin associated with polysomes (Fig 3.8 A, B). However, the effects of Rapamycin are much more pronounced on the polysomal levels of ODC RNA suggesting that the PI3K/mTOR pathway specifically regulates ODC translation through changes in stability of ODC RNA.

One potential target of mTOR that has been shown to be essential for maintaining stability of CyclinD1 and Myc is Tristetraprolin (TTP) (Marderosian et al., 2006). TTP presents an attractive target as it has been shown to destabilize RNAs by binding to specific AU rich elements in their 3'UTR and has been shown to accumulate in response to Rapamycin (Marderosian et al., 2006). Interestingly, examination of TTP levels exhibited a strong correlation with the ODC RNA stability results obtained in our study. In Ras12V cells, ODC RNA is quite stable when compared to RIE-1 cells and this correlates with the levels of TTP, which are much lower in these cells than RIE-1 cells (Fig 3.9). Treatment with Rapamycin renders ODC RNA less stable although not as unstable as seen in RIE-1 cells, and this also correlates with the level of TTP induced by Rapamycin, but again not as much as that observed in RIE-1 cells (Fig 3.9). These results support the idea that TTP plays a role in destabilizing ODC RNA.

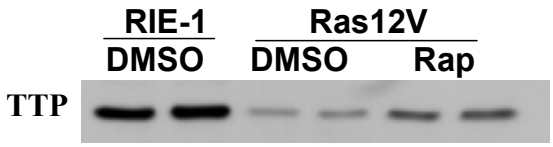

Figure 3.9. Correlation of destabilization of ODC RNA with TTP levels

Levels of the RNA destabilizing factor TTP were measured in whole cell extracts of RIE-1 and Ras12V cells treated with DMSO. Ras12V cells were also treated with 100nM Rapamycin (Rap) added directly to the plates and incubated for 24 hrs of growth. 30μg of total protein was loaded per lane and duplicate samples were examined using western blot analysis as described in Methods. Results were confirmed by performing the experiment in duplicate.

Regulation of ODC translation by phosphorylation of eIF4E

In response to Ras activation, RIE-1 cells exhibit an increase in both total and phosphorylated levels of eIF4E (Fig 3.1A). While there is sufficient evidence to suggest that over-expressing eIF4E induces ODC translation, not much is known about the specific role of eIF4E phosphorylation in regulating ODC activity. We utilized an inhibitor of Mnk1/2, CGP57380 to understand the effect of inhibiting eIF4E phosphorylation on ODC synthesis. Mnk is the kinase that phosphorylates eIF4E and has been shown to be activated by the Ras-activated Raf-MEK-ERK pathway (Waskiewicz et al., 1997). 20 μM of CGP57380 was effective in inhibiting eIF4E phosphorylation without affecting the total eIF4E levels and also did not result in any feedback activation of ERK (see Chapter IV- Fig 4.8 B, C). CGP57380 reduced ODC activity in Ras12V cells by about 25% within 2 hrs of treatment in comparison to the DMSO treated cells and its effect at 2 hrs of treatment was more potent in comparison to both the MEK inhibitor PD98059 and Rapamycin (Fig 3.10A). However, after 24 hrs of treatment the CGP57380 reduced ODC activity by more than 50% (Fig 3.10B) and this inhibition was very similar to the treatment with PD98059 and Rapamycin for 24 hrs (Chapter II Fig 2.7A). Inhibition of Mnk also resulted in a similar inhibition of ODC activity in 4E-P2 cells (Fig 3.10C), which are transformed by over-expression of eIF4E (these cells are described in more detail in Chapter IV). These results suggest that dephosphorylation of eIF4E inhibits ODC activity but other factors contribute to the elevated ODC in the Ras12V cells as the levels of ODC activity remaining after CGP57380 treatment are still higher than the activity measured in RIE-1 cells (see Chapter II Fig 2.3A).

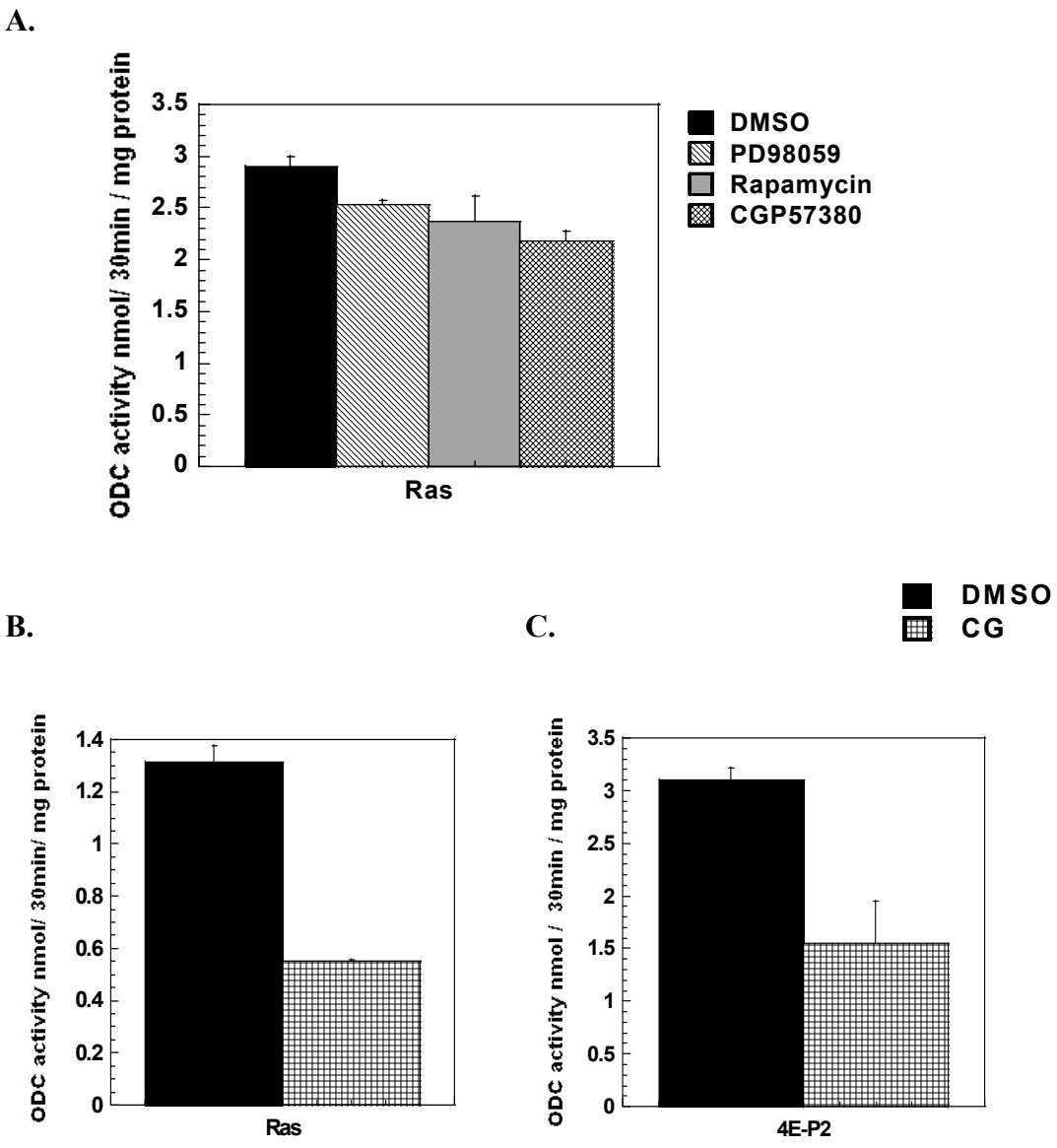

Figure 3.10. Effect of eIF4E-phosphorylation on ODC activity

(A) Ras12V cells were treated for 2hrs with DMSO or with inhibitors 20 μM CGP57380, 100nM Rapamycin, or 50 μM PD98059 (added in fresh media) and ODC activity was measured as described in Methods of chapter II. ODC activities were also measured after a prolonged treatment of 24 hrs with DMSO or 20 μM CGP57380 (CG) in **(B)** Ras12V and **(C)** 4E-P2 cells.

To determine if increased phosphorylation of eIF4E induces ODC synthesis by increasing the transcription levels, Ras12V cells were co-transfected with a vector expressing Firefly luciferase derived from ODC promoter and a renilla luciferase expression plasmid, used as a normalization control. ODC promoter activity was not significantly affected by treatment with CGP57380 for 24 hrs in comparison to the DMSO treated controls (Fig 3.11). Alterations in ODC RNA stability were also determined as described previously. Treatment with CGP57380 for 24 hrs slightly reduced ODC RNA stability in comparison to the DMSO treated controls but the effect was minimal in comparison to Rapamycin (Fig 3.7A, B). Also, total ODC RNA levels as observed in comparisons between DMSO and CGP57380 at 0 hrs of ActD treatment were found to be similar (Fig 3.7A, B). These results suggest that dephosphorylation of eIF4E does not affect rates of ODC transcription and has only a minor effect on ODC RNA stability.

We then wished to determine whether eIF4E phosphorylation affects translation of ODC using polysome analysis. Interestingly, treatment of Ras12V cells with CGP57380 for 2 hrs caused a significant and reproducible shift in ODC RNA from the heavier polysomal fractions to the lighter polysomal fractions in comparison to the DMSO treated controls (Fig 3.12A, B). Quantitation of ODC RNA levels associated with the polysomes demonstrated a dramatic shift in ODC RNA from fractions 9, 10, and 11 into fractions 6, 7, 8 (Fig 3.14A). However, treatment with CGP57380 for 2 hrs did not affect the levels of Cyclophilin RNA associated with the polysomes, suggesting that dephosphorylation of eIF4E specifically inhibits translation of ODC (3.12A, B and 3.14B). Since eIF4E dephosphorylation has also been shown to inhibit translation of

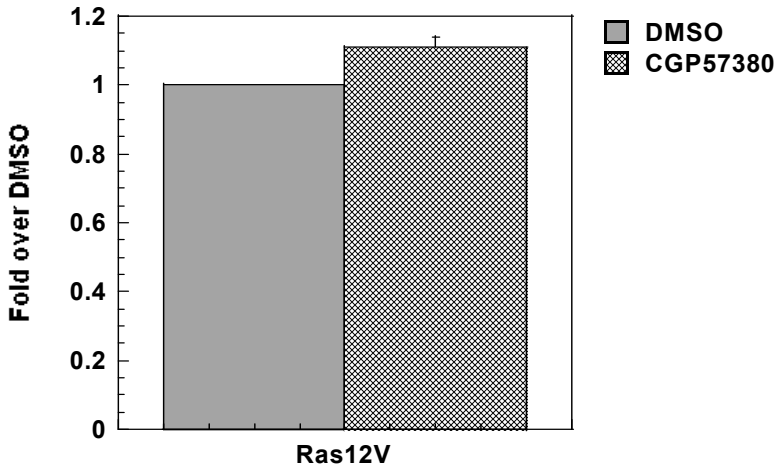

Figure 3.11. Effect of inhibiting eIF4E phosphorylation on ODC promoter activity

Ras12V cells were co-transfected with the PGL3-pODC vector expressing Firefly luciferase derived from the ODC promoter and with pRL-SV40 vector expressing Renilla luciferase (control for transfection efficiency). Transfected cells were treated for 24 hrs with either DMSO or 20 μM CGP57380 and the inhibitors were added directly to the plates. Luciferase activities were measured as described in the Methods of chapter IV. Graph represents fold change in ODC promoter activity compared to DMSO treated cells, measured by normalizing Firefly luciferase activity to renilla luciferase activity. Triplicate samples were measured for each experiment and the experiment was repeated twice.

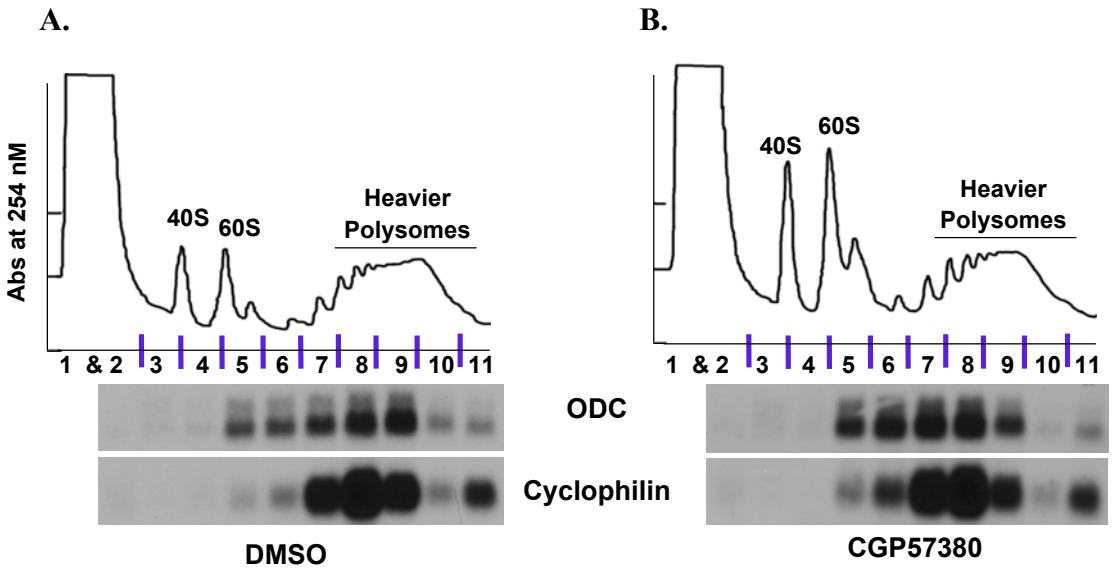

Figure 3.12. Effect of eIF4E phosphorylation on polysomal association of ODC

Ras12V cells were treated for 2hrs with either **(A)** DMSO or **(B)** 20 μM CGP57380 (added in fresh media) and polysome analysis was carried out as described in Methods. Northern blots were simultaneously probed for ODC and Cyclophilin RNA.

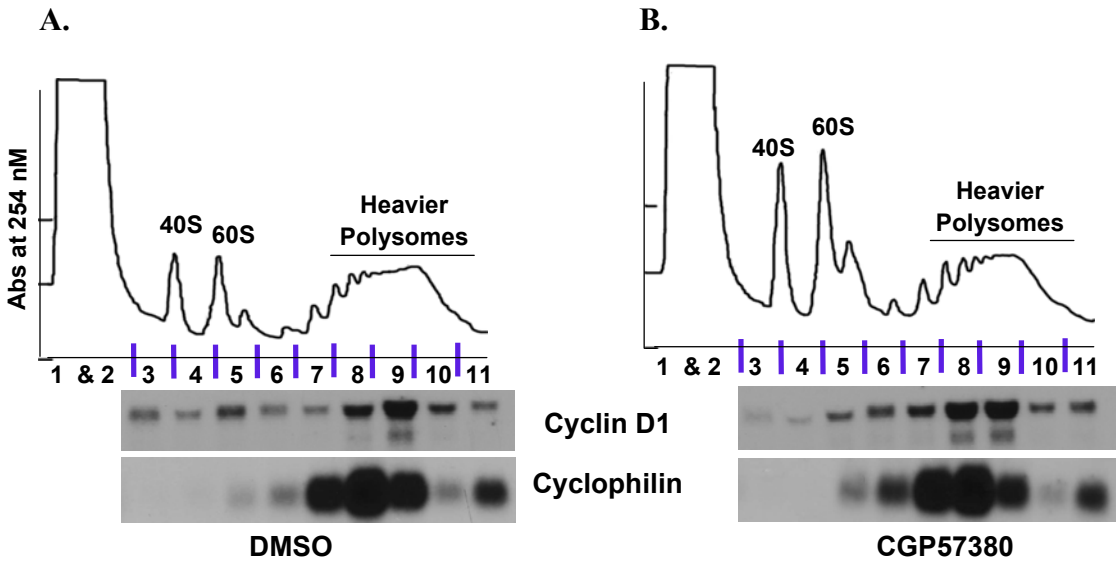

Figure 3.13. Effect of eIF4E phosphorylation on polysomal association of Cyclin D1

To analyze effect of **(B)** CGP57380 compared to **(A)** DMSO on Cyclin D1 translation, northern blots used in Figure 3.12 were stripped and reprobed for Cyclin D1 using a cDNA probe complementary to the 3'end of the Cyclin D1 transcript.

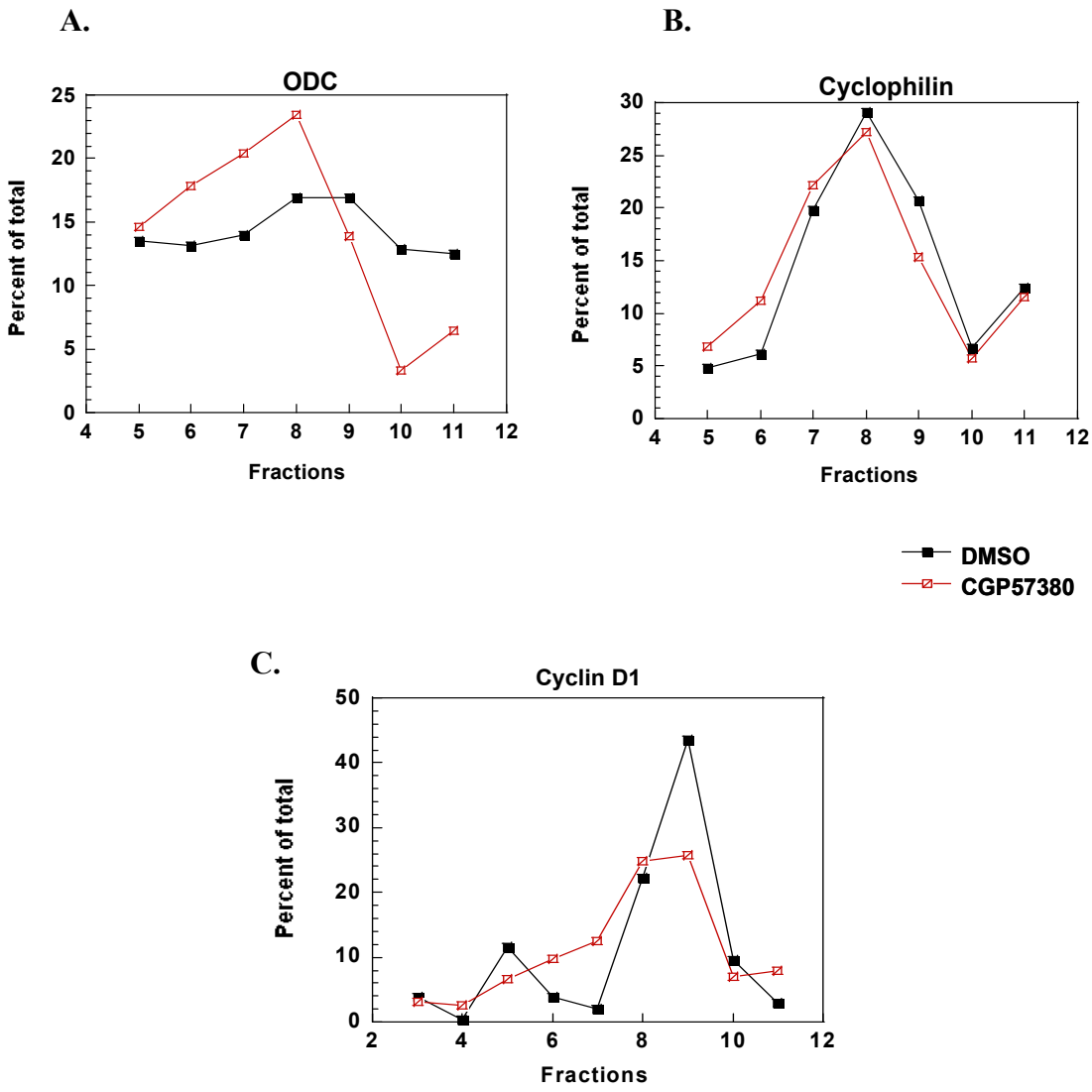

Figure 3.14. Effect of eIF4E phosphorylation on polysomal association of ODC and Cyclin D1

For graphical depiction of results in Figure 3.12 and 3.13, percent RNA in each fraction was determined by summing up the amount of **(A)** ODC, **(B)** Cyclophilin or **(C)** Cyclin D1 RNA in the 11 fractions and each fraction was represented as a percent of the total. Graphs represent a single experiment and the experiment was repeated twice with similar results.

Cyclin D1, we analyzed polysomal association of Cyclin D1 RNA in the presence of CGP57380. Unlike ODC RNA, only a single fraction shift of Cyclin D1 RNA from fraction 9 to fraction 8 was observed in comparison to the DMSO treated controls (Fig 3.13A, B & 3.14C). These results suggest that in the Ras12V cells, dephosphorylation of eIF4E does not affect translation efficiency of Cyclin D1, at least after 2 hrs of treatment with CGP57380.

It is noteworthy that treatment with CGP57380 affected the overall polysome profile as determined from the absorbance at 254 nM. Compared to the DMSO treated controls, peaks corresponding to 40S, 60S and 80S ribosomal subunits were induced in response to Mnk inhibition without much effect on the polysomal peak (Fig 3.12 A, B). However, treatment with CGP57380 for 2 hrs had only a mild effect on global protein synthesis rates, as measured by incorporation of S^{35}-Methionine into protein (Fig 3.15). This is consistent with the observation that CGP57380 does not affect polysome profiles of Cyclophilin.

Surprisingly, treatment with Rapamycin for 2 hrs barely affected translation efficiency of ODC (Fig 3.16 A, B) and also had no effect on global protein synthesis (Fig 3.15). In contrast, treatment with Rapamycin for a prolonged time for 24 hrs affected the levels of ODC RNA associated with the polysomes (Fig 3.8). However, 2 hrs of Rapamycin treatment did inhibit translation of one of the TOP RNAs EF1A (Elongation factor 1 alpha) by causing a shift in EF1A RNA from the polysomal fractions to sub and non polysomal fractions (Fig 3.17 A, B) suggesting that the Rapamycin was having the desired effect on its target genes in Ras12V cells. These results confirm the previous observations that Rapamycin does not regulate ODC synthesis by affecting its translation

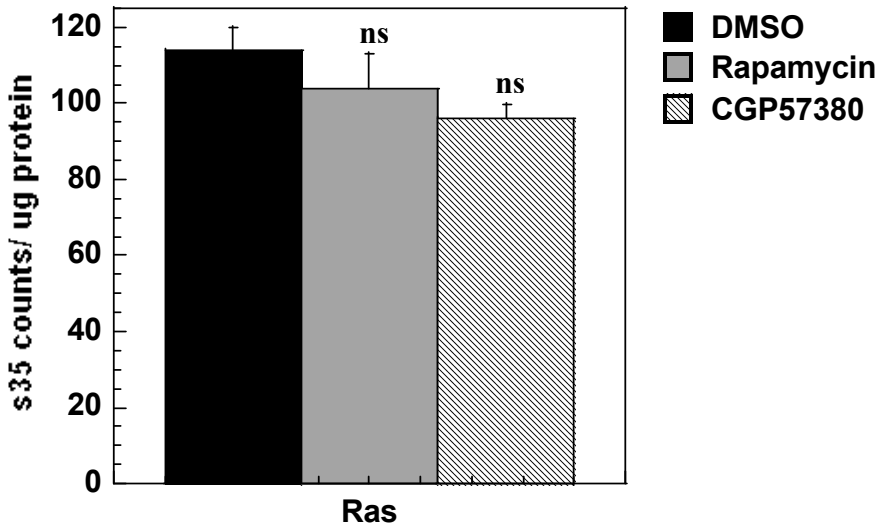

Figure 3.15. Effect of eIF4E phosphorylation and PI3K/mTOR pathway on global protein synthesis

Ras12V cells were treated with either DMSO or 100nM Rapamycin or 20 μM CGP57380 for 2hrs (added in fresh media) and global protein synthesis rates were determined by incorporation of S^{35}-Methionine into protein during the last 30 min of treatment as described in Methods. Graph y-axis represents S^{35} counts measured per μg of total protein. Triplicate samples were analyzed for each treatment and the experiment was repeated twice. Difference between DMSO and Mnk inhibitor treatment and Rapamycin was found to be ns = not significant as determined using a two-tailed T-test.

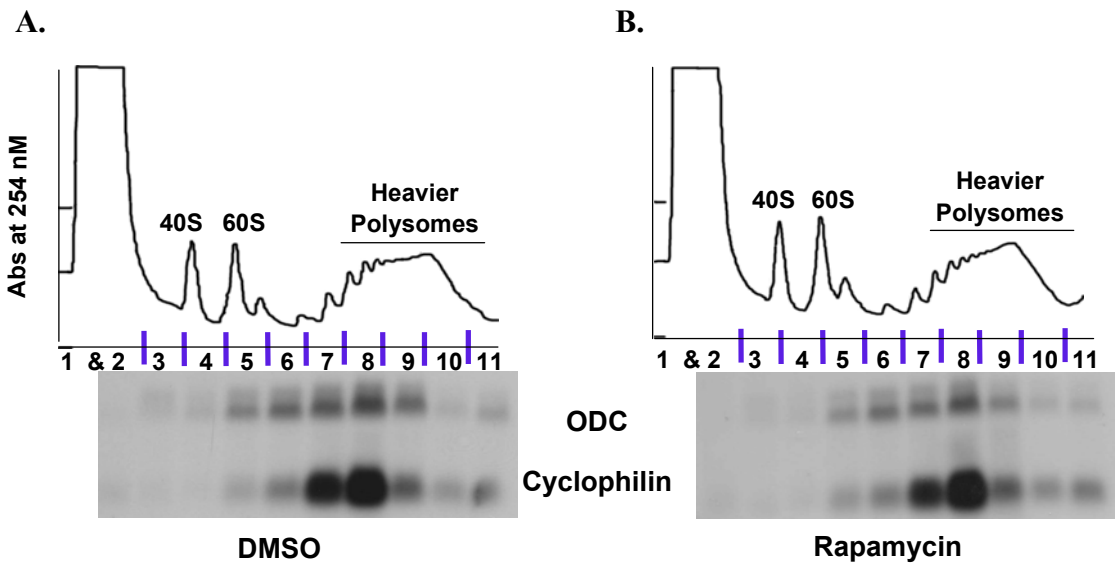

Figure 3.16. Effect of PI3K/mTOR pathway on translation initiation of ODC

Ras12V cells were treated with either **(A)** DMSO or **(B)** 100nM Rapamycin for 2 hrs (added in fresh media) and polysome analysis was carried out as described in Methods. Northern blots were simultaneously probed for ODC and Cyclophilin. The experiment was performed in duplicate.

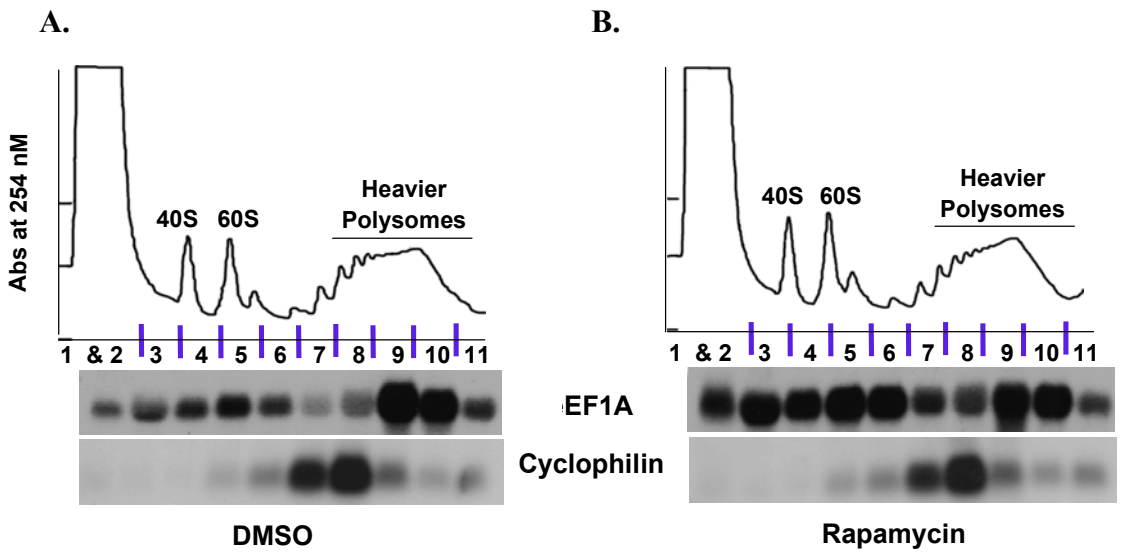

Figure 3.17. Effect of PI3K/mTOR pathway on translation initiation of EF1A

Northern blots used in Figure 3.16 were stripped and reprobed for EF1A in **(A)** DMSO treated and **(B)** Rapamycin treated Ras12V cells.

efficiency but rather by affecting ODC RNA stability.

One puzzling question remains as to how dephosphorylation of eIF4E can inhibit ODC translation? To understand the mechanism we compared the effects of CGP57380 and Rapamycin on interactions between the inhibitor of translation initiation 4EBP1 and eIF4E and interactions between eIF4G with eIF4E. Rapamycin as expected increased the association of 4EBP1 with eIF4E as assayed by IP analysis of eIF4E (Fig 3.18A, B) and by m7GTP sepahrose chromatography analysis (Fig 3.18C). IP analysis also revealed a decrease in the association of eIF4G with eIF4E, suggesting that Rapamycin does inhibit cap complex formation in the Ras12V cells (Fig 3.18A). However, CGP57380 did not affect association of 4EBP1 with eIF4E (Fig 3.18B, C) or eIF4G with eIF4E (Fig 3.18B), suggesting that the dephosphorylation of eIF4E does not affect translation by inhibiting cap complex formation in Ras12V cells. Hence the mechanism involved in regulation of ODC synthesis by the phosphorylation status of eIF4E still remains elusive.

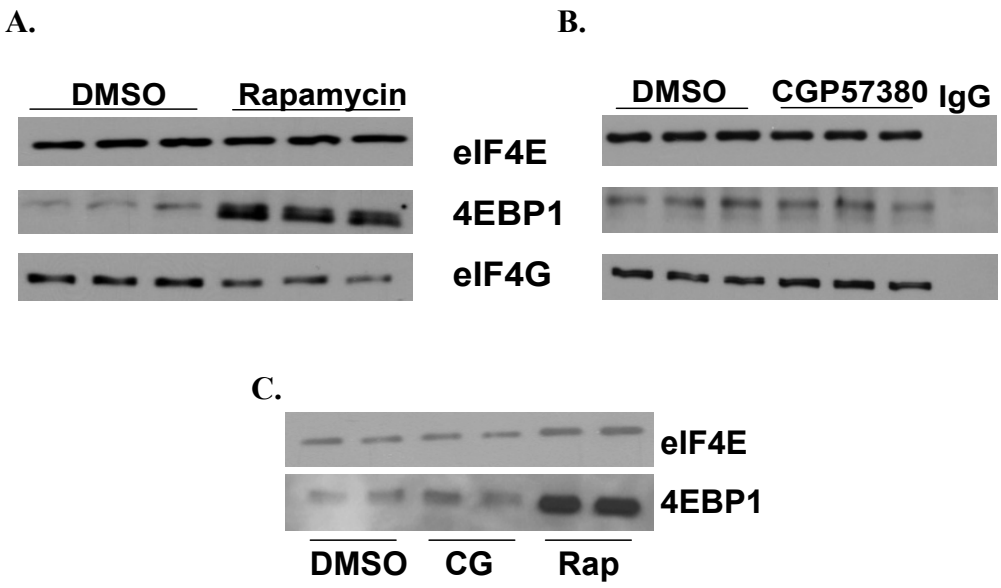

Figure 3.18. Effect of eIF4E phosphorylation and PI3K/mTOR pathway on formation of the cap-complex

Ras12V cells were treated with either DMSO or 100nM Rapamycin (Rap) or 20 μM CGP57380 (CG) for 2hrs (added in fresh media) and subjected to either **(A, B)** IP analysis or **(C)** m7GTP sepharose chromatography. **(A, B)** Using IP of total eIF4E, amount of 4EBP1 or eIF4G associated with eIF4E was determined by western blot analysis. **(C)** m7GTP sepharose chromatography was performed as described in Methods and the amount of eIF4E or 4EBP1 associated with the m7GTP cap was analyzed by a western blot. **(B)** IP analysis using mouse IgG served as a negative control.

Discussion

In response to constitutive activation of Ras, ODC activity is induced 20-fold in the RIE-1 cells; however there is only a 2-fold increase in transcription and about a 2-fold increase in the stability of ODC protein, suggesting that ODC synthesis must be predominantly regulated by a translational mechanism. The complex secondary structure and the increased length of the 5'UTR of ODC RNA makes it an ideal target for translational regulation, and indeed ODC is poorly translated under normal conditions (Shantz & Pegg, 1994). However, in cells transformed by over-expressing the cap binding factor eIF4E (4E-P2 cells), ODC RNA exhibits a shift from the lighter to heavier polysomal fractions and its activity is induced, suggesting ODC is efficiently translated in these cells (Rousseau et al., 1996; Shantz et al., 1996b). Since the Ras12V cells exhibit increased levels of eIF4E we wished to determine if translation is the predominant regulator of ODC synthesis using polysome analysis.

Interestingly, polysome profiles revealed that Ras increases translation of ODC in Ras12V cells by increasing the levels of ODC RNA associated with polysomes rather than an increase in translation initiation (in spite of the increased levels of eIF4E). Notably, increased association of ODC RNA with polysomes (2-fold) was also observed in 4E-P2 cells and it was attributed to a 25% decrease in nuclear localization of ODC RNA (Rousseau et al., 1996). However in Ras12V cells, nuclear localization of ODC RNA was decreased only mildly (Fig 3.5), and the levels of ODC RNA associated with the polysomes was increased by more than 5-fold (Fig 3.4) This suggests that Ras must regulate the polysomal levels of ODC RNA by other mechanisms such as alterations in stability of ODC RNA. Indeed, we found that ODC RNA stability was increased by Ras

to a large extent in our system. Even after 8 hrs of ActD treatment, only about 20% of the ODC RNA was degraded in Ras12V cells. Our present data suggests that in response to Ras, ODC RNA is markedly stabilized and is available to be recruited onto polysomes, resulting in increased ODC synthesis.

We found that the effect of Ras on ODC RNA stability is mediated at least partly by mTOR. Our results show that inhibition of mTOR reduces ODC synthesis by greater than 50% with no effect on ODC promoter activity. In addition, even though Rapamycin has the expected effect on the cap complex formation in the Ras12V cells it does not affect translation initiation of ODC RNA. Thus, unlike previous work in fibroblasts (Rousseau et al., 1996), we find that in an epithelial model that Ras-mediated induction of mTOR up regulates ODC synthesis by a novel mode of regulation involving stabilization of ODC RNA. Recent studies have shown that mTOR also affects the stability of RNAs such as Cyclin D1 and Myc in an AKT-dependent manner (Marderosian et al., 2006). Interestingly, ODC RNA belongs to the same class of RNAs as Cyclin D1 and Myc, as they are all characterized by a complex secondary structure in their 5'UTR and contain AU rich elements in their 3'UTRs (Lovkvist Wallstrom et al., 2001). It is possible that apart from translation initiation, regulation of ODC RNA stability is likely a common mechanism of regulation and may vary based on the physiological stimulus, since it has been shown that the degradation of Cyclin D1 and Myc RNAs is induced by Rapamycin only in cells containing active AKT (Marderosian et al., 2006). For instance, in cells over-expressing eIF4E such as 4E-P2 cells, ODC synthesis is induced by increased translation initiation, whereas under conditions where Ras is activated, resulting in an induction of a complex network of effectors including

AKT, ODC synthesis is predominantly regulated by RNA stability. To determine the contribution of increased RNA stability to overall ODC activity in Ras cells, we determined the half-life of ODC RNA approximately by extending out the analysis to 20 hours. Turn over rate of ODC RNA was found approximately to be 19 hrs in Ras cells, which is about 5.5 fold greater than the half-life of ODC RNA in control cells with a t1/2 = 3.5 hrs. The 5.5 fold increase in RNA stability and the 2-fold increase in transcription could be the predominant cause of the 20-fold increase in ODC activity in the Ras cells.

One noteworthy observation is that the levels of ODC RNA associated with the polysomes are increased by 5-fold, but this increase is not reflected by the total levels of ODC RNA. In response to Ras, total ODC RNA is increased only by 2-fold and can be explained by transcriptional activation by the Raf/MEK/ERK pathway, since treatment with the MEK inhibitor PD98059 reduced the total ODC RNA levels to control levels without significantly affecting ODC RNA stability. Also, treatment with Rapamycin increases the degradation of ODC RNA but does not affect the total ODC RNA levels. Finally, cytoplasmic localization of ODC RNA is not significantly altered by Ras activation, which puts forth the question as to why decreased degradation of ODC RNA and increased recruitment into polysomes is not reflected by the total RNA levels? One possible hypothesis is that ODC RNA is stored in cytoplasmic storage bodies called P-bodies (mRNA processing bodies) in RIE-1 cells and upon Ras transformation ODC RNA is released from these bodies to be recruited into polysomes. It is possible that our polysome analysis did not include P-bodies since the supernatant loaded onto the gradients was obtained by centrifugation of the whole-cell lysate at 10000 rpm for 10min rather than a careful separation of cytoplasm and nucleus.

Cytoplasmic P-bodies are sites for both RNA storage and RNA degradation via the deadenylation and decapping mechanism (Eulalio et al., 2007). Our hypothesis is based on a recent study in yeast, which showed that under translationally inhibited conditions such as the stationary growth phase, RNAs were stored in P-bodies. When translation was restored, RNA was recruited into polysomes from P-bodies, followed by a decrease in the number and size of P-bodies formed (Brengues et al., 2005). Since most of the P-body components are similar between yeast and mammalian systems, it was proposed that a similar mechanism of RNA storage may exist in mammalian systems (Brengues et al., 2005). To address this hypothesis in future experiments, the number of P-bodies formed and the localization of ODC RNA to P-bodies can be compared between Ras12V and RIE-1 cells and also in the presence of Rapamycin.

One question that still remains to be addressed is whether Ras activation typically induces ODC synthesis predominantly by increasing the RNA stability. It has been shown previously in NIH/3T3 fibroblasts that Ras transformation does greatly increase ODC RNA stability. However, the contribution of RNA stability to the overall synthesis of ODC protein was not analyzed (Holtta et al., 1988). To determine the contribution of changes in RNA stability to the overall synthesis of ODC, RNA binding factors that regulate ODC RNA stability must be identified and the functional consequence of their interactions determined. One potential target is TTP, as it can be activated by Rapamycin in an AKT- dependent manner and in turn binds to Cyclin D1 and Myc 3'UTRs to increase degradation of these RNAs (Marderosian et al., 2006). Also, over-expression of TTP specifically in Ras transformed fibroblasts functioned as a tumor suppressor by increasing degradation of RNAs such as IL-3 (Stoecklin et al., 2003).

Since TTP levels correlate with the status of ODC RNA stability in our cells, RNA-protein interaction studies should be carried out to determine if TTP binds to the AU rich motifs in the 3'UTR of ODC and regulates the stability of its RNA. One other potential target is HuR (HU-antigen R), an RNA stabilizing factor that has been shown to respond to polyamine levels (Zou et al., 2006). Our preliminary data analyzing the pull down of cytoplasmic lysates using biotin labeled RNA shows that HuR binds to both the 5' and 3'UTR of ODC in RIE-1 cells but not to the coding region (data not shown). It is also interesting to note that HuR has been reported to regulate IRES-mediated translation of p27 (Kullmann et al., 2002). Further analysis is being carried out to determine if the amount of HuR bound to ODC is regulated by Ras.

In conclusion, we have determined a novel mechanism of ODC regulation induced by Ras transformation involving alterations in RNA stability and this function of Ras is controlled through mTOR, which we show for the first time, can not only regulate initiation of ODC translation but also regulate stability of ODC RNA.

Effect of eIF4E phosphorylation on ODC translation

The role of the phosphorylation of eIF4E in mediating its functions as a translation initiation factor is a highly debated area of research (Scheper & Proud, 2002). Using the Mnk inhibitor CGP57380, our study for the first time shows that dephosphorylation of eIF4E inhibits ODC activity induced by Ras. Both total and phosphorylation levels of eIF4E are induced in these cells, and the induction of eIF4E is blocked by MEK inhibition suggesting that the Raf-MEK-ERK pathway is the predominant pathway activating Mnk and phosphorylating eIF4E (Fig 4.7). The effects of the Mnk inhibitor on ODC activity were comparable to the effects of inhibition of MEK.

While inhibiting MEK reduced ODC promoter activity, Mnk inhibition did not affect ODC promoter activity, total ODC RNA levels or ODC RNA stability, suggesting that inhibition of Mnk affects ODC synthesis solely at a translational level. Interestingly, polysome analysis of cells treated with CGP57380 revealed a shift in ODC RNA to the lighter polysome fractions, suggesting that dephosphorylation of eIF4E decreases translation efficiency of ODC. The effects of Mnk inhibition were specific for ODC as they did not affect translation efficiency of Cyclophilin and had only a minor effect on both Cyclin D1 translation and global protein synthesis rates. Previous studies showed that treatment of fibroblasts over-expressing eIF4E with CGP57380 decreased synthesis of Cyclin D1, which was attributed to the decreased transport of Cyclin D1 RNA from the nucleus to the cytoplasm (Topisirovic et al., 2004). Our polysome analysis did not reveal any decrease in the levels of Cyclin D1 RNA associated with the polysomes. However, the difference in results could be due to the oncogene used for transformation since our studies over-express Ras and in an epithelial cell context.

Our polysome analysis also revealed an increase in the 40S, 60S and 80S ribosomal subunits upon Mnk inhibition suggesting a possible disaggregation of polysome assembly. However, this did not have a significant effect on global protein synthesis. Similar results were observed in human kidney cells treated with CGP57380 (Morley & Naegele, 2002). Treated cells recovered from a hypertonic shock without any effects on protein synthesis but the polysome profiles did display a shift towards smaller polysomes, suggesting that dephosphorylation of eIF4E does affect polysome assembly (Morley & Naegele, 2002). Although these results have to be substantiated with further *in vitro* studies, they suggest that this slight impairment of polysome assembly is not

sufficient to affect global protein synthesis but may affect sensitive RNAs such as ODC that are in general inefficiently translated. The polysome profiles, along with the shift in ODC RNA to lighter polysomes in CGP57380 treated cells, suggest that dephosphorylation of eIF4E could affect the process of translation initiation. To determine if CGP57380 affected cap complex formation, we analyzed interactions between eIF4G and eIF4E as well as 4EBP1 and eIF4G. As reported earlier (Herbert et al., 2000; Saghir et al., 2001), we did not observe any effect of Mnk inhibition on their interactions, suggesting that dephosphorylation of eIF4E does not affect formation of the eIF4F complex. Further studies have to be carried out to determine what stage of protein synthesis is affected by the phosphorylation status of eIF4E.

Studies in Drosophila show that expression of a non-phosphorylatable mutant of eIF4E affects normal growth of the flies (Lachance et al., 2002). Studies in mammalian systems have left the significance of eIF4E phosphorylation an unresolved issue. While some studies suggest that phosphorylation of eIF4E has a negative effect on protein synthesis, possibly by decreasing its affinity for the cap (Knauf et al., 2001; Scheper et al., 2002), there are other studies suggesting that phosphorylation does not have any effect on global protein synthesis (McKendrick et al., 2001; Morley & Naegele, 2002; Ueda et al., 2004). Our results do suggest that dephosphorylation of eIF4E does not affect global protein synthesis. However, since ODC activity is specifically inhibited by CGP57380, our results also suggest that dephosphorylation of eIF4E affects synthesis of specific RNAs especially under transformed conditions. A previous study by Topisirovic et. al., showed that phosphorylation of eIF4E is needed for the transformation properties of eIF4E (Topisirovic et al., 2004). Since induction of ODC is also required with the

transformation properties of eIF4E (Shantz et al., 1996a), and our study shows that dephosphorylation of eIF4E inhibits ODC activity, it is possible that phosphorylation of eIF4E specifically induces translation of RNAs such as ODC to mediate transformation.

In conclusion, our results suggest that dephosphorylation of eIF4E specifically inhibits ODC synthesis by affecting its translation efficiency, without affecting global protein synthesis levels or cap complex formation under Ras transformed conditions. Using a non-phosphorylatable mutant of eIF4E or knocking down Mnk in future experiments may help shed further light on the mechanism involved.

.

Chapter IV

Effect of Ras activation on cap-independent translation of ODC

Specific Aim: To analyze if Ras activation stimulates cap-independent translation of ODC and to determine which Ras effectors regulate ODC IRES-mediated activity and the mechanism involved.

Introduction

Ras activation in response to growth factors, and constitutively active Ras mutants, induce ODC activity by a complex mechanism involving transcription, translation and changes in protein stability (Holtta et al., 1988; Shantz, 2004; White et al., 1987). While the contribution of each of these processes cannot be ruled out, previous studies suggest that ODC synthesis is regulated predominantly by translation, especially at the level of initiation (Graff et al., 1997; Rousseau et al., 1996; Shantz et al., 1996b). One of the early steps in translation initiation is the recognition of the m7GTP cap by the rate-limiting translation initiation factor eIF4E, which is part of the eIF4F cap-binding complex (Gebauer & Hentze, 2004; Gingras et al., 1999). The eIF4F complex also contains two other major factors, the eIF4G scaffolding factor and the RNA helicase eIF4A, which help recruit the ribosomal subunits to the 5'UTR of mRNAs to initiate translation (Gebauer & Hentze, 2004; Gingras et al., 1999) . Activation of Ras facilitates enhanced translation initiation by activating PI3K, which in turn activates Akt and mTOR to facilitate the phosphorylation of the eIF4E Binding Protein 4EBP1(Proud, 2004; Richter & Sonenberg, 2005). Hypophosphorylated 4EBP1 interferes with eIF4F complex formation by competing with eIF4G to bind to eIF4E, and thus inhibits translation initiation (Proud, 2004). Additionally, phosphorylation of eIF4E itself can be regulated by Ras through activation of the Mnk1/2 kinases, which are controlled by the Raf/MEK/ERK pathway (Waskiewicz et al., 1997). Although the defined role of eIF4E phosphorylation in regulating translation has yet to be defined, recent studies suggest that phosphorylation may play a significant role in the transformation properties of eIF4E (Topisirovic et al., 2004).

Translational regulation of ODC is unique, as it belongs to a special class of RNAs that possess very long and highly structured 5'UTRs that, in general hinder efficient translation (Shantz & Pegg, 1994). However, conditions that increase the presence of translation initiation factors such as eIF4E allow efficient translation of ODC, which is sufficient to maintain the transformed state, since inhibiting ODC in cells over-expressing eIF4E reverses their transformed phenotype (Rousseau et al., 1996; Shantz et al., 1996a). While translation via the cap is the predominant mode of ODC translation, under specific conditions such as the G2-M phase of the cell cycle or during apoptosis, ODC has been shown to be translated in a cap-independent manner (Pyronnet, 2000; Pyronnet et al., 2005). Cap-independent translation is well documented for viral RNAs that lack a cap structure and are translated efficiently by recruiting ribosomes directly onto regions within their 5'UTR termed Internal Ribosome Entry Sites (IRES) (Gallego, 2002; Jang et al., 1990). IRES-mediated translation has also been reported for several cellular RNAs important for cell growth, including Myc and cyclin D1 (Stoneley & Willis, 2004). ODC exhibits a biphasic induction of activity, once at the G1-S boundary and again at the G2-M phase of the cell cycle (Fredlund et al., 1995). Previous studies showed that ODC activity is increased during G2-M in spite of an overall inhibition of global protein synthesis, and ODC activity during this phase was not responsive to the effects of Rapamycin, which inhibits mTOR (Pyronnet, 2000). These results suggested that ODC activity during G2-M is regulated in a cap-independent manner.

Our studies for the first time analyze the effects of oncogenic Ras on ODC synthesis by cap-independent translational mechanisms. Ras activation enhanced IRES-mediated translational activity of ODC, which is regulated by both the Raf/MEK/ERK

and PI3K pathways. While the PI3K pathway regulates ODC IRES-mediated translation indirectly by altering cell-cycle progression, our studies also show that ODC IRES activity can be regulated independent of cell cycle changes through the Raf/MEK/ERK pathway. Moreover, such regulation hinges upon the phosphorylation status of eIF4E.

Materials and Methods

Screening for ODC 5'UTR splice variants

Total RNA was isolated using RNaqueous-4PCR kit (Ambion) from growing Ras12V and Control RIE-1 cells, and using the oligo (dT) primer cDNA was synthesized from 2 µg of total RNA as per the GC-rich Superscript^{tm} First-Strand cDNA synthesis kit instructions (Invitrogen). Four percent of the cDNA synthesized was then used in subsequent PCR amplification reactions. The ODC 5'UTR was cloned into the bicistronic plasmid pRΔEF between Renilla and Firefly luciferase reporters also containing an inactive EMCV sequence between the two reporters (a kind gift of Dr. P. Sarnow, Stanford University). The entire ODC 5'UTR was amplified from cDNA and using the following forward and reverse primers, EcoRI overhangs were introduced into the 5'end and 3'end of the ODC 5'UTR: (Forward- ODC6F: 5'-ATATGAATTCTGTCAGTCCTGCAGCCGCC- 3'; Reverse: ODC6R 5'-ATATGAATTCGGTTGGTTCTCGATGTGCC- 3'). Both the empty pRΔEF vector and the amplified ODC 5'UTR were then digested with EcoRI, ligated together and transformed into competent bacterial cells. Twenty bacterial clones for Ras12V and control cells were sequenced with a reverse primer Fluc01 (5'-GGCGCCGGGC CTTTCTTTATG- 3') complementary to the 5' end of Firefly luciferase to identify the presence of ODC 5'UTR in sense or antisense orientations. Sequencing also revealed the presence of four splice variants of 5'UTR in both the Ras12V and control cells of 273, 286, 290 and 303bp in length.

For transfection experiments, the entire bicistronic sequence with or without the four 5'UTR splice variants in the sense orientation between Renilla and Firefly luciferase were cloned into the pcDNA3.0 plasmid backbone. For each splice variant, the

bicistronic sequence from the pRΔEF plasmid described above was doubly digested with SacI and XbaI and the expected 4kb product was then gel-purified and digested further with NheI. The expected 3.4kb NheI and XbaI digested product was then gel purified and ligated with the empty pcDNA3.0 plasmid also digested with NheI and XbaI. A bicistronic sequence with the EMCV viral sequence(Carter & Sarnow, 2000), and a bicistronic sequence with the 303bp ODC 5'UTR variant in the antisense orientation were also cloned into the pcDNA3.0 plasmid to generate a positive and negative control, respectively.

Dual Luciferase assay and cell cycle analysis

For dual luciferase assays, 140,000 control RIE-1 cells, 160,000 Ras12V cells RIE-1 and 125,000 4E-P2 cells were plated per well of a 6-well plate and transfected with the pcDNA3.0 bicistronic plasmids using lipofectamine 2000 (Invitrogen). Twenty four hrs following transfection, cells were extracted in the passive lysis buffer (Promega) and assayed using the Dual-Luciferase kit (Promega). For inhibitor treatments, six hrs after transfection, the medium was replaced with DMEM supplemented with 10% FCS and treated with either the vehicle DMSO or 100nM Rapamycin, 20 μM LY294002, 50 μM PD98059, or 20 μM CGP57380. Twenty four hrs following transfection, cells were extracted as described above for luciferase assays or fixed in 70% ethanol, washed with PBS and stained with propidium iodide (Sigma) for flow-cytomteric analysis. Percent of cells in each phase of the cell-cycle was estimated using the ModFit software.

Western blot analysis

For analysis of p38 and eIF2-alpha levels cells were treated with 50 μM PD98059, 20 μM LY294002 and 100nM Rapamycin or 20 μM CGP57380 in serum free media for 2

hrs and western blot analysis was carried out as described in chapter II except that the blots were probed with antibodies against total and phosphorylated p38 MAPK, p38-delta and phosphorylated (ser51) eIF2-alpha, phosphorylated (ser209) and total eIF4E (Cell Signaling Technology). For apoptosis induction cells were treated with 1μM staurosporine (Sigma) and extracted in 4E-HB buffer at the indicated time points and probed with antibodies against PARP (Santa Cruz) and eIF4G (a kind gift of Dr. Scot Kimball, PSU).

Northern analysis, RT-PCR and promoter assay to analyze the integrity of the bicistronic transcript

To analyze the integrity of the bicistronic transcript, Ras12V cells were transfected with the bicistronic plasmids as described above and total RNA was isolated using the RNAqueous-4PCR kit (Ambion). 20 μg of total cellular RNA were separated on a 1.2% (w/v) agarose-formaldehyde gel, transferred to Hybond N+ membrane (Amersham Biosciences) and UV cross-linked using a Stratalinker (Stratagene). A Renilla Luciferase cDNA probe was PCR-amplified from the bicistronic plasmid on the pcDNA3.0 backbone using the forward primer 5'-GCTATGAGCATCAAGATAAGATC -3' and reverse primer 5'-GAGAACTCGCTCAACGAACG- 3'. The cDNA probe complementary to the 3' end of the Renilla Luciferase transcript was then radio labeled with P32 dCTP using the Rad prime DNA radiolabeling kit (Invitrogen) as per the manufacturer's instructions. Radiolabeled membranes were then developed by exposure to an X-ray film. For RT-PCR analysis the empty bicistronic pcDNA3.0 vector or the bicistronic pcDNA3.0 plasmid with the 303bp ODC 5'UTR was transfected into Ras12V cells and 24 h following transfection total RNA was isolated using the RNA isolation kit

(Ambion). cDNA was synthesized from 2 µg of total RNA as described above. A gene-specific reverse primer FFREV (5'-CAGAATGTAGCCATCCATCC -3') complimentary to the 3' end of Firefly luciferase coding sequence (excluding the last 390 bases) was used to synthesize the cDNA. Using about four percent of the cDNA synthesized and using a forward primer spanning the start codon of Renilla luciferase RLATG (5'-GCTAGCCACCATGACTTC- 3') and the FFREV primer mentioned above, most of the bicistronic transcript was amplified and analyzed on a 0.8% agarose gel.

To replace Renilla luciferase with the CAT reporter, the pRΔEF plasmid was initially digested with SacI and HindIII followed by digestion with NheI and XhoI restriction enzymes. This cloning strategy was used since pRΔEF has two NheI restriction sites that would generate similar sized products and to remove one of the NheI sites, the following PCR primers were used on the pRΔEF vector:

Forward-Bicis NheID 5'ACCGAGCTCTTACGCGTGCAAGCCCGATCT 3'

Reverse-Bicis HindIII 5'CTGTTGTGTCAGAAGAATCAAGCTTTTTGC 3'

The forward primer overlapped with a Sac I restriction site and carried a single base change that would remove one of the NheI sites, and the reverse primer overlapped with a HindIII site. The PCR product was then digested with SacI and HindIII, and ligated with pRΔEF digested with the same restriction enzymes to generate the NheI D-pRΔEF plasmid. To generate CAT reporter carrying overhangs with NheI and XhoI sites, the following PCR primers were used on the pPL-CAT vector:

Forward-CAT NheI primer 5'ATAGGTAGCCACCATGGAGAAAAAAATCACTGG 3'

Reverse-CAT XhoI primer 5'GGCGCTCGAGTTACGCCCCGCCCTGCCACT 3'

The PCR product was digested with XhoI and NheI restriction enzymes and ligated to

NheI D-pRΔEF plasmid digested with the same enzymes to generate the pCAT-F plasmid.

For analysis of cryptic promoter activity of the ODC 5'UTR, the 303bp ODC 5'UTR was cloned into the XhoI and HindIII sites of a promoterless Basic pGL3 plasmid (Promega) containing Firefly luciferase as the reporter enzyme. The ODC 5' 303bp pGL3 plasmid was then compared to the Basic pGL3 vector and to a control pGL3 plasmid (Promega) containing a potent SV40 promoter. Cells were extracted in the passive lysis buffer (Promega) and luciferase activity was measured using the Luciferase assay kit (Promega).

Distribution of 5' UTR variants

ODC 5'UTR cDNA was PCR amplified using the following primers:
Forward – ODC 5F: 5'CCTTCAGTCAGCAGCTCGGC 3'; Reverse – ODC 6R 5'ATATGAATTCGGTTGGTTCTCGATGTGCC- 3'. PCR conditions were as follows: initial denaturation 95°C-3min, denaturation 94°C-30 sec, annealing 61.4°C-30 sec, elongation 72°C-30sec and final elongation 72°C-10 min and PCR was set up as a 30 cycle reaction and also repeated using a 25 cycle amplification reaction. The PCR samples were analyzed by capillary electrophoresis (CE) using the HDA-GT12 CE instrument (Transgenomic Inc). A 2kb DNA Mass Standard was mixed with each PCR sample and analyzed in the same capillary at the same time to determine the concentration of each PCR product. Normalized Area (NA) under each peak was measured using the BIOCAL software. DNA concentration for each peak was determined using the NA under the 2kb DNA standard. Total NA under each region was added together to determine DNA concentration for each expected PCR product.

Results

Identification of alternate splice variants present in the mRNA of ODC

To test if any mutations or alternative splicing could be detected in the ODC sequence in Ras12V cells, total RNA was isolated and reverse transcribed to cDNA. Using specific primers, the ODC coding region, 3'UTR and 5'UTR were amplified by PCR and sequenced. Sequencing revealed no alterations induced by Ras transformation in the ODC open reading frame or 3'UTR. However, several overlapping sequences were observed in the ODC 5'UTR. To analyze these possible splice variants, the 5'UTR cDNA sequences from both cell lines were transformed into E.coli. Screening of clones by sequencing revealed the presence of four splice variants of the ODC 5'UTR in both Ras12V cells and untransformed controls. These species were 303bp, 290bp, 286bp, and 273bp in length, and differed from each other in the presence or absence of an additional 13bp and 17bp intronic sequence (Fig 4.1A). The 17bp intronic sequence is also present in the mouse ODC 5'UTR (data not shown), and a conserved pyrimidine-rich sequence within the 13bp intron is present in the human ODC 5'UTR (Pyronnet, 2000).

The relative distribution of each variant in both cell lines was analyzed by capillary electrophoresis to identify any effects in response to Ras. Among the four ODC transcripts, the most abundant in both control and Ras12V cells was the 286bp 5'UTR variant (Fig 4.1B). However, the distribution trend of these transcripts was different in normal versus transformed cells. When comparing percent abundance in each cell line, the shorter 5'UTR species of 273 bp and 286 bp were more abundant in the control cells. However, the longer 290 bp and 303 bp species were more abundant in the Ras12V cells. This suggests a Ras-responsive selection of alternative ODC transcripts that contain

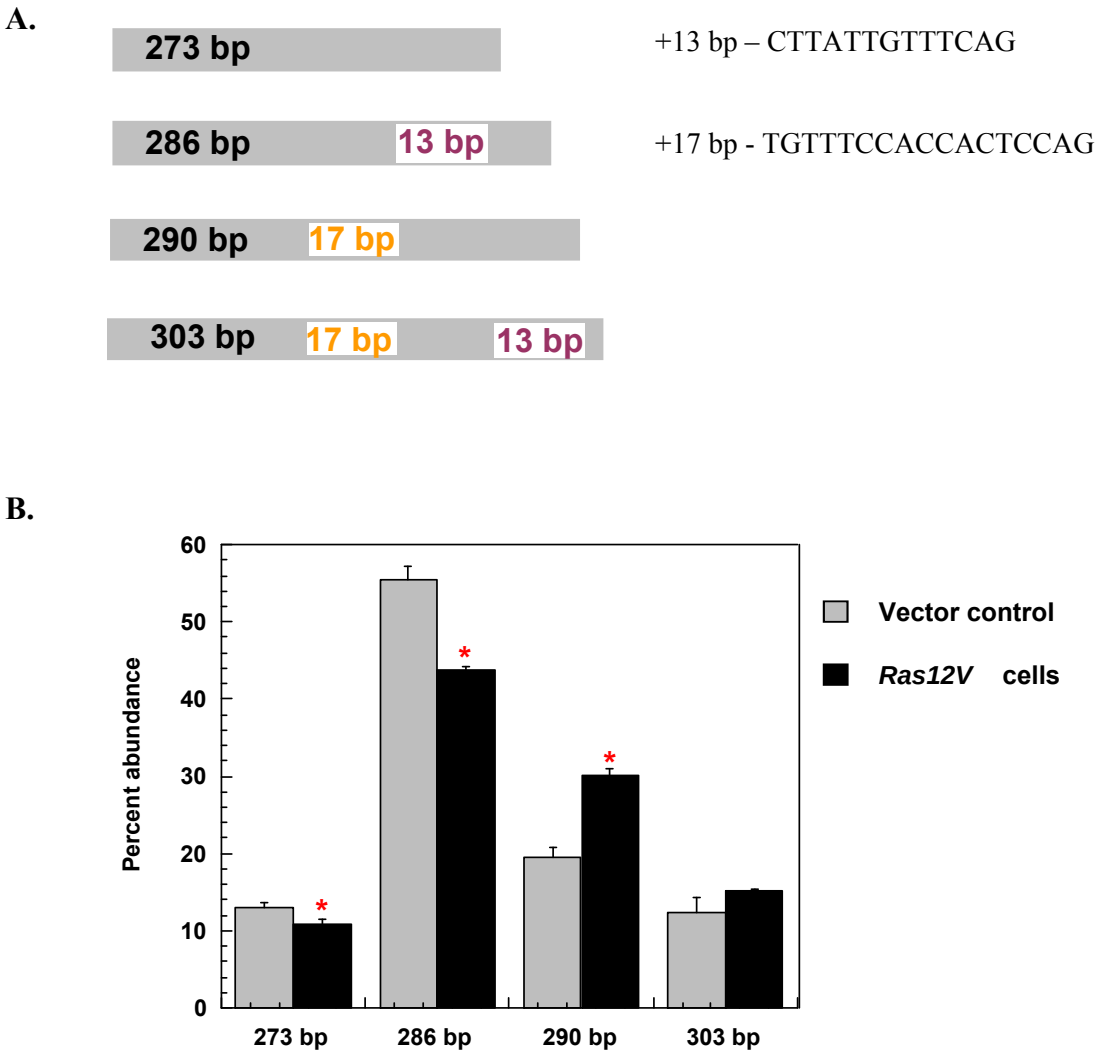

Figure 4.1. Identification of four splice variants of ODC 5'UTR sequence and estimation of their distribution (See next page for figure legend)

Figure 4.1. Identification of four splice variants of ODC 5'UTR sequence and estimation of their distribution

(A) Schematic representing the lengths of four splice variants of ODC 5'UTR identified in both Ras12V and control RIE-1 cells. It also indicates the presence or absence of a 17bp or 13bp intronic sequence in each variant.

(B) Distribution of each splice variant relative to each other in Ras12V cells and control was determined by capillary electrophoresis as described in the Methods. Graph represents the average of two separate experiments with triplicate samples per experiment. Difference in the distribution of 273bp in Ras12V cells compared to controls was statistically significant with a $*p<0.05$, and also significant for 286bp and 290bp with a $*p<0.0001$ as calculated by a two-tailed T-test.

intronic sequences (Fig 4.1B).

Cap-independent translation of ODC

To analyze if the observed ODC 5'UTR splice variants can initiate translation in a cap-independent manner, and to determine if there is a difference in the efficiency of IRES-mediated translation among these splice variants, a bicistronic plasmid assay was used. This plasmid contains, on the pcDNA3.0 plasmid backbone (Invitrogen), two reporter sequences produced as a single transcript. The first reporter, Renilla luciferase, is translated in a cap-dependent manner. The second reporter, Firefly luciferase, can be translated efficiently only in a cap-independent manner that is initiated from a sequence containing a putative IRES. To assay for the presence of IRES activity in the ODC 5'UTR, the four variant 5'UTR sequences were cloned into the bicistronic plasmid between Renilla luciferase and Firefly luciferase, transfected into cells during log-phase growth, and the luciferase activities were measured. The ratios of Firefly to Renilla luciferase activities were expressed as fold change over ratios obtained with an empty bicistronic control plasmid. An attenuated viral EMCV sequence previously reported to exhibit IRES activity (a kind gift from Dr. P. Sarnow, Stanford University) was used as a positive control (Carter & Sarnow, 2000).

All the ODC splice variants assayed in the bicistronic assay supported IRES-mediated translational activity (Fig 4.2B), and the strongest IRES activity in both normal and transformed cells was exhibited by the 303 bp 5'UTR variant. However, Ras transformation had a striking stimulating effect on IRES activity from all of the ODC 5'UTR species; increasing IRES-mediated translation up to 6-fold compared to the control cells (Fig 4.2B). A 303bp 5'UTR in the antisense orientation served as a negative

A.

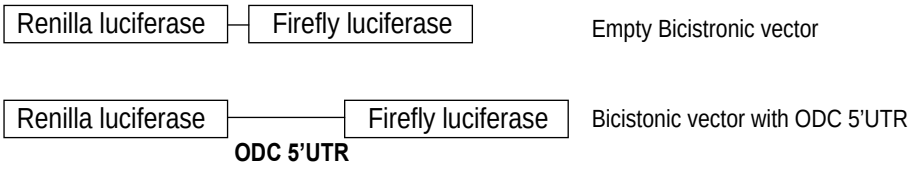

B.

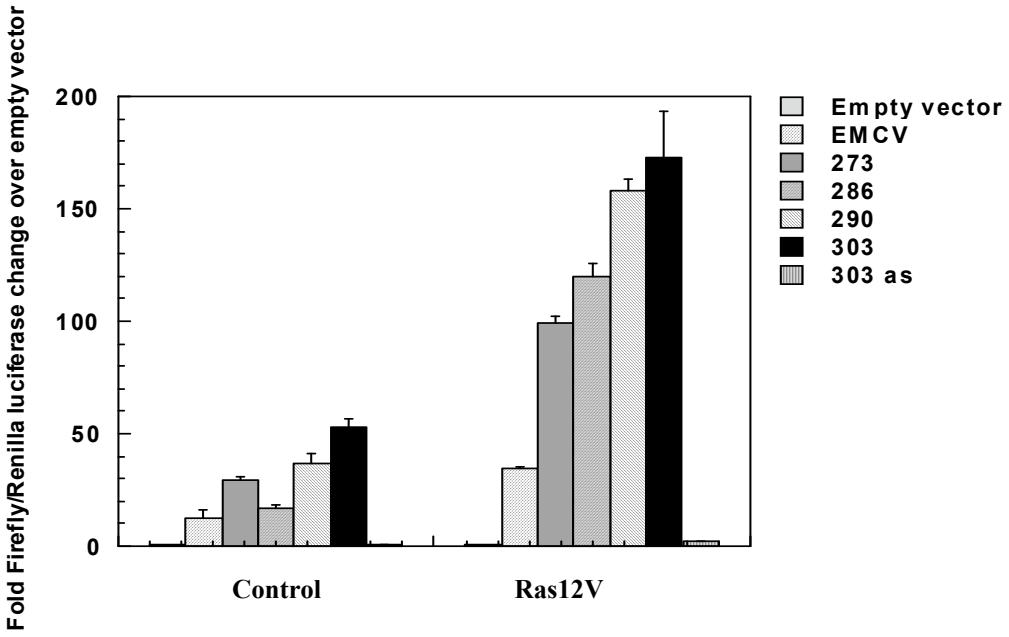

Figure 4.2. Comparison of IRES mediated translation of ODC in Ras 12V cells and RIE-1 cells. (See next page for figure legend)

Figure 4.2. Comparison of IRES mediated translation of ODC in Ras 12V cells and RIE-1 cells

(A) Schematic of the empty bicistronic vector displaying the reporter sequences (above) and bicistronic vector with ODC 5'UTR (below).

(B) Cells were transfected with either the empty Renilla-Firefly bicistronic plasmid or with the plasmid containing one of the four splice variants of ODC 5'UTR cloned in between Renilla (cap) and Firefly (cap-independent) luciferase sequences. 24 hrs following transfection, luciferase activities were measured. 303 as-antisense, containing the 303bp sequence cloned in antisense orientation, was used as a negative control. As a positive control, an attenuated IRES from the EMCV virus was used. The X- axis represents ratios of Firefly to Renilla luciferase activities measured for each plasmid and expressed as a fold change over the ratios measured for the empty bicistronic plasmid. This plot represents the average of two experiments with triplicate samples measured per experiment

length control and as expected exhibited minimal IRES activity (Fig 4.2B). While Ras12V cells exhibited a 5'UTR length-dependent increase in IRES activity, in the control cells the IRES activity of the 286bp 5'UTR variant was consistently significantly lower than the 273bp variant (Fig 4.2B).

Effect of inhibitors on IRES-mediated translation of ODC

The ability of ODC to be translated in a cap-independent manner more efficiently in the Ras-transformed cells puts forth an interesting question as to whether this IRES activity is regulated by Ras signaling. To evaluate the role of Ras effector pathways on ODC IRES activity, both transformed and control cells were transfected with the 303bp bicistronic plasmid, which exhibited the strongest IRES activity, and following transfection these cells were first treated with PI3K pathway inhibitors. Compared to the vehicle treated controls, cap-independent translation was decreased by more than 50% in the presence of LY294002 or Rapamycin in the control cells but was unaltered in the Ras12V cells (Fig 4.3A). However cap-dependent translation as reflected by the Renilla luciferase activity of the bicistronic vector was inhibited in the presence of both these inhibitors in the control and Ras12V cells (Fig 4.5). Renilla luciferase activity was reduced to about 50% in the presence of Rapamycin in both the cell-lines compared to the DMSO controls and was also reduced in the presence of LY294002, with the effects being more obvious in the control RIE-1 cells (Fig 4.5).

ODC IRES activity has been reported to be stimulated during the G2-M phase of the cell cycle, where global cap-dependent translation is inhibited (Pyronnet et al., 2000; Pyronnet et al., 2005). Hence, in order to explain the differential effects of LY294002 and Rapamycin on IRES activity in the two cell lines, cell-cycle

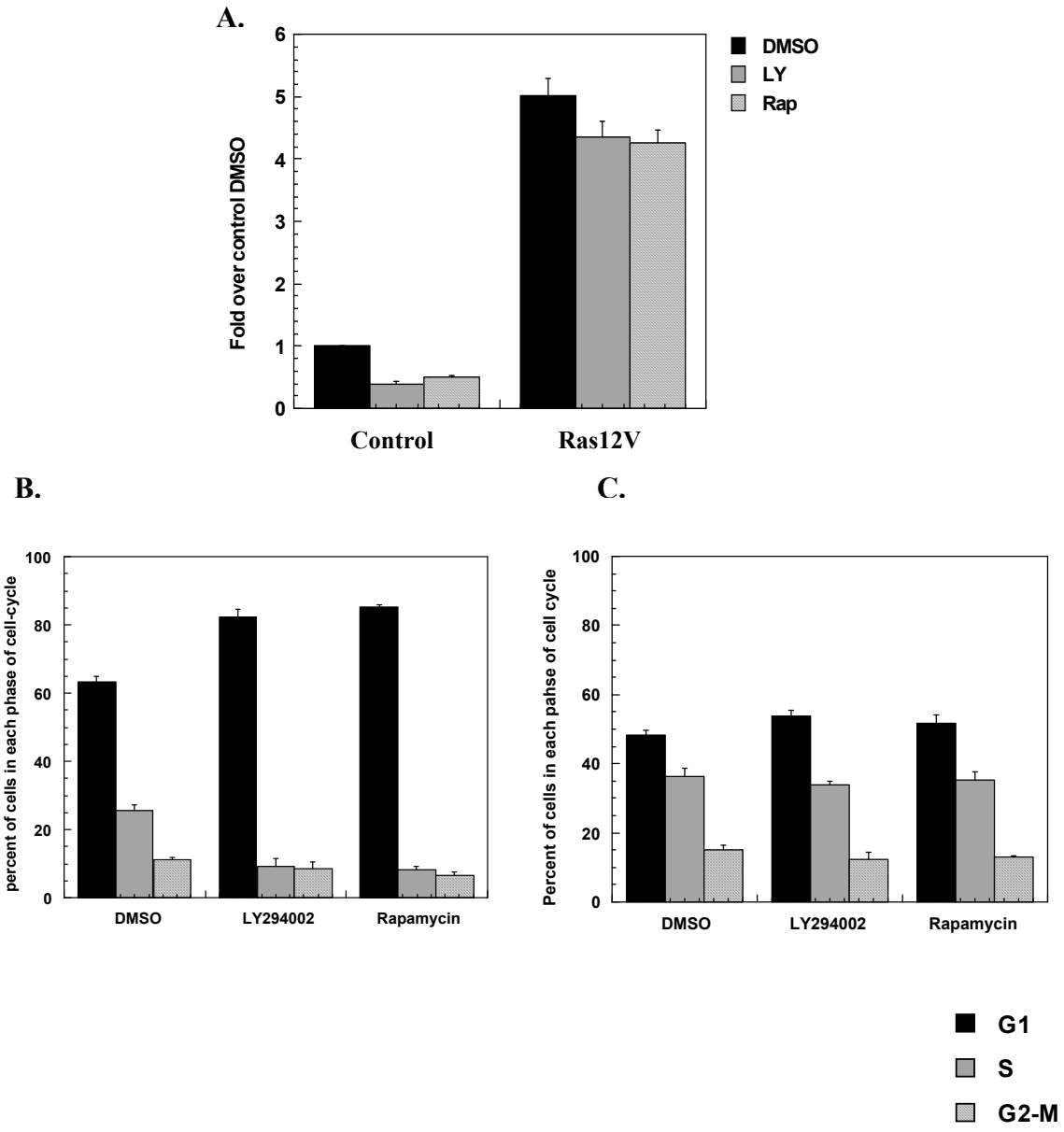

Figure 4.3. Effect of inhibition of the PI3K/mTOR pathway on ODC IRES-mediated translational activity and cell-cycle progression in Ras12V and parental RIE-1 cells

(See next page for figure legend)

Figure 4.3. Effect of inhibition of the PI3K/mTOR pathway on ODC IRES-mediated translational activity and cell-cycle progression in Ras12V and parental RIE-1 cells

Both control and Ras12V cells were transfected with the 303bp bicistronic plasmid. Immediately following transfection, cells were serum-starved for 6 h, and serum was added back along with the vehicle DMSO, 20 μM LY294002 (LY) or 100nM Rapamycin (Rap). 24 hrs following transfection, luciferase activities were measured and cell cycle progression was analyzed.

(A) For luciferase assays, the y-axis represents the fold change in Firefly luciferase (IRES) activity normalized to the activity observed in DMSO-treated parental control cells. Graph represents the average of triplicate samples and the experiments were performed in duplicate.

(B) and **(C)** Cell cycle progression was analyzed in **(B)** RIE-1 cells and **(C)** Ras12V cells by Flow Cytomtery as described in the Methods. The number of cells in each phase of the cell cycle is represented as a percent of the total (y-axis). Graphs represent the average of three independent experiments.

progression was analyzed. The percentages of cells in the G1, S and G2-M phases of the cell cycle were 63%, 26% and 11%, respectively, in the control cells and 49%, 36% and 15%, respectively, in the Ras12V cells (Fig 4.3B,C). In non-transformed cells in the presence of LY294002 or Rapamycin, the percent of cells in the G1 phase increased to about 85%, while the percent of cells in the S phase was reduced to 8-9%, and in the G2-M phase to 6-8% (Fig 4.3B, C). On the other hand, these inhibitors had no effect on cell cycle distribution in Ras12V cells, although western blot analysis confirmed inhibition of the PI3K/mTOR pathway (Chapter II-Fig 2.5, 2.6).

In contrast to PI3K pathway inhibition, inhibition of MEK surprisingly caused ODC IRES activity to increase in both the Ras12V and control cells (Fig 4.4A). This stimulatory effect was exclusive to cap-independent translation as cap-dependent translation (Renilla luciferase activity) was not affected by PD98059 at all in Ras12V cells and had a mild stimulatory effect in control RIE-1 cells (Fig 4.5). To examine the IRES-stimulating effects of PD98059, cell cycle progression was also analyzed in the presence of this compound. Contrary to the effects of the inhibitors of the PI 3K/mTOR pathway, MEK inhibition did not alter the cell cycle distribution significantly in either cell line. Specifically, the percent of cells in G2-M was not different compared to the DMSO control (Fig 4.4B, C).

Since both the Raf and PI3K pathways cooperate to regulate ODC activity in response to Ras, the effect of the PI3K/mTOR pathway in stimulating ODC IRES activity in the presence of MEK inhibition was analyzed. ODC IRES activity was measured in the presence of a combination of inhibitors consisting of PD98059 plus LY294002, or PD98059 plus Rapamycin. In the presence of these inhibitor combinations, increased

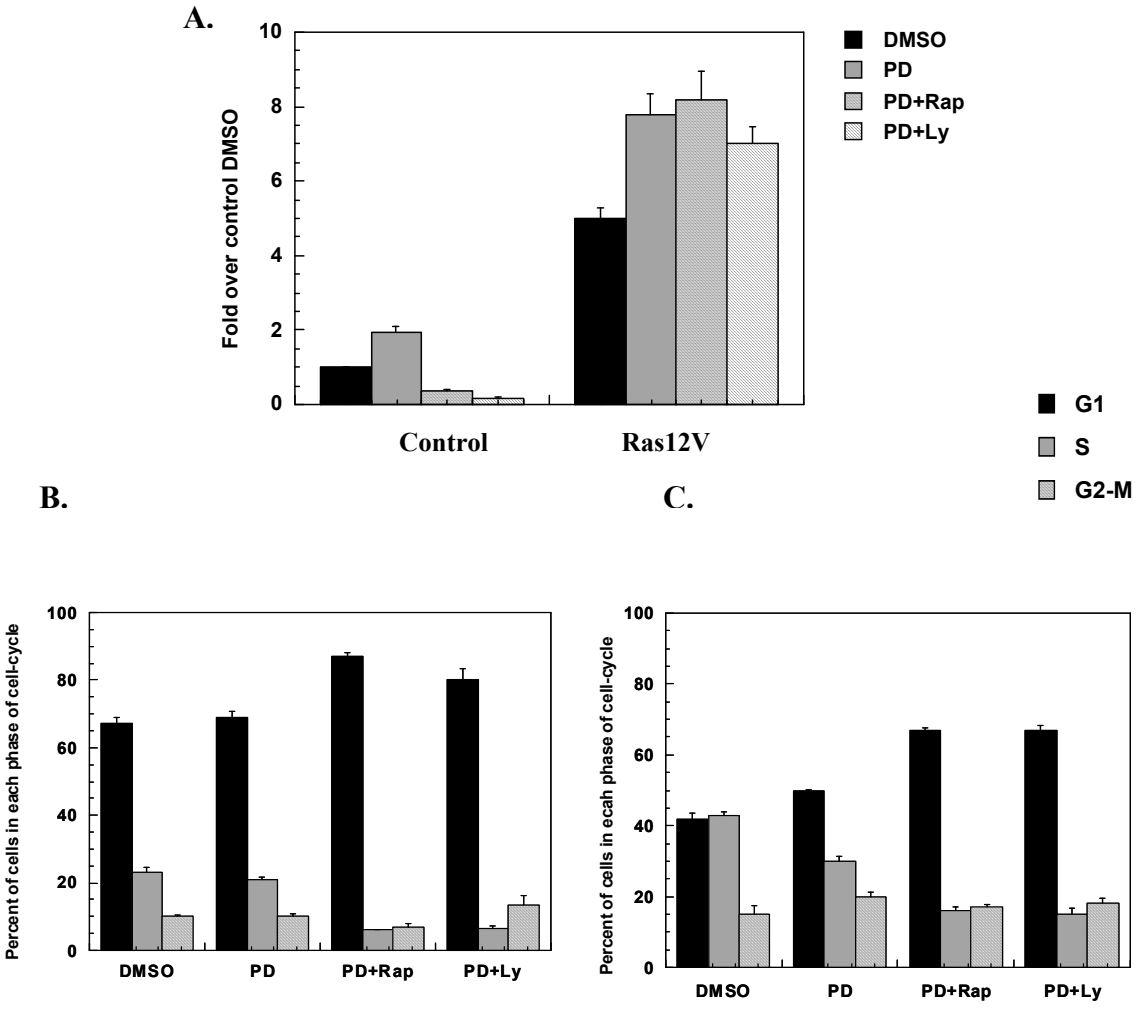

Figure 4.4. Effects of inhibition of either MEK or both MEK and PI3K/mTOR on ODC IRES-mediated translational activity and cell cycle progression in control and Ras12V cells (See next page for figure legend)

Figure 4.4. Effects of inhibition of either MEK or both MEK and PI3K/mTOR on **(A)** ODC IRES-mediated translational activity and cell cycle progression in **(B)** control and **(C)** Ras12V cells

Both control and Ras12V cells were transfected with the 303bp bicistronic plasmid. Immediately following transfection, cells were serum-starved for 6 h, then serum-containing medium was added with either the vehicle DMSO, 50 μM PD98059 (PD), PD and 20 μM LY294002, or PD and 100nM Rapamycin (Rap). 24 hrs following transfection, luciferase activities were measured and cell cycle progression was analyzed as described in Figure 4.3.

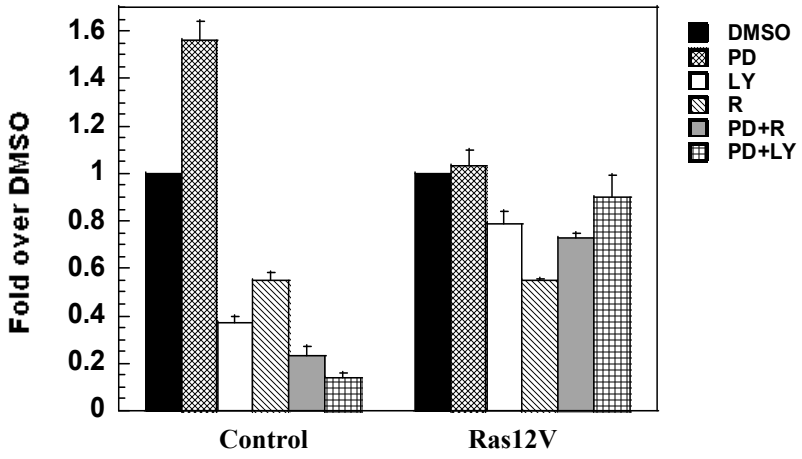

Figure 4.5. Effect of the inhibitors on expression of Renilla luciferase (cap-dependent translation)

Cells were transfected with the 303bp bicistronic vector and luciferase activity was measured as described for Fig 4.3. Graphs represent the average of triplicate samples and the experiment was performed in duplicate. Y-axis represents the Renilla luciferase (cap) activity expressed as a fold over DMSO treatments in either control or Ras 12V cells.

ODC IRES activity was maintained in Ras12V cells, but IRES activity was markedly inhibited in control cells compared to their DMSO-treated counterparts (Fig 4.4A). Inhibition of IRES activity in control cells paralleled the inhibitory effect of dual inhibitors on cap-dependent translation (Renilla luciferase activity), however in contrast to the stimulated IRES activity, cap-dependent translation was mildly inhibited in the presence of dual inhibitors in the Ras12V cells (Fig 4.5). Treatment of control cells with the dual inhibitors was accompanied by increased G1 arrest, as the number of cells in the G1 phase of the cell cycle was increased to about 90% compared to the 65% in the DMSO treated control cells (Fig 4.4B). On the other hand, all of the inhibitor combinations produced only a minor effect on cell cycle progression in Ras12V cells (Fig 4.4C).

Studies analyzing the effects of PD98059 were thus far carried out using the 303bp ODC 5'UTR splice variant, which incited the question if the effects of PD98059 were splice variant specific, that is if the presence of the intronic sequences were necessary for the stimulatory effects of PD98059. To address this possibility, 273bp bicistronic vector that lacked the additional 13 and 17bp intronic sequences was transfected into the Ras12V cells and treated with PD98059 and compared to the 303bp bicistronic vector. PD98059 stimulated 273bp ODC IRES activity to an extent similar to the 303bp ODC IRES activity suggesting that the effect of PD98059 was not influenced by the presence of the additional intronic sequences (Fig 4.6).

To explain the effects of PD98059, the possibility of a compensatory induction in the p38 MAPK pathway in response to MEK inhibition was assessed (Fig 4.7A). Levels of both phosphorylated and total p38 MAPK, as well as the p38 delta isoform

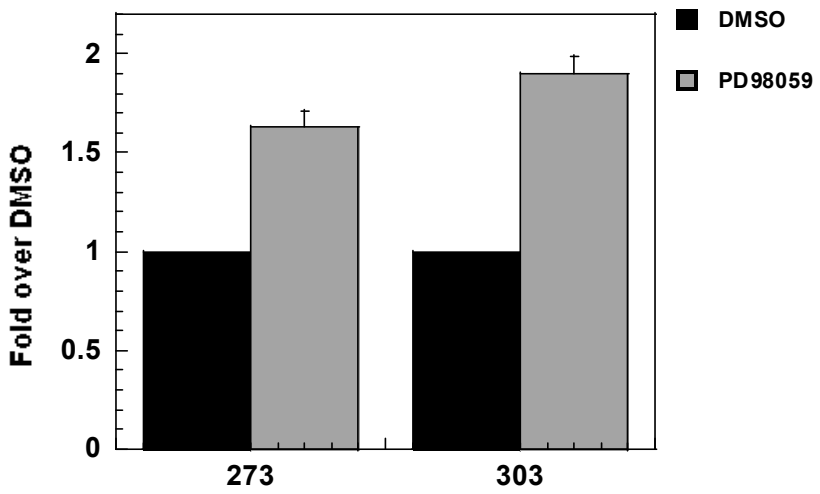

Figure 4.6. Effect of MEK inhibition on splice variant specific ODC IRES-mediated translational activity

Ras12V cells were transfected with either the 273bp or 303bp ODC 5'UTR bicistronic plasmid and treated with either the vehicle DMSO or 50 μM PD98059. Firefly luciferase (IRES) activities were measured as described for figure 4.3. Y-axis represents the Firefly luciferase (IRES) activity expressed as fold over DMSO treatments and the graph represents the average of triplicate samples.

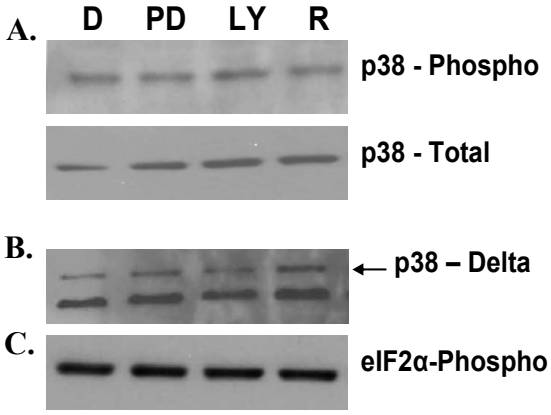

Figure 4.7. Effect of inhibition of MEK and PI3K-mTOR on p38 MAPK and eIF2-alpha levels

Ras12V cells were treated with vehicle D-DMSO, 50 μM PD98059 (PD), 20 μM LY294002 (LY) or 100nM Rapamycin (R). 40μg of total protein was loaded per lane and Western blot analysis was carried out to determine levels of **(A)** phosphorylated and total p38-MAPK levels**, (B)** total levels of the isoform p38-delta and **(C)** phosphorylated levels of translation initiation factor eIF2-alpha. The blots were repeated with extracts from two independent experiments.

shown previously to interact with ERK (Efimova et al., 2003), were analyzed in the presence of PD98059 or the inhibitor combinations. However, no changes in p38 MAPK were observed, making it unlikely that this pathway influences ODC IRES activity (Fig 4.7A, B). Also, since increased activation of translation initiation factor eIF2-alpha has been shown to stimulate ODC IRES activity during the G2-M phase of cell-cycle (Tinton et al., 2005), phosphorylated levels of eIF2-alpha were analyzed in the presence of PD98059. Again, no increase was observed in either the total or phosphorylated level of eIF2-alpha (Fig 4.7C).

Regulation of ODC by eIF4E phosphorylation

The increase in IRES activity seen in the presence of MEK inhibition, coupled with the lack of compensation by other pathways, suggest that elements downstream of MEK control ODC IRES activity in Ras-transformed RIE-1 cells. The Mnk1 and Mnk2 kinases are crucial targets of ERK, which upon activation phosphorylate the translation initiation factor eIF4E (Waskiewicz et al., 1997), and Ras12V cells contain increased levels of phosphorylated eIF4E (Chapter III –Fig 3.1A). Therefore, we next investigated the role of this phosphorylation in ODC regulation. In the Ras12V cells, phosphorylation of eIF4E was almost completely inhibited in the presence of PD98059, without affecting total eIF4E levels, but neither LY294002 nor Rapamycin had a substantial effect on phosphorylation of eIF4E (Fig 4.8A). To assess the contribution of eIF4E phosphorylation to ODC IRES activity, the specific Mnk inhibitor CGP57380 (CG) was used. To ensure that the Mnk inhibitor was affecting its intended target, phosphorylated levels of eIF4E were analyzed. As expected, Mnk inhibition greatly reduced the phosphorylation of eIF4E without affecting the total levels (Fig 4.8B). When

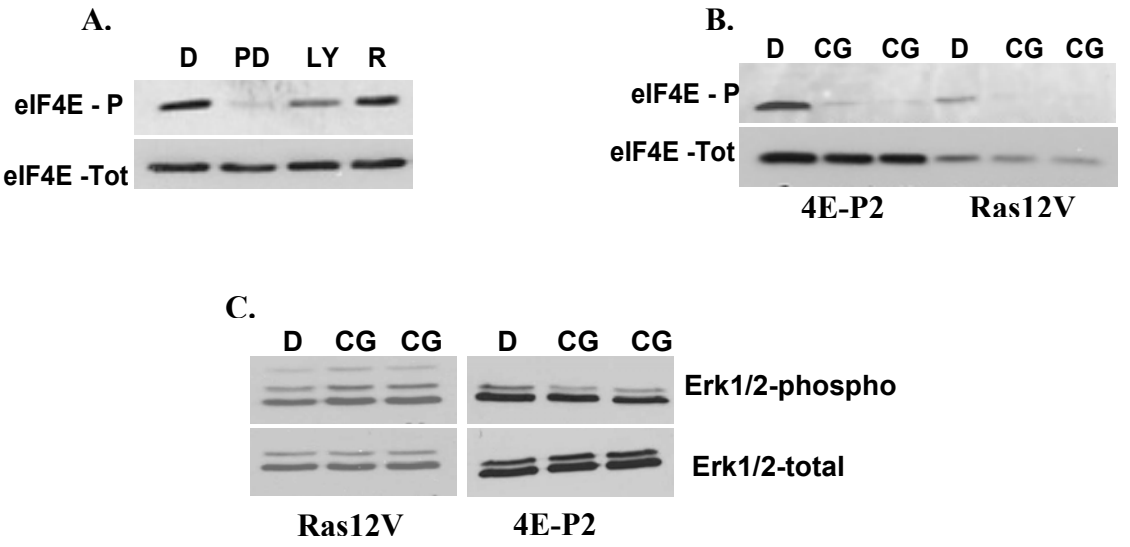

Figure 4.8. Effect of CGP57380 on eIF4E phosphorylation and ERK phosphorylation in Ras12V and 4E-P2 cells

Western blot analysis of **(A)** Ras12V cells treated with either the vehicle DMSO, 50 μM PD98059 (PD), 20 μM LY294002 (LY) or 100nM Rapamycin (R) and **(B)** both Ras12V and 4E-P2 cells treated with either DMSO or 20 μM CGP57380 (CG). Blots were probed with antibodies against total and phosphorylated eIF4E. Cells were grown in the presence of serum for 24 h and treated with inhibitor in serum-free media for 2 hrs. 40μg of total protein was loaded per lane. Samples were analyzed in duplicate for each treatment. The experiment was repeated twice to confirm the results.

(C) Samples were prepared as described for (B), instead the blots were probed with antibodies against total and phosphorylated ERK1/2.

ODC activity was measured in the presence of CG, it was reduced by about 60% compared to vehicle-treated Ras12V cells (Chapter III –Fig 3.10), suggesting that dephosphorylation of eIF4E is sufficient to inhibit ODC activity, and represents a crucial target of the MEK pathway in regulating ODC. Also no non-specific effect was observed on ERK phosphorylation in the presence of Mnk1 inhibition (Fig 4.8C).

To analyze if the phosphorylation status of eIF4E contributes to ODC IRES regulation, the effect of Mnk inhibition on ODC IRES-mediated translation was analyzed. At a concentration of 20 μM, CG moderately but significantly increased ODC IRES activity by about 1.5 fold in comparison to DMSO treatment in both Ras12V cells and control cells (Fig 4.9). These results suggest that dephosphorylation of eIF4E can stimulate ODC IRES activity while decreasing overall ODC protein synthesis. However, the effect of Mnk inhibition was not as potent as PD98059, suggesting that, in control and transformed RIE-1 cells; there are other targets of ERK that can regulate ODC IRES-mediated translation.

To further clarify the role of eIF4E in ODC synthesis, the effect of the Mnk inhibition was studied in 4E-P2 cells. These cells present a good model to analyze the direct effects of eIF4E, as they are transformed by over-expression of eIF4E and consequently circumvent much of the complex regulation associated with Ras over-expression (Rousseau et al., 1996). Western blot analysis confirmed that in spite of over-expression of eIF4E, 20 μM CG was sufficient to significantly block phosphorylation of eIF4E in 4E-P2 cells, without affecting either total eIF4E levels (Fig 4.8B) or phosphorylated levels of ERK (Fig 4.8C). Treatment of these cells with CG was also quite effective in inducing ODC IRES-mediated translation, exhibiting more than a

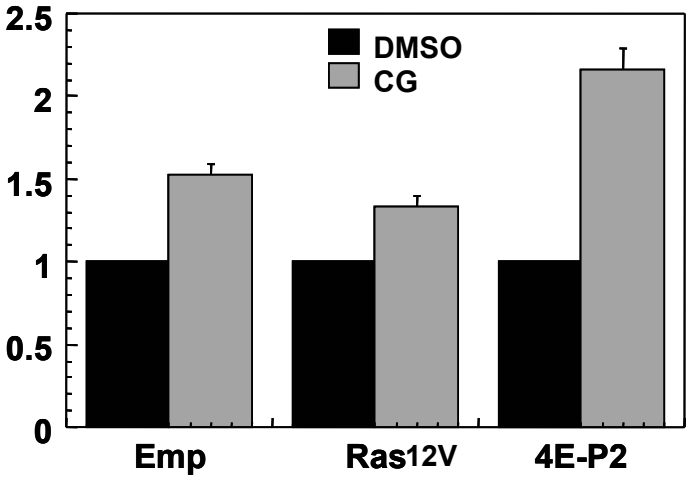

Figure 4.9. Effect of dephosphorylation of eIF4E on ODC IRES activity

For luciferase assays, RIE-1 cells, Ras12V cells and 4E-P2 cells were transfected with either the empty or 303bp bicistronic plasmid as described in Figure 4.3 and treated with either DMSO or 20 μM CGP57380 (CG). The Y-axis represents the fold change in Firefly luciferase (IRES) activity normalized to the activity observed in DMSO treated cells. Graph represents the average of triplicate samples and the experiment was performed in duplicate.

2-fold increase in comparison to the DMSO-treated controls (Fig 4.9). This treatment did not affect cap-dependent translation (Renilla luciferase activity) in comparison to the DMSO treated controls in either cell line (Fig 4.11).

A further correlation between ODC IRES activity and eIF4E phosphoylation was observed when ODC cap-independent translation exhibited a dose-dependent response to changes in eIF4E phosphorylation obtained by using a range of inhibitor concentrations (Fig 4.10A). To explain the effects of Mnk inhibition, cell-cycle progression was also analyzed in 4E-P2 cells. Interestingly, treatment with 20 μM CG resulted in a 90% reduction in the number of G2-M phase cells in comparison to the DMSO-treated controls, yet up-regulated ODC IRES-mediated translation (Fig 4.10B). These results suggest that dephosphorylation of eIF4E positively regulates ODC IRES translational activity, and this effect is uncoupled from regulation by cell cycle progression.

Analysis of Integrity of the bicistronic transcript

One of the valid concerns with the bicistronic plasmid assay is the possibility of non-specific splicing that result in a Firefly luciferase transcript independent of Renilla luciferase, allowing translation of Firefly luciferase in a cap-dependent manner. Also the inserted 5'UTR can act as a promoter allowing synthesis of Firefly luciferase in a cap-dependent manner. To assay for the presence of aberrant transcripts, cDNA was synthesized from cells transfected with the pcDNA 303bp bicistronic plasmid and most of the bicistronic transcript was PCR amplified using the primers whose positions are indicated in Figure 4.12A. As expected only a 2.7 kb product was detected for the empty bicistronic plasmid and a 3.0 kb product was detected for the 303bp variant, suggesting an absence of spurious splicing (Fig 4.12B). These results were further confirmed by

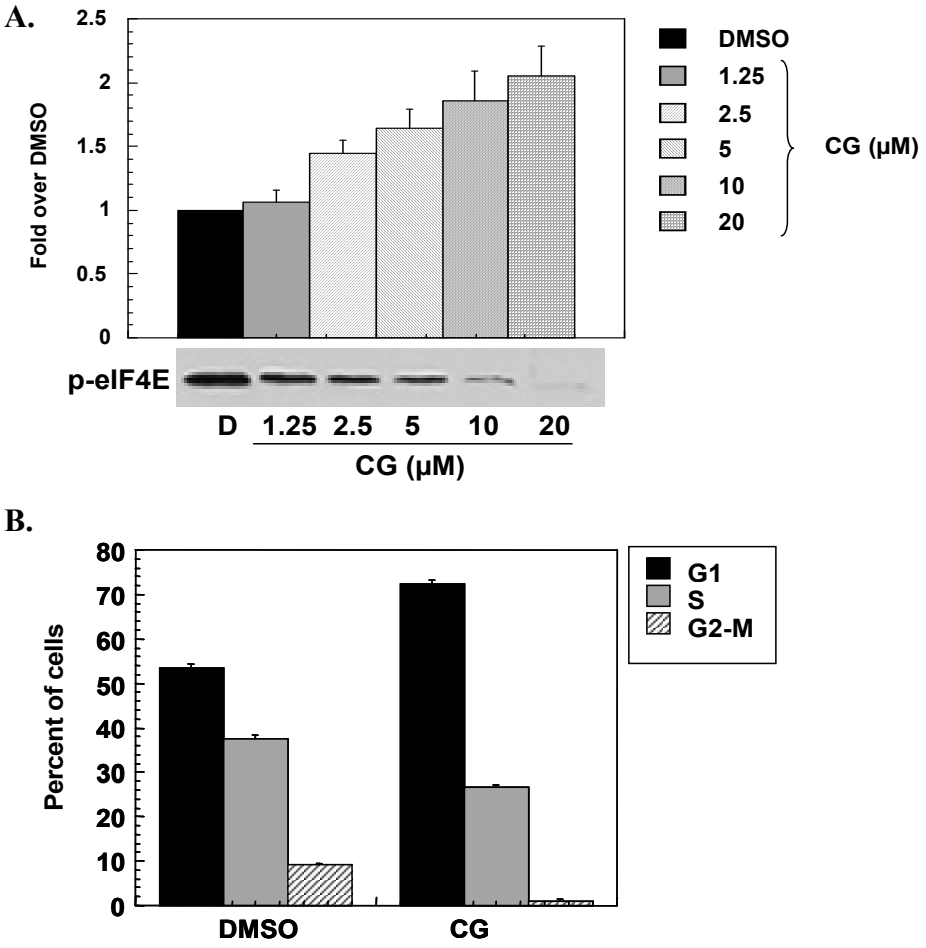

Figure 4.10. ODC IRES-mediated translation in response to varying doses of the Mnk inhibitor (See next page for figure legend)

Figure 4.10. ODC IRES-mediated translation in response to varying doses of the Mnk inhibitor

4E-P2 cells were transfected with either the empty or 303bp bicistronic plasmid. For dose-response effect **(A)**, cells were treated with CGP57380 at doses ranging from 1.25 to 20 μM and luciferase activities were measured as described in Figure 3. The Y-axis represents the fold change in Firefly luciferase (IRES) activity normalized to the activity observed in DMSO-treated cells. The graph represents the average of triplicate samples and each experiment was performed in duplicate. Western blot below the graph displays effect of varying doses of the Mnk inhibitor on levels of eIF4E phosphorylation. For cell-cycle progression analysis **(B)**, cells were treated with either DMSO or 20 μM CGP57380 (CG) and analyzed as described in Figure 4.3. Graphs represent the average of three independent experiments.

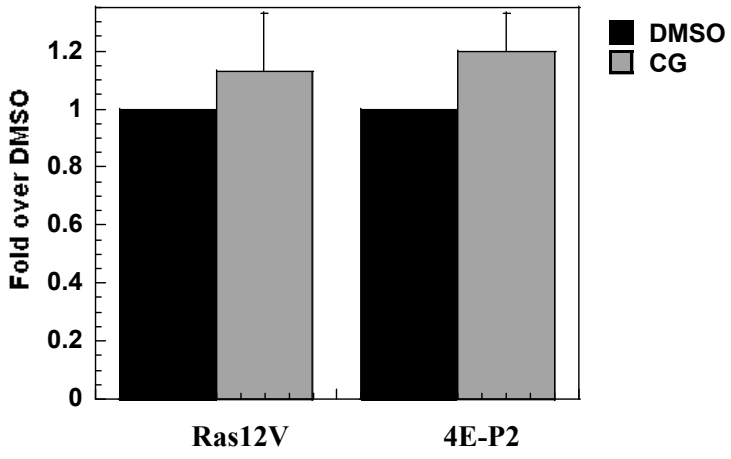

Figure 4.11: Effect of the Mnk inhibitor on expression of Renilla luciferase (cap-dependent translation).

Cells were transfected with the 303bp bicistronic vector and luciferase activity was measured as described for Fig 4.9. Graphs represent the average of triplicate samples and the experiment was performed in duplicate. Y-axis represents the Renilla luciferase (cap) activity expressed as a fold over DMSO treatments in either Ras12V cells or 4E-P2 cells.

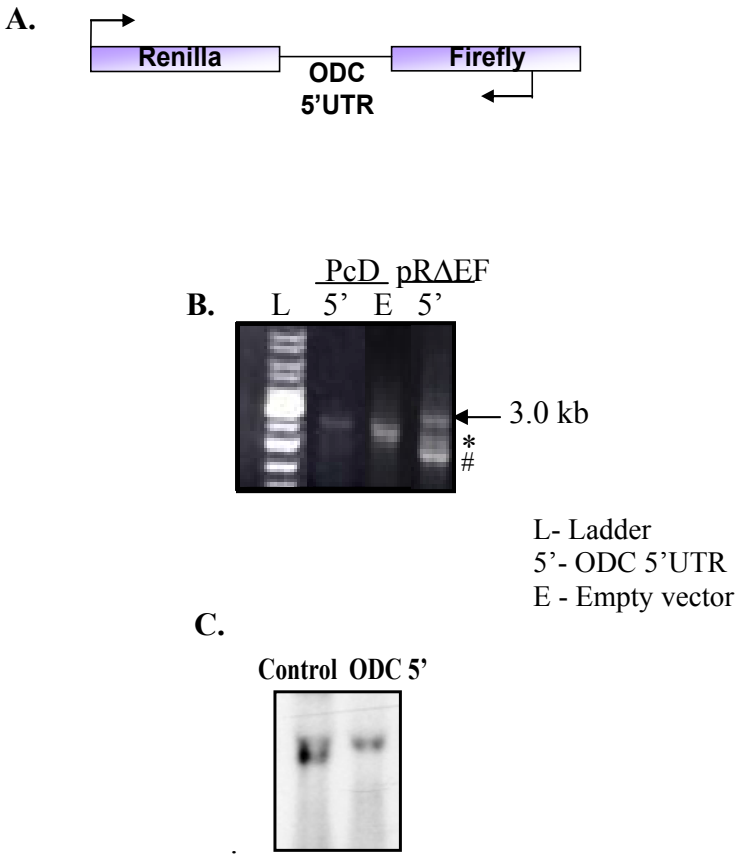

Figure 4.12: Analysis of the integrity of the pcDNA 303bp bicistronic transcript.

(See next page for figure legend)

Figure 4.12: Analysis of the integrity of the pcDNA 303bp bicistronic transcript.

(A) and **(B)** RT-PCR analysis of bicistronic mRNA was carried out by processing cDNA from RNA isolated from cells transfected with either the empty or ODC5'UTR pcDNA (pCD) bicistronic plasmid or pRΔEF ODC 5'UTR bicistronic plasmid.
(A) Bicistronic cDNA was amplified using primers spanning the start site of Renilla luciferase and close to the 3'end of Firefly luciferase as indicated and **(B)** analyzed on a 0.8% agarose gel. PCR products of ODC 5'UTR containing bicistronic cDNA was compared to the empty bicistronic cDNA and to the 303bp pRΔEF bicistronic cDNA. Arrow represents the expected size of the bicistronic product. * represents the additional 2.5kb and # represents the 2 kb splice product observed only with the pRΔEF bicistronic plasmid.
(C) Northern blot analysis of pcDNA bicistronic RNA was carried out as described in methods. Expected size for ODC 5'UTR bicistronic transcript is about 3.7kb and for control transcript is about 3.4 kb. The experiment was repeated twice.

northern blot analysis, which detected only the expected intact 3.7kb bicistronic transcript for the 303bp and a slightly shorter product for the empty bicistronic plasmid (Fig 4.12C). Possible cryptic promoter activity of the ODC 5'UTR was also ruled out by expression of the 303 bp variant in a pGL3 promoterless plasmid, which resulted in luciferase activity near the background levels produced by an empty vector in both the control and Ras12V cells (Fig 4.13A,B).

Northern blot analysis of the 303bp bicistronic plasmid on the pcDNA3.0 plasmid backbone used in all of our studies did not reveal the presence of any additional bicistronic transcripts other than the expected 3.7kb sized transcript, as described above. However, it is important to note that northern blot analysis of 303bp bicistronic plasmid on a pRΔEF plasmid backbone (schematic of pRΔEF plasmid Fig 4.14A) (Carter & Sarnow, 2000) revealed the presence of additional transcripts other than the expected bicistronic transcript (data not shown), although no such non-specific transcripts were found in the EMCV IRES pRΔEF bicistronic plasmid or with the empty pRΔEF bicistronic plasmid as reported previously (Carter & Sarnow, 2000) (Fig 4.14B,C). Northern blot analysis of 303bp pRΔEF bicistronic transcript displayed the expected 4.0 kb transcript representing the intact bicistronic RNA and also displayed two additional transcripts about 2.5kb and 1.7kb in length (Fig 4.14B). These additional transcripts were also observed with the 290bp pRΔEF RNA but were not observed with either the pRΔEF RNA containing 290 or 303bp ODC 5'UTR cloned in the antisense orientation (Fig 4.14C). These results suggested that the pRΔEF plasmid with ODC 5'UTR in the sense orientation is subject to non-specific splicing. Additionally cDNA analysis revealed the expected 3.0 kb PCR product but also showed two other PCR products about 2 and 2.5kb

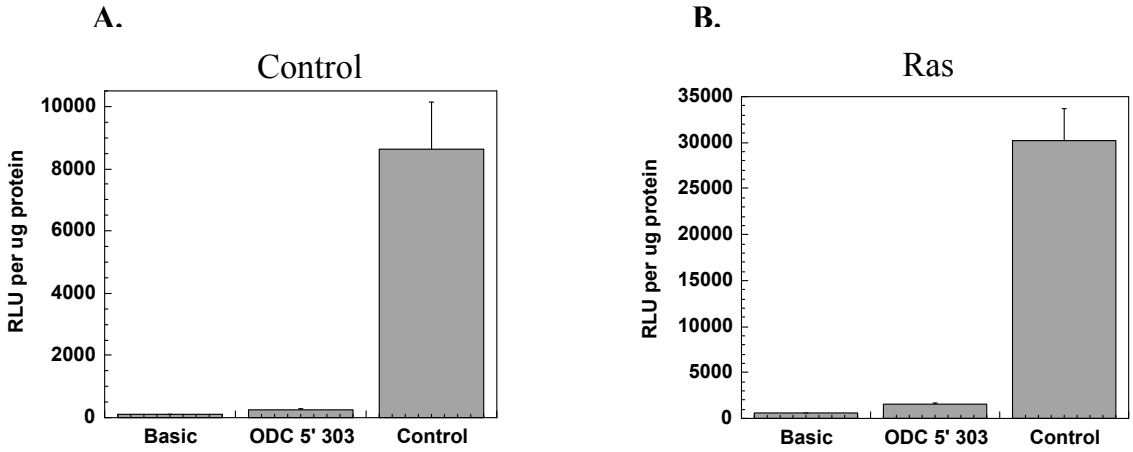

Figure 4.13. Analysis of promoter activity of ODC 5'UTR

To determine promoter activity of ODC 5'UTR, 303bp ODC 5'UTR was cloned into a promoterless luciferase expression vector and transfected into either the **(A)** RIE-1 or **(B)** Ras12V cells. 24 hrs following transfection luciferase activities were measured as described in Methods. Graph y-axis represents luciferase activity normalized per ug of total protein. Basic (promoterless) and Control (SV40 promoter) luciferase expression vectors were used as negative and positive controls respectively. Graph represents the average of triplicate samples and the experiment was performed in duplicate.

in length, further confirming that the pRΔEF 303bp transcript undergoes non-specific splicing. To determine the potential location of splicing, the 2 and 2.5kb PCR products were sequenced. Sequencing of the 2kb PCR product interestingly revealed that this product may be the result of splicing involving the 3'end of Renilla luciferase and one of the introns of ODC 5'UTR. However sequencing of the 2.5kb product was not as successful as it produced a set of overlapping sequences.

Based on the sequencing results and a previous report that the 3'end of Renilla luciferase has a potential splicing site (Holcik et al., 2005), we replaced the Renilla luciferase reporter in the pRΔEF plasmid with a Chloramphenicol Acetyltransferase (CAT) reporter to eliminate the non-specific splicing sites. However, northern analysis revealed that replacing Renilla luciferase with the CAT reporter still resulted in a non-specific transcript (Fig 4.14D). Replacing Renilla luciferase did not remove spurious splicing sites in our experiments and the possible explanation for the discrepancy between our results and the previous report by Holcik et.al., is that we analyzed the effect of an alternate reporter sequence in the same plasmid, however Holcik et.al., replaced Renilla luciferase with an alternate reporter sequence but also used a different plasmid backbone (pcDNA3.0). Also most of the reports indicating absence of non-specific splicing associated with cellular 5'UTR bicistronic plasmids have used a pcDNA backbone for their bicistronic plasmid assays (Holcik et al., 2005; Pyronnet et al., 2000; Ray et al., 2006). Based on these observations we replaced the pRΔEF plasmid backbone with the pcDNA 3.0 plasmid backbone and did not detect any non-specific splicing transcripts either by northern analysis or by cDNA analysis (Fig 4.14A, B, C). The differences between these two plasmids lie in both the plasmid backbone and

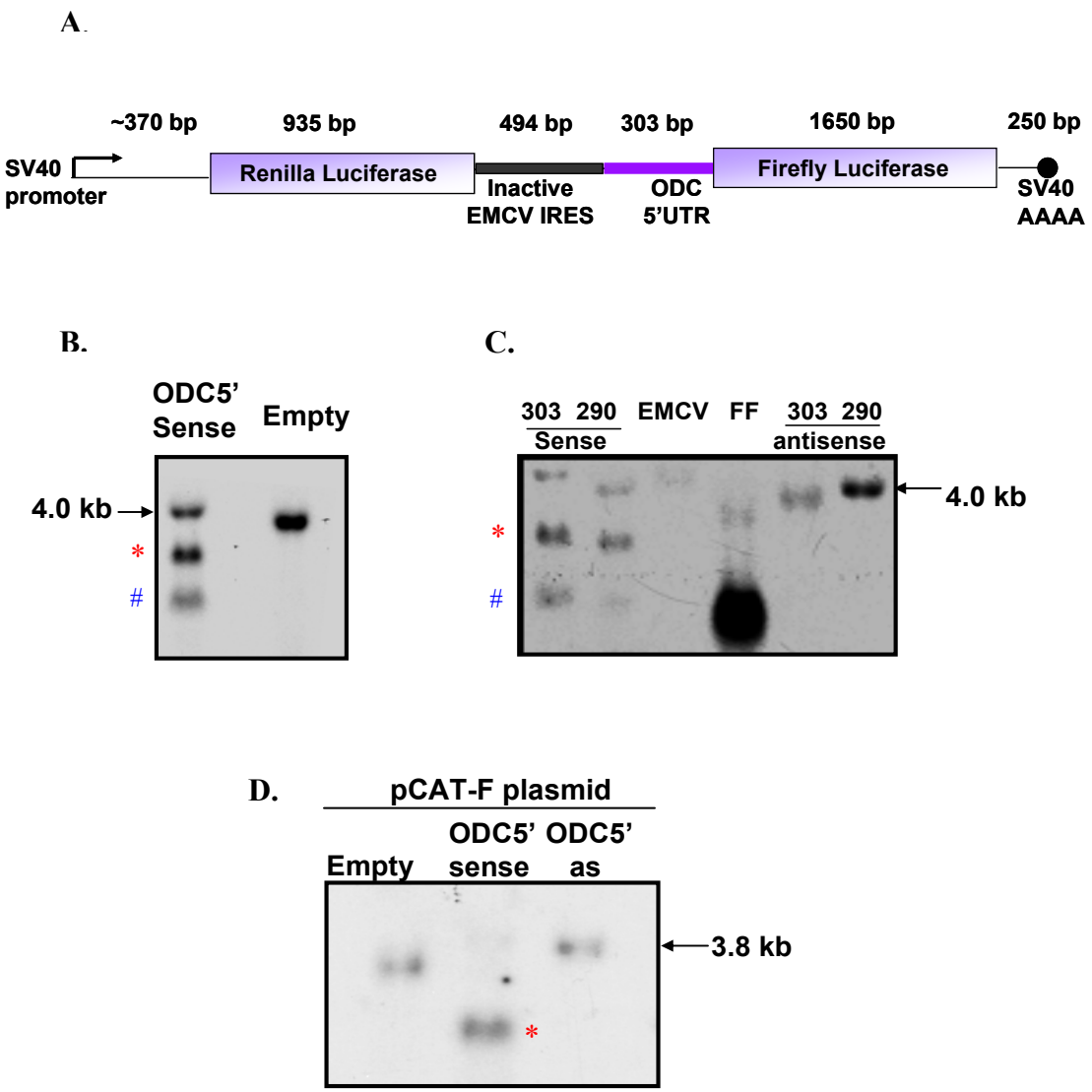

Figure 4.14: Spurious splicing of pRΔEF –ODC 5'UTR bicistronic RNA

(See next page for figure legend)

Figure 4.14: Spurious splicing of pRΔEF-ODC 5'UTR bicistronic RNA.

To analyze integrity of the pRΔEF-ODC 5'UTR, cells were transfected with either the empty or 303bp sense and antisense or 290bp sense and antisense and EMCV IRES containing bicistronic plasmids into the Ras12V cells. 24 hrs following transfection, RNA was isolated from the transfected cells and 20µg of total RNA was loaded per lane and northern analysis was carried out as described in Methods.

(A) Schematic represents the entire length of the pRΔEF bicistronic transcript and the sizes of the reporter sequences, promoter and ODC 5'UTR. Arrow indicates the direction of transcription.

(B) Northern blot analysis of 303bp ODC 5'UTR pRΔEF bicistronic RNA compared to the empty vector. Expected size of the full length transcript is about 4kb. * represents an additional transcript about 2.5kb in length and # represents another transcript about 1.7 kb in length representing products of non-specific splicing.

(C) Northern analysis of 303bp sense and antisense, EMCV IRES and 290bp ODC 5'UTR sense and antisense pRΔEF bicistronic RNA. FF represents Firefly luciferase expressing monocistronic plasmid which was also transfected into the Ras12V cells and utilized as a size marker in the northern analysis.

(D) Northern analysis of bicistronic RNA where the Renilla luciferase reporter in the pRΔEF plasmid was replaced with a CAT reporter (pCAT-F). Empty pCAT-F RNA was compared to pCAT-F RNA containing ODC 5'UTR in either the sense or antisense (as) orientation. * represents an additional 2.5 kb transcript other than the expected 3.8kb transcript.

also in that the pcDNA 3.0 plasmid has a CMV promoter and enhancer instead of the SV40 promoter and enhancer present in the pRΔEF plasmid (Bert et al., 2006). The type of promoter/enhancer could make a difference as a recent report showed that the SV40 enhancer associated with the pRΔEF plasmid also contributes to the non-specific splicing (Bert et al., 2006). These results and observations thus suggest that the plasmid backbone and possibly the type of promoter/enhancer could contribute to non-specific splicing that has been consistently reported with the pRΔEF bicistronic plasmid containing cellular 5'UTRs (Holcik et al., 2005).

Additional control to confirm ODC has IRES mediated translational activity

Cellular genes that contain IRES elements utilize the IRES mode of translation under specific conditions such as apoptosis or during the G2-M phase of cell-cycle, when cap-dependent translation is in an inefficient state (Spriggs et al., 2005). The earlier results in this chapter show that ODC has an IRES activity that is induced in response to Ras and is under the control of G2-M phase of cell-cycle in control RIE-1 cells. To further confirm that ODC has a true IRES, IRES-mediated translational activity of ODC was also assayed during apoptosis when cap-dependent translation is inhibited (Spriggs et al., 2005). Apoptosis was induced in Ras12V cells by treating the cells with staurosporine. Induction of apoptosis was confirmed by cleavage of Poly (ADP-ribose) polymerase (PARP), a nuclear enzyme that during apoptosis is cleaved by caspases into a 89 kDa, and a 24 kDa fragment (Duriez & Shah, 1997). Treatment with staurosporine was effective in cleaving PARP within 4 hrs, suggesting that the cells were undergoing apoptosis at this time point (Fig 4.15A).

Another characteristic of apoptosis is the cleavage of translation initiation factor eIF4G

into 150 kDa and 76 kDa fragments, which has the critical consequence of global inhibition of cap-dependent translation (Clemens et al., 2000). Treatment with staurosporine caused a mild reduction in the full length 220 kDa eIF4G levels at 8 hrs, further confirming that the cells are undergoing apoptosis and also suggesting a possible inhibition of cap-dependent translation (Fig 4.15B). Interestingly after 4 hrs of staurosporine treatment ODC IRES activity was stimulated to about 2-fold and doubled thereafter at 8hrs in comparison to the DMSO treated controls (fig 4.15B). This stimulatory effect was limited to cap-independent translation, since cap-dependent translation measured by Renilla luciferase activity was unaltered at both 4 and 8hrs of treatment when compared to the DMSO treated controls (Fig 4.15C). These results suggest that ODC has an IRES activity that is also induced under conditions of apoptosis when cap-dependent translation is inhibited.

To analyze if this stimulated IRES activity of ODC contributes to maintain the overall synthesis of ODC protein under apoptotic conditions, we measured ODC activity at 4 and 8 hrs of staurosporine treatment (data not shown). However, unlike the IRES activity, total ODC activity decreased at 4 hrs and further at 8 hrs (data not shown) suggesting that the contribution of IRES-mediated translation of ODC is not sufficient to maintain the elevated ODC activity in the Ras12V cells. However, it is possible that the IRES activity is sufficient to maintain the basal ODC activity when cap-dependent translation is inhibited. Another report that cap-independent translation of ODC could be stimulated during apoptosis comes from a recent microarray study that found ODC as one of the RNAs translated efficiently by associating with the heavier polysomal fractions during a TRAIL (TNF-related apoptosis inducing ligand) induced apoptotic condition (Bushell et al., 2006). However, in our

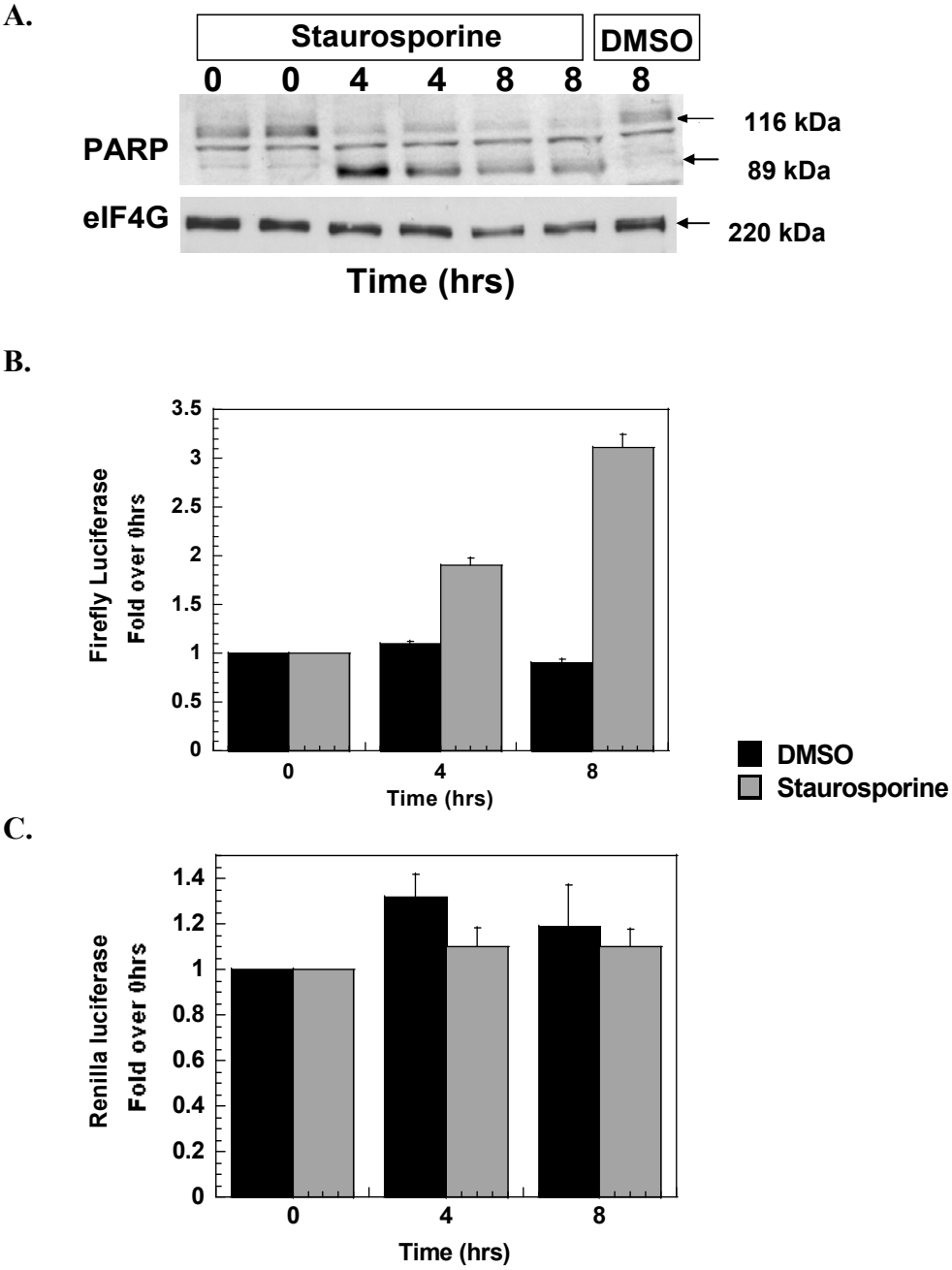

Figure 4.15. Effect of apoptosis on ODC IRES activity

(See next page for figure legend)

Figure 4.15. Effect of apoptosis on ODC IRES activity

Ras12V cells were transfected with the 303bp bicistronic plasmid as described in fig 4.3 and 24 hrs following transfection, apoptosis was induced by treating the cells with 1μM (final) staurosporine and DMSO was used as the vehicle control. Immediately after adding staurosporine, cells were rinsed and analyzed as time 0 hrs and samples were also collected 4 or 8 hrs after staurosporine treatment. Luciferase activities and western blot analysis was carried out as described in Methods. The entire experiment was repeated twice.

(A) Western blot analysis was carried out using antibodies against PARP and full-length eIF4G (220 kDa). 116 kDa represents full-length PARP and 89kDa represents the major cleaved product of PARP during apoptosis.

(B) Graph represents Firefly luciferase activity (ODC IRES) expressed as a fold over 0 hrs of staurosporine or DMSO treatment and the activities were measured at the indicated time points.

(C) Graph represents Renilla luciferase activity (cap) expressed as a fold over 0 hrs of staurosporine or DMSO treatment and the activities were measured at the indicated time points.

model of staurosporine induced apoptosis we did not observe any induction of ODC protein synthesis as measured by ODC activity. It is possible that the mode of inducing apoptosis either by staurosporine or TRAIL and the type of caspase signaling cascade activated could impact the overall synthesis of ODC protein. Alternately, apoptosis may alter the stability of ODC RNA transcript, which could result in a reduction of ODC activity, irrespective of the increase in efficiency of IRES-mediated translation.

Discussion

ODC RNA studied previously in rat pancreatic carcinoma cells has been reported to contain several 5'UTR splice variants that exhibit IRES activity (Pyronnet et al., 1996). Analysis of the ODC 5'UTR in both RIE-1 and Ras12V cells identified the presence of four alternate splice variants of 273, 286, 290 and 303bp in length that differed from each other in the presence or absence of an additional +13 or +17 intronic sequence. This is the first report of these splice variants in normal, non-transformed rat cells. Normal pancreatic acinar cells expressed only the 273bp species (Pyronnet et al., 1996), and this was also the species first identified in rat (Manzella & Blackshear, 1990).

ODC belongs to a unique subset of mRNAs that are characterized by a long GC-rich 5'UTR with a complex secondary structure. Such long structured 5'UTRs are in general inhibitory to cap-dependent translation, but can allow translation under specific conditions through a cap-independent, IRES-mediated mechanism (Kangas et al., 1998; Pyronnet, 2000; Saito et al., 2000). Analysis using a bicistronic plasmid assay confirmed that all of the observed 5'UTR variants contained active IRES sequences, and IRES-mediated activity was markedly activated in cells transformed by Ras. In both the Ras-transformed and non-transformed cells, the presence of both the +17 and +13 intronic sequences produced the strongest IRES activity. This may be attributed to the presence of a pyrimidine rich sequence in both the +17 and +13 intronic sequence, with sequence similarities to certain viral IRES elements (Pyronnet, 2000).

While IRES activity was observed in both Ras12V and parental control cells, the efficiency of IRES activities among the four splice variants differed depending on the cell line. Specifically, in Ras12V cells the IRES activity generally increased with increasing

length of the 5'UTR sequence. In contrast, the +13 species exhibited less efficient IRES activity than either the +17 species or the intronless 273bp species in non-transformed cells. A possible explanation is that certain inhibitory IRES transacting factors that can recognize the sequences in the +13 intron are up-regulated in non-transformed cells in comparison to the Ras12V cells. Precedence for such a possibility is a recent report on a rhinovirus IRES inserted into the poliovirus genome (Merrill et al., 2006). Expression from this rhinovirus IRES was shown to be regulated in a cell-specific manner by a DRBP76 RNA binding IRES transacting factor, which upon binding inhibited its IRES activity (Merrill et al., 2006). While DRBP76 was expressed in both neuronal and cancerous glioma cells, it bound to rhinovirus IRES only in the normal neuronal cells, thus enhancing IRES activity in malignant glioma cells (Merrill et al., 2006; Merrill & Gromeier, 2006).

Intriguingly, several known IRES transacting factors are also factors associated with aberrant splicing under cancerous conditions (Venables, 2006). Our studies found such a difference in splice variant abundance, with the distribution of ODC 5'UTR splice variants 290bp and 303bp species being more abundant in Ras12V cells in comparison to the normal RIE-1 cells. Although the difference was moderate, it may have a significant functional consequence to overall ODC activity in Ras12V cells, as both these splice variants exhibited increased cap-independent translational activity in comparison to the other two variants, and ODC IRES activity of all the splice variants was clearly increased in response to Ras transformation. Certain IRES transacting factors such as PTB and HnRNPA1 have been shown to exhibit increased activity in specific types of cancers (Venables, 2006). Although neither of these factors was found to regulate ODC IRES

activity *in vitro* (Pyronnet et al., 2005), detailed cell-specific analysis must be carried out to identify ODC IRES trans-acting factors.

It is also noteworthy that the fold increase in ODC IRES activity in comparison to the empty bicistronic plasmid is more pronounced in both cell lines used in the current studies in comparison to a previous report in HeLa cells (Pyronnet, 2000; Pyronnet et al., 2005). A possible explanation is that the HeLa cells are of human origin and these splice variants have been derived from the rat. Earlier studies have specified cell-type differences in IRES regulating factors (Merrill et al., 2006). As this study was carried out in RIE-1 cells using splice variants derived from the same cell type, ODC IRES activity measured may be in a more physiologically relevant context.

To determine which Ras effector pathways regulate ODC IRES activity, inhibitors were used to target the MEK, PI3K or mTOR signaling intermediates. Compared to vehicle-treated controls, cap-independent translation was decreased by more than 50% in the presence of LY294002 or Rapamycin in parental RIE-1 cells. This was accompanied by an increase in the number of G1 phase cells, and a corresponding decrease in S-phase and G2-M phase cells. These results are in agreement with previous studies suggesting that ODC IRES activity is induced during the G2-M phase of the cell cycle (Pyronnet, 2000), and further suggest that the ODC IRES is positively controlled by the PI3K pathway in non-transformed control cells (Fig 4.16). In contrast, these inhibitors had no effect on cell cycle distribution in Ras-transformed cells, and did not alter IRES activity (Fig 4.16). The resistance of Ras-transformed cells to cell cycle arrest by these inhibitors implies that the PI3K pathway fails to respond appropriately to inhibitory signals, allowing IRES-mediated ODC translation to proceed in the rapidly proliferating

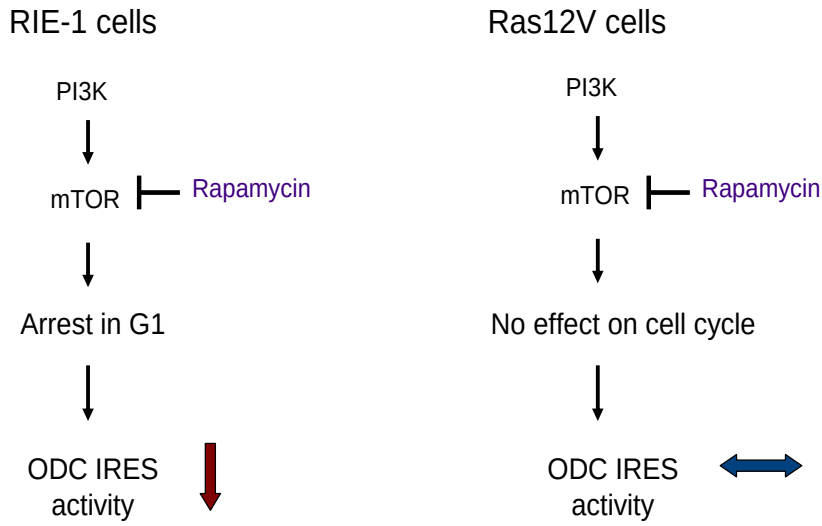

Figure 4.16. Schematic represents the effect of Rapamycin on ODC IRES-mediated translational activity.

Treatment of non-transformed RIE- cells with the mTOR inhibitor Rapamycin results in the expected cell-cycle arrest in the G1 phase and consequently down-regulates ODC IRES activity. However, in the Ras transformed cells Rapamycin unexpectedly has no effect on cell-cycle and as a result has no effect on the translation of ODC via the IRES. These results suggest that the PI3K pathway regulates ODC IRES activity through its effects on the cell-cycle progression.

Ras-transformed cells. However, inhibition of PI3K or mTOR causes ODC activity to be reduced by about 50-60% in Ras12V cells, supporting a regulatory role for this pathway in control of cap-dependent ODC translation through 4EBP1 in the Ras-transformed cells.

Inhibition of MEK using PD98059 did not significantly affect the number of G2-M phase cells in either cell line, yet surprisingly increased ODC IRES activity by about two-fold in both the control and Ras12V cells. These results suggest that the ODC IRES can be negatively regulated by the Raf/MEK/ERK pathway, and this effect appears to be independent of the transformed status of the cells (Fig 4.17A). It is possible that a specific trans-acting factor is repressed by this pathway, and is released upon inhibition. A recent study showed enhancement of Hepatitis C viral IRES-mediated translation also in the presence of PD98059 (Murata et al., 2005). To expand these results, cells were treated simultaneously with the MEK inhibitor and either LY294402 or Rapamycin. IRES activity in control cells was inhibited by this treatment, suggesting that the PI3K-pathway may have a dominant role in regulating the ODC IRES in the non-transformed cells (Fig 4.17B). On the other hand, the increased ODC IRES activity was maintained in the Ras12V cells subjected to either inhibitor combination, suggesting the Raf-controlled pathway dominates in Ras-transformed cells (Fig 4.17B).

A previous study showed that both Myc and CyclinD1 IRES elements are positively regulated by the MEK and p38 MAPK pathways (Shi et al., 2005). However, no compensation by p38 MAPK takes place in our system, and p38 MAPK levels are extremely low in both cell line. To assess the contribution of eIF4E phosphorylation to ODC IRES activity, a specific Mnk inhibitor was used. The Mnk1/2 kinases are activated

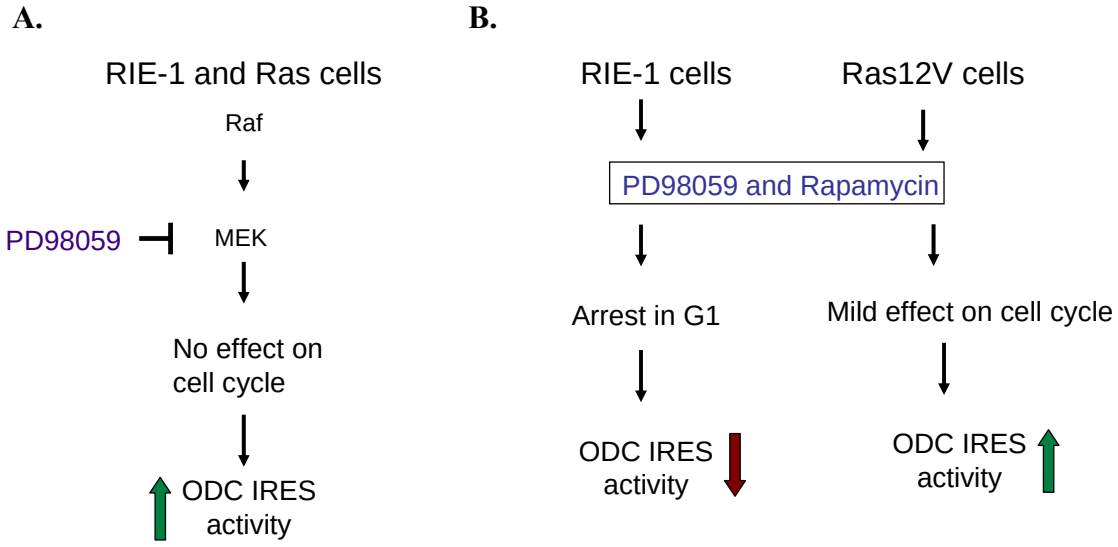

Figure 4.17. Schematic represents the regulation of cap-independent translation of ODC by both the Raf-kinase and PI3K pathways.

(**A)** Inhibition of the Raf-kinase pathway up-regulated ODC IRES activity in both the Ras and RIE-1 cells and this effect was independent of the effects on cell-cycle.

(B) Inhibition of both the Raf-kinase and PI3K pathways arrested the non-transformed RIE-1 cells in the G1 phase and consequently down-regulated ODC IRES activity suggesting that the predominant regulator of ODC IRES activity in these cells is the PI3K pathway. On the other hand, in the Ras transformed cells, inhibition of both these pathways had only a mild effect in arresting cell-cycle progression, and the ODC IRES activity remained induced suggesting that the Raf-Kinase pathway is the chief regulator of ODC IRES activity in these cells.

by ERK and/or p38 MAPK, with Mnk1 regulating inducible phosphorylation of eIF4E and Mnk2 affecting basal phosphorylation levels (Ueda et al., 2004). The low p38 MAPK levels in both cell lines described here suggest that Mnk1 appears to be controlled almost entirely by the Raf/MEK/ERK pathway. Thus, using a Mnk inhibitor would replicate the effects of PD98059 on phosphorylation of eIF4E, without affecting the upstream components of the Raf/MEK/ERK pathway. Interestingly, inhibition of Mnk enhanced ODC IRES activity significantly, suggesting that changes in eIF4E phosphorylation contribute to ODC IRES regulation.

To further understand the role of eIF4E phosphorylation in regulating ODC IRES activity, 4E-P2 cells were treated with the Mnk inhibitor. These cells stably over-express eIF4E, resulting in cellular transformation, and we and others have shown previously that ODC translation is increased as a result of this over-expression (Rousseau et al., 1996), (Shantz,1999). When Mnk was inhibited in these cells, we observed a dose-dependent increase in ODC IRES activity that was directly correlated with levels of phosphorylated eIF4E, but again was unrelated to the percent of G2-M phase cells. Such a robust effect of eIF4E dephosphorylation on IRES-mediated translation of ODC in these cells points to a direct relationship between eIF4E phosphorylation and regulation of the ODC IRES, which can only be inferred in the Ras-transformed cells, due to the multitude of downstream targets activated by Ras.

The role of phosphorylation in regulating the functions of eIF4E is still the topic of debate, especially since Mnk1/2 double knockout mice did not reveal any significant growth or developmental defects(Ueda et al., 2004). However, these findings do not negate the possibility of functional involvement of phosphorylation of eIF4E in specific

physiological situations (Ueda et al., 2004). Phosphorylation of eIF4E is generally thought to decrease its affinity for the cap, and this has been interpreted to have positive and negative effects on translation (Herbert et al., 2000; Knauf et al., 2001; Lachance et al., 2002; Scheper et al., 2002; Walsh & Mohr, 2004). The effect of eIF4E dephosphorylation was previously correlated with stimulating the IRES activity of an egg-laying hormone (ELH) in Aplysia neurons after an afterdischarge (AD) (Dyer et al., 2003; Ross et al., 2006). After an AD, Aplysia neurons exhibited increased dephosphorylation of eIF4E and a global reduction in cap-dependent translation, but conversely stimulated IRES activity of ELH (Dyer et al., 2003). Inhibition of cap-dependent translation upon eIF4E dephosphorylation may increase the availability of specific translation initiation factors such as eIF4G and eIF4A to carry out cap-independent translation. In addition, eIF4E has been shown to be dephosphorylated during the G2-M phase of the cell cycle (Pyronnet et al., 2001), perhaps further correlating eIF4E phosphorylation with regulation of ODC IRES activity.

In summary, the studies described here show for the first time that cap-independent translation of ODC can be activated in response to Ras transformation, and is differentially controlled by elements downstream of Ras in both normal and Ras-transformed RIE-1 cells. The IRES element appears to be regulated by the phosphorylation status of eIF4E, and dephosphorylation of eIF4E either by MEK or Mnk1/2 inhibition increases ODC IRES activity in both cell lines. In situations where both the Raf/MEK/ERK and PI3K/mTOR pathways are inhibited in normal cells, ODC IRES activity is very low, and most cells arrest in G1. However, when both of these pathways are inhibited in Ras-transformed cells, cell cycle arrest does not occur and ODC

IRES activity is induced, thus helping to maintain high ODC activity. While these studies do not address the relative contribution of cap-dependent versus cap-independent translation of ODC in Ras-transformed cells, even a minor contribution to ODC translation by a cap-independent mechanism under transformed conditions may help ensure maintenance of elevated polyamine content in these rapidly growing cells.

Chapter V

Identification of genes regulated by antizyme to inhibit MEK-induced tumorigenesis

Specific Aim: To use a genomic approach to identify genes that are regulated by antizyme (an endogenous inhibitor of ODC), that are important for its tumor suppressor properties in MEK-induced skin tumors

Introduction

Several *in vivo* models have shown ODC to be an essential mediator of Ras transformation (Feith et al., 2005; Feith et al., 2006; Hayes et al., 2006; Megosh et al., 1998; Smith et al., 1998). ODC has been shown to cooperate with Ras to induce spontaneous tumor formation in a transgenic mouse model that over-expresses ODC from a K6 (Keratin 6) skin promoter (Hayes et al., 2006; Smith et al., 1998). One of the prominent pathways regulating ODC in response to Ras is the Raf-MEK-ERK pathway (Shantz, 2004). Previous results from our lab have shown that activation of MEK can induce ODC activity *in vivo* and this induction is necessary for tumorigenesis (Feith et al., 2005; Feith et al., 2006). Transgenic mice over-expressing MEK from a K14 (Keratin 14) skin promoter developed spontaneous tumors, which could be inhibited by treating the mice with DFMO, an irreversible inhibitor of ODC (Feith et al., 2005).

Further evidence for the vital role of ODC in Ras-mediated tumorigenesis was obtained, when expression of antizyme (AZ), an endogenous inhibitor of ODC, inhibited tumor formation induced by MEK in the K14-MEK mice (Feith et al., 2006). AZ is a highly regulated target of polyamines. AZ expression is induced by high levels of polyamines and in turn, it checks polyamine levels by down-regulating their synthesis through inhibition of ODC activity (Hayashi et al., 1996; Murakami et al., 1992; Murakami et al., 1989). AZ dimerizes with ODC to prevent the formation of enzymatically active ODC homodimers and targets it for degradation by the proteasome (Coffino, 2001a; Murakami et al., 1992). It also maintains the polyamine levels by inhibiting their transport into the cell (Suzuki et al., 1994).

Since AZ inhibits ODC and consequently down-regulates polyamine levels, its

effects on inhibiting tumorigenesis were analyzed *in vivo* by crossing the K14-MEK mice with mice expressing AZ from a K5 and a K6 promoter (Feith et al., 2006). K5 and K14 are comparable promoters as they are expressed in the same layers of skin, the outer root sheath (ORS) and interfollicular epidermis. The K6 promoter, when unstimulated, is expressed in very low levels in the ORS but in response to hyperproliferation stimulus such as that provided by MEK its expression is induced, thus ensuring that the cells expressing MEK are also expressing AZ (Powell et al., 1991). Supporting the tumor-suppressor functions of AZ, the MEK/K5-AZ and MEK/K6-AZ transgenic mice developed fewer tumors and had delayed tumor formation in comparison to the K14-MEK mice (Fig 5.1A) (Feith et al., 2006).

A possible mechanism for reduced tumorigenesis in these mice involves increased transit through the G2-M phase of cell-cycle, suggested by a decrease in the number of cells in mitotic phase and a smaller decrease in the number of cells in the S phase of the cell-cycle (Feith et al., 2006). The double transgenic mice also had reduced ODC activity in tumors, suggesting that the effects of AZ in suppressing MEK-induced tumorigenesis could be mediated by down regulating polyamines (Feith et al., 2006) (Fig 5.1B). Recent studies have shown that AZ may have targets other than ODC, such as Cyclin D1 and Smad1, although levels of Cyclin D1 were not altered in the MEK/AZ mice in comparison to the K14-MEK mice (Feith et al., 2006). To identify such AZ regulated targets that contribute to its anti-tumorigenic properties, we carried out a genomic analysis to determine any differences in the genetic profiles of MEK/K5-AZ and MEK/K6-AZ tumors compared to tumors with MEK expression only.

In this study, microarray analysis revealed that the expression of AZ from the K6

promoter altered the expression of a greater number of genes by at least 2-fold in the MEK-induced tumors in comparison to AZ derived from the K5 promoter. This perhaps reflects the more general expression of the K6 promoter in the tumor tissue. To further characterize the genes altered, we carried out a preliminary analysis by selecting four genes; each involved in a distinct set of cellular processes and validated the changes in their expression levels using real-time PCR.

A.

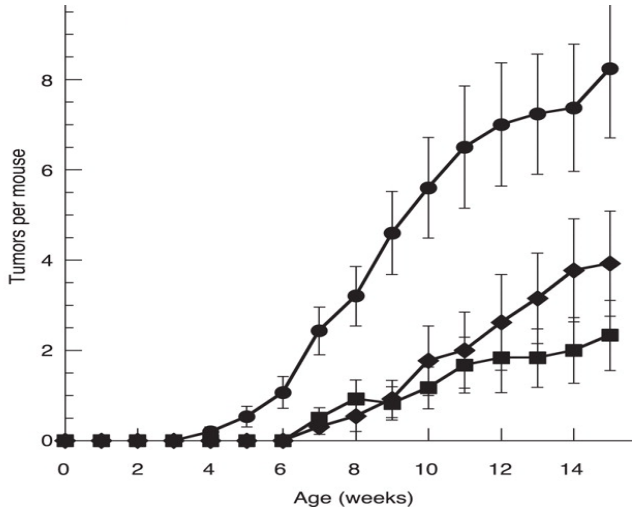

B.

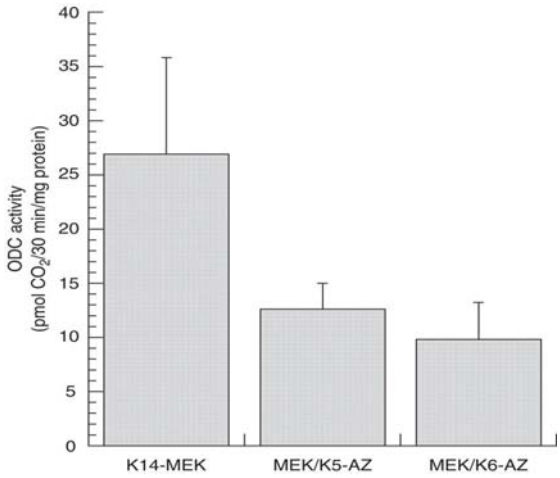

Figure 5.1. Tumor incidence and ODC activity in MEK/K5-AZ and MEK/K6-AZ mice compared to K14-MEK mice (Feith et al., 2006).

Study by Feith *et.al.*(Feith et al., 2006), **(A)** shows the number of tumors formed in K14-MEK mice (filled circle, $N = 30$), double transgenic MEK/K5-AZ mice (filled square, $N = 12$) and MEK/K6-AZ mice (filled diamond, $N = 13$). **(B)** ODC activity was measured in tumors from K14-MEK mice ($N = 6$), MEK/K5-AZ mice ($N = 5$) and MEK/K6-AZ mice ($N = 4$) (Feith et al., 2006).

Materials and Methods:

Breeding and handling of transgenic mice

K14-MEK males on the ICR background were backcrossed with C57BL/6J non transgenic females for at least 5 generations to obtain K14-MEK mice on the C57BL/6J background. K14-MEK males were then bred with K5-AZ and K6-AZ transgenic females on the same C57BL/6J background to reduce genetic variability, and the genotype of pups was determined by PCR analysis on DNA isolated from tail clips as described (Feith et al., 2006) .

RNA isolation from tumors

To isolate tumors, mice were sacrificed at 14-16 weeks of age. Isolated tumors were rapidly frozen in liquid nitrogen and RNA was isolated from tumor sections weighing approximately 50-100 mg. Frozen tumors were crushed rapidly in an ice-cold mortar using a pestle and immediately transferred to an ice-cold eppendorf tube filled with 750µl ice-cold Trizol (Invitrogen). Keeping extracts on ice and using a hand-held homogenizer (Thomas Sci), the extracts were briefly homogenized and 250 µl ice-cold Trizol was added to make the total volume to 1ml. Samples were then briefly spun at 13000 rpm, 4°C for 10min to remove debris. The supernatant was transferred to a new eppendorf tube and RNA was isolated exactly as per Trizol kit instructions (Invitrogen). RNA was dissolved in a final volume of 50 µl nuclease free water. Quality of RNA was assessed using the Agilent 2100 Bioanalyzer (Agilent) by the Penn State University Functional Genomics core facility. Once quality was confirmed, 3 µg of total RNA extracted from each of four mice was combined as one 12 µg sample for each genotype. Tumors were combined from 2 males and 2 females for the MEK and MEK/K6-AZ genotype and from

3 females and 1 male for the MEK/K5-AZ genotype.

Microarray analysis

Chip analysis was performed by Genome Explorations Inc. For hybridizations, Affymetrix mouse 430 2.0 chips were used. These chips contain 45000 probe sets, which recognize more than 34000 mouse genes (Affymetrix). Using 12 μg of total RNA for each genotype first and second strand cDNA was synthesized using a cDNA synthesis kit (Invitrogen). Biotinylated cRNA was synthesized using the Bioarray High yield RNA labeling kit (Enzo Diagnostics). cRNA was hybridized to the chip by incubation at 45°C for 16hrs, washed and stained with phycoerythrin-conjugated streptavidin. The fluorescent images were scanned using the GCS 3000 high-resolution confocal laser scanner (Affymetrix).

Scanned chip images were analyzed using the Gene Chip Operating System v1.2 (GCOS; Affymetrix) software and also confirmed by Gene Spring software analysis (Silicon Genetics). Data were analyzed as described previously (Lockhart et al., 1996). Eleven probe pairs were used for each transcipt and each pair consisted of a perfect match and a mismatch probe. Signal intensity for each gene was calculated as the average intensity difference, represented by [Σ(PM - MM)/(number of probe pairs)], where PM and MM denote perfect-match and mismatch probes.

Real-Time PCR

2μg of pooled RNA used for microarray analysis was also used for synthesis of cDNA using the Superscript first strand cDNA synthesis kit (Invitrogen) as per the manufacturer's instructions. Samples were analyzed by relative real-time PCR as per Quantitect Sybr green PCR kit instructions (Qiagen). 1/12 th of the cDNA was used for

sample measurements. For standard curve analysis a combination of equal volumes of MEK and MEK/K6-AZ cDNA diluted 1 to 4 was used as the starting dilution and diluted eight times thereafter to set up a dilution series. Primers used for validating the genes are as follows:

Egr-1 forward 5'GCAGGCACAGCCTTGCAG 3'

Egr-1reverse 5'GCTCAGGTCTCCCTGTTGTTG-3',

β-Catenin forward 5'GCTTCCAGACATGCCATCATG 3'

β-Catenin reverse 5'GGTTGTGCAGAGTCCCAGC 3'

Cdkn2b forward 5'GTAGATGAGAGGCACTGAAGTG 3'

Cdkn2b reverse 5'CTTGTCGAGCTGGAGGTGAC 3'

Cyclophilin forward 5'GCAGGTCCATCTACGGAGAG 3'

Cyclophilin reverse 5'CTGGGAACCGTTTGTGTTTGG3',

Tgf-β1 forward 5'CGTCACTGGAGTTGTACGGC 3'

Tgf-β1 reverse 5'GATCCCGTTGATTTCCACGTG 3'

PCR reactions and data analysis were carried out using the Applied Biosystems real-time PCR 7300 system (Genomic Core Facility, HMC, Penn State University) using PCR conditions as follows: Denaturation 95°C-15 sec, annealing 57°C-30sec, elongation 72°C-30sec and the cycle was repeated 39 times.

Results

Changes in global gene expression profiles

Microarray analysis was carried out to determine variations in gene expressions between the genotypes MEK, MEK/K5-AZ and MEK/K6-AZ. To minimize biological variation between samples, RNA was pooled from four different mice to generate one sample per genotype. The number of genes that were changed significantly and at least 2-fold was higher in comparisons between MEK/K6-AZ and MEK mice than between MEK/K5-AZ and MEK mice. The majority of these genes were down-regulated rather than up-regulated in the MEK/K6-AZ tumors in comparison to the MEK-induced tumors (Table 5.1). However, several interesting genes were up-regulated especially a subset of immediate early transcription factors (Table 5.2). Several of these genes were identified as involved in processes such as translation initiation, transcription, cell-cycle progression, Wnt signaling and TGF-β signaling pathways, suggesting that inhibition of ODC by AZ could regulate these processes (Table 5.2). Very few of these genes such as the translation initiation factors eIF2A and eIF4A, were found to be down-regulated in tumors from both MEK/K5-AZ and MEK/K6-AZ in comparison to MEK. This suggests that these genes respond to AZ irrespective of any variations in expression levels of AZ (Table 5.2), especially since the AZ levels in tumors from MEK/K5-AZ mice were very low (Feith et al., 2006).

Validating gene expression changes using real-time PCR

To validate genes using real-time PCR four genes, each belonging to different pathways, were selected. Cyclophilin, which was found to be unaltered between the two genotypes MEK/K6-AZ and MEK, was selected as the normalization control

Genotype comparisons	Genes changed at least 2- fold	
	Down	Up
MEK/K5-AZ vs. MEK	108	174
MEK/K6-AZ vs. MEK	795	186
MEK/K6-AZ vs. MEK/K5-AZ	630	211

Table 5.1. Comparison of genes changed at least 2-fold between genotypes MEK, MEK/K5-AZ and MEK/K6-AZ

Table represents a comparison between genotypes carried out using a statistically significant 2-fold change as the cut-off.

	MEK/K6-AZ vs. MEK	MEK/K5-AZ vs. MEK
Translation factors		
eIF2A	3.2	2.5
PKR	2.1	< 2
eIF4A1	5.6	2.6
Wnt signaling pathway		
Fzd6	4.6	< 2
beta -Catenin	8	< 2
Dishevelled	3	< 2
Wisp1	< 2	2
Immediate early transcription factors		
Egr -1	2.2	< 2
Egr -2	2.1	< 2
Fos	3.7	< 2
G1/S phase transition factors		
Cdkn2b	2.2	< 2
Trp53	2.6	< 2
Tgf -β signaling pathway		
Tgf β1	3	< 2
Stat1	2.1	< 2
Stat3	2.5	< 2

Table 5.2. Analysis of fold-change in genes belonging to specific functional categories

Table displays a subset of genes categorized based on function and the fold change in their expression levels in MEK/K6-AZ and MEK/K5-AZ tumors in comparison to MEK tumors. Genes whose expression between genotypes compared did not change above 2-fold are represented as < 2. Those increased are represented in red and those decreased are represented in green.

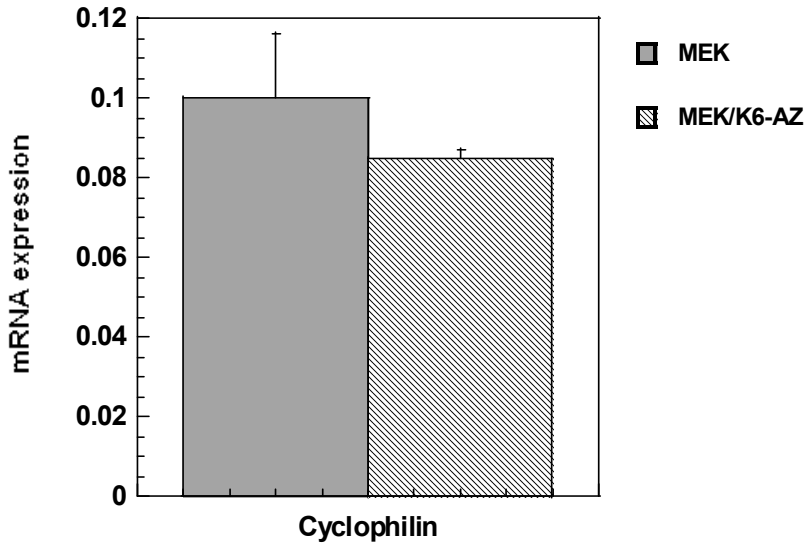

Figure 5.2. Analysis of Cyclophilin as a normalization control for quantitation by real-time PCR

Real-time PCR analysis was carried out as described in Methods. Graph represents the average of 3 experiments and quadruplicate samples were measured for each PCR run. The expression levels of Cyclophilin were not found to be significantly different between MEK and MEK/K6-AZ with p=0.36 (not significant) as determined by a two-tailed T-test.

(Fig 5.2). One of the genes selected was β-Catenin, which is a key player in the Wnt (wingless-type MMTV integration site family member) signaling pathway, and our genomic analysis also revealed changes in a few other members of the Wnt pathway such as Frizzled (Fzd) and Disheveled (Dsh) (Table 5.2) (Barker & Clevers, 2000; Barker & Clevers, 2006). Wnt ligand, upon binding to its receptor Fzd inhibits proteosomal degradation of β-Catenin, which then translocates into the nucleus to activate the Tcf/Lef transcription family (Barker & Clevers, 2006). Unchecked activation of this pathway is associated with tumorigenesis in several types of cancers (Barker & Clevers, 2006; Larue & Delmas, 2006; Lee et al., 2006; Segditsas & Tomlinson, 2006). Genomic analysis revealed an 8-fold decrease in β-Catenin levels in the MEK/K6-AZ tumors compared to MEK (Table 5.2). Real-time PCR analysis confirmed the decrease in β-Catenin RNA levels but only a 3-fold change was observed (Fig 5.3). However, the decrease in β-Catenin levels suggests that the Wnt signaling pathway could possibly be regulated by AZ.

One other gene found to be down-regulated in the MEK/K6-AZ tumors when compared to the MEK tumors is Tgf-β1 (Tumor growth factor beta1), which was selected for further validation. Tgf-β1 belongs to a family of ligands including Tgfβ2 that bind to Tgf binding receptors and activate the Smad family of transcription factors (Derynck et al., 2001; Miyazono et al., 2003). Tgf-β1 is an interesting target to examine as it is involved in cancer as a tumor suppressor at the initial stages of cancer formation and as a promoter of tumor invasiveness at later stages of tumor growth (Derynck et al., 2001; Miyazono et al., 2003). However, the 3-fold decrease in Tgf-β1 transcript levels in the MEK/K6-AZ tumors compared to MEK as determined by chip analysis (Table 5.2) could

not be validated as a significant change using real-time PCR analysis, suggesting that Tgf-β1 may not be implicated in AZ-mediated inhibition of tumorigenesis. The reason for this difference is not known, but it could reflect an instability in the Tgf β1 RNA, since the same sample used for the array analysis was also used for real-time PCR analysis but after a few cycles of freezing and thawing.

The other two genes selected were Egr-1 and Cdkn2b, which were each increased by 2.2 fold in the MEK/K6-AZ tumors in comparison to MEK (Table 5.2). Egr-1(Early growth response-1) is a transcription factor that is induced as an immediate-early gene that responds to growth factor stimulation. It has been implicated as a tumor-suppressor gene that is down-regulated by Ras activation to facilitate cancer formation (Lucerna et al., 2006; Shin et al., 2006). Cdkn2b (Cyclin dependent kinase inhibitor 2b), also known as p15Ink4B, is an inhibitor of a cell-cycle dependent kinase (Cdk4/6) that regulates the transition from G1 to S phase of cell-cycle (Lee & Yang, 2001). Deletions and silencing methylation in this gene have been implicated in carcinogenesis, especially in the later stages of cancer progression (Krug et al., 2002; Okuda et al., 1995). Both Egr-1 and Cdkn2b were confirmed to be enhanced by real-time PCR analysis, with Egr-1 RNA exhibiting a 3 fold increase and Cdkn2b only about a 1.3 fold increase. However, this was found to be a significant difference in the MEK/K6-AZ tumors compared to MEK (Fig 5.3). These results are noteworthy as both these genes are considered as suppressors of tumor formation and both are up-regulated upon AZ expression in skin tumors.

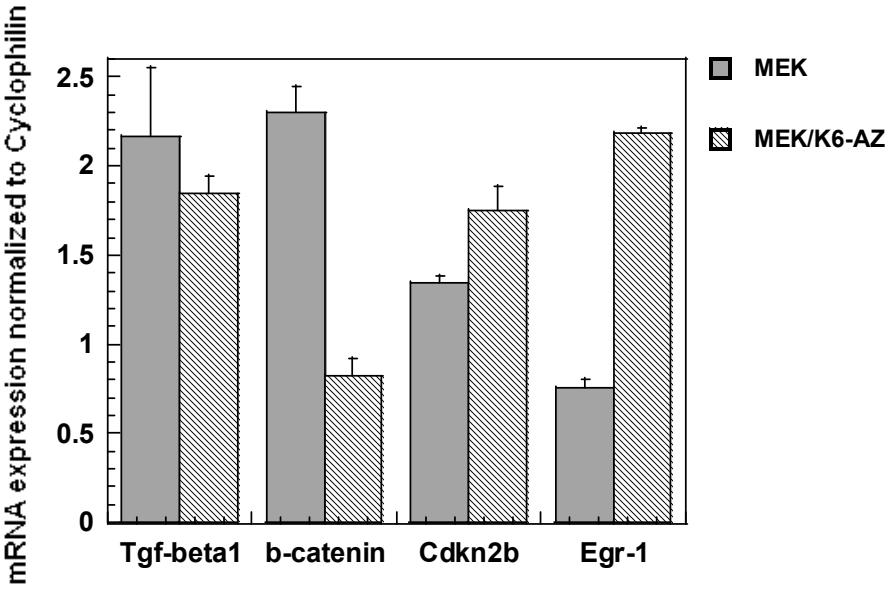

Figure 5.3. Relative expression levels of genes selected for validation as determined using real-time PCR

Real-time PCR analysis was carried out as described in Methods. Y-axis represents mRNA expression levels of genes normalized to Cyclophilin. Graph represents the average of quadruplicate samples and the experiment was repeated twice. For genes β-Catenin, Cdkn2b and Egr-1 the difference in expression levels between MEK and MEK/K6-AZ were found to be statistically significant with a $p=0.0001$, $p=0.032$, $p<0.0001$ respectively. For Tgf-β1 the difference was not found to be statistically significant with a $p=0.4$, as measured by a two-tailed T-test.

Discussion

Analysis of global gene expression profiles in tumors isolated from MEK/K6-AZ, MEK/K5-AZ and MEK mice revealed several potential targets that could be regulated by AZ. Genomic changes were more prolific in the tumors expressing AZ from the K6 promoter than tumors expressing AZ from the K5 promoter. This may be explained by the difference in the expression levels of AZ expressed from the K5 and the K6 promoter (Feith et al., 2006). Immunohistochemistry analysis by Feith et al. showed that AZ expression driven by the K5 promoter was much less pronounced than the K6 induced AZ expression and the K5-AZ expression was more localized to the basal layer (Feith et al., 2006). It is possible that isolated changes in gene expression were concealed by performing the analysis on the entire tumor sample without selecting for cells that specifically expressed K5-AZ, but it is notable that the minimal K5-AZ expression is sufficient to inhibit MEK-induced tumor growth as potently as K6-AZ expression on the C57BL/6J background (Feith et al., 2006). These differences in global genomic profiles between genotypes must be interpreted cautiously as these analyses were done using a single chip per genotype and to determine significant changes replicate samples have to be analyzed.

We selected a few genes to validate changes in gene expressions and confirmed that β-Catenin, Egr-1 and Cdkn2b exhibited significant changes in expression between MEK/K6-AZ and MEK tumors. Down-regulation of β-Catenin by AZ may have a significant consequence as activation of β-Catenin has been shown to induce transcription of growth regulatory proteins such as Myc and Cyclin D1 and regulate cell-cell adhesion, which is deregulated in cancer cells (Barker & Clevers, 2006; Moon, 2005). Also, β-

Catenin is implicated in several types of cancers, especially in colon cancers carrying mutations in APC (Adenomatous Polyposis Coli) (Barker & Clevers, 2006; Segditsas & Tomlinson, 2006). Studies have shown that β-Catenin increases expression of metastatic factors such as S100A4 and increases tumor invasiveness. Its accumulation in the nucleus has been correlated with a severe colonic tumor progression model, suggesting that some of the effects of AZ through down-regulation of β-Catenin, could involve inhibition of tumor progression and invasiveness (Brabletz et al., 2001; Stein et al., 2006; Wong et al., 2004). It would be interesting to examine if AZ does decrease levels of β-Catenin protein through regulation of RNA levels and the functional consequence of this regulation. Also, an effect of AZ on expression of other members of the Wnt signaling pathway such as Fzd and Dsh has to be validated.

The genes identified by the genomic analysis could either be regulated by effects of AZ on polyamine synthesis or be regulated by AZ in a polyamine independent manner. One target that could potentially be regulated by polyamines is the transcription factor Egr-1. Studies show that Ras activation, which induces polyamines, also suppresses Egr-1. The ODC promoter has been predicted to contain Egr-1 binding sites, which upon Egr-1 binding may regulate ODC promoter activity in a cell-type dependent manner (Moshier et al., 1996; Shin et al., 2006). Our lab is currently pursuing studies to understand the relationship between Egr-1 and polyamines and the effect of their interaction on tumorigenesis.

Future studies will involve validating several genes other than the ones described in this chapter that are significantly different between MEK/K6-AZ and MEK tumors. It also must be determined if changes in these genes are merely a consequence of AZ-

mediated inhibition of tumorigenesis, or alternately, if changes in the expression of these genes actually play a causative role in tumor formation.

Chapter VI

Overall conclusions and Significance (Fig 6.1)

The main aim of this project was to understand the regulation of ODC by Ras in the context of an epithelial cell model (RIE-1). We found that activation of Ras results in elevated ODC synthesis and that the induction of ODC involves a complex mechanism involving regulation at the levels of transcription, translation and degradation. Ras elevated transcription of ODC by about 2-fold, and this induction was found to be regulated by the Raf-MEK-ERK pathway. One potential mechanism involves the activation of the transcription factor Myc by ERK. So far, Myc has been correlated with the induction of ODC transcription by Ras (Auvinen et al., 2003). However, further studies have to be carried out to determine if Myc is the mediator of Ras-activated transcription of ODC, and determine the consequence of this regulation on Ras-induced transformation.

Besides Myc, it is possible that other transcription factors also regulate ODC, such as Egr-1. Our microarray analysis of skin tumors from mice over-expressing MEK and AZ revealed that expression of AZ induced Egr- 1 (Chapter V). Since the ODC promoter has been found to contain binding sites for Egr-1 and expression of Egr-1 is suppressed by Ras, it is possible that induction of Egr-1 inhibits ODC transcription to combat MEK-induced tumorigenesis (Shin et al., 2006). The role of Egr-1 as a transcription factor for ODC is currently being examined in our lab.

Since transcription was induced only 2-fold in the Ras transformed cells but ODC activity was induced 20-fold, we also examined the role of translation in regulating ODC. Polysome analysis revealed that Ras regulates ODC translation by increasing the amount

of RNA associated with the polysomes, rather than shifting the RNA to the lighter or non polysomal fractions. This increase in the amount of polysomal RNA was found to be the result of increased stability of ODC RNA. Rapamycin inhibited the stability of ODC RNA without affecting translation efficiency or transcription of ODC. Since Rapamycin affected ODC activity by greater than 50%, this suggested that inhibition of ODC RNA stability can significantly affect ODC activity. It would therefore be crucial to determine the factors that regulate ODC stability in response to Ras.

Two such factors that we are currently examining are TTP and HuR. TTP is a RNA destabilizing factor that binds to AU rich elements in the 3'UTR of RNAs such as Cyclin D1 to increase degradation of the mRNA (Stoecklin et al., 2003). Analysis of TTP levels revealed that they are inversely correlated with the stability of ODC RNA, with the TTP levels being higher in RIE-1 cells and lower in Ras12V cells. TTP was also elevated in response to Rapamycin. Analysis of pull down of proteins bound to biotin-labeled 3'UTR of ODC will help determine whether TTP binds to the ODC 3'UTR, especially in the RIE-1 cells and in response to Rapamycin. Using the above mentioned biotin-pull down assay, we can also analyze if the RNA stabilizing factor HuR is bound to the ODC RNA. Interestingly, preliminary studies show that HuR binds to both the 3' and 5'UTR of ODC RNA, but not to the coding region. We are currently trying to determine if levels of HuR bound to the 3'UTR of ODC RNA is different between Ras and RIE-1 cells. Also, by manipulating the levels of HuR using siRNA or by over expressing TTP in Ras cells, we intend to determine the effects of these factors on the stability of ODC RNA. Since the predominant mode of ODC regulation in epithelial cells involved changes in RNA stability, it would be interesting to analyze if Ras has similar

effects on ODC in cells of a mesenchymal origin or if Ras-mediated regulation of ODC varies between cell-types.

Adding complexity to the above-described mechanisms of ODC regulation is the observation that Ras induces cap-independent translation of ODC. The IRES-mediated translation of ODC was found to be negatively regulated by the Raf-kinase pathway, which was partly influenced by the phosphorylation status of eIF4E. Since dephosphorylation of eIF4E did not up-regulate ODC IRES activity to the same extent seen with MEK inhibition, this suggested that additional MEK effectors must also be essential for ODC IRES activity. To identify these factors, we are currently using the above mentioned biotin-pull down assays using the 5'UTR of ODC to detect bound factors. One such factor identified by our preliminary studies is HuR. Further studies have to be carried out to determine the contribution of HuR to ODC IRES activity. Manipulation of factors such as HuR will help us determine the contribution of cap-independent translation to overall synthesis of ODC protein in response to Ras.

The final mechanism of ODC regulation that poses interesting questions is the effect of eIF4E phosphorylation on ODC synthesis. Dephosphorylation of eIF4E using the Mnk inhibitor CGP57380 inhibited ODC activity and reduced translation efficiency of ODC without affecting transcription or RNA stability. ODC has been shown to be essential for eIF4E-induced transformation, as inhibition of ODC by its inhibitor DFMO reversed the transformation of cells over expressing eIF4E (Shantz et al., 1996a). Also, it has been shown that phosphorylation of eIF4E is essential for the transforming properties of eIF4E (Topisirovic et al., 2004). Based on these studies, it would be interesting to

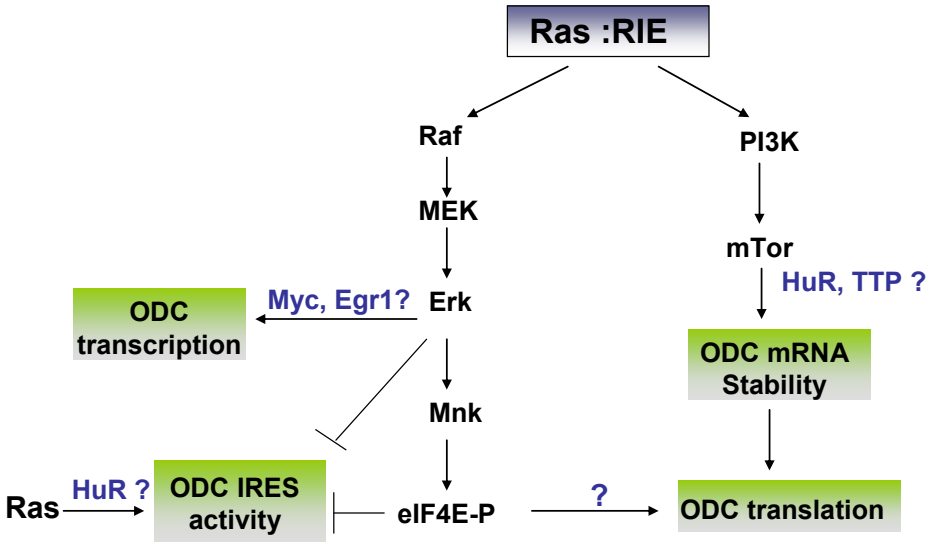

Figure 6.1. Regulation of ODC by Ras in RIE-1 cells

See text for details

analyze if the effects of eIF4E phosphorylation on ODC activity are essential for eIF4E-induced transformation. Some of these questions could be answered by using cells that over-express a non-phosphorylatable mutant of eIF4E and analyzing the effects on ODC activity and transformation.

In conclusion, induction of ODC synthesis by Ras is a complex process. Since many cancers carry Ras activating mutations and are of epithelial origin, understanding how Ras affects ODC synthesis would help us determine what potential drugs can be used to treat these cancers by targeting ODC. Inhibiting ODC using the clinical inhibitor DFMO has been shown to inhibit as well as prevent tumorigenesis. Although DFMO is currently in clinical trials as a chemopreventive agent, it was not effective as a chemotherapeutic agent. Given that DFMO can be used in humans without profound side effects, it still shows promise for cancer treatment in combination with other chemotherapeutic agents such as Rapamycin and inhibitors of MEK. This may particularly be helpful in tumors that are resistant to drugs such as Rapamycin. The Ras12V cells present an interesting model as these cells are not cytostatic in response to Rapamycin, suggesting that they are resistant to the effects of Rapamycin. Also, Rapamycin did not completely inhibit ODC in these cells. In such cancer cells combining DFMO with Rapamycin may be sufficient to completely inhibit ODC activity and reverse tumorigenesis. Thus, to design better therapeutic strategies it is critical to understand how ODC synthesis is regulated, specifically under cancerous conditions.

Bibliography

Albig, A.R. & Decker, C.J. (2001). *Mol Biol Cell*, **12,** 3428-38.

Andersson, G. & Heby, O. (1972). *J Natl Cancer Inst*, **48,** 165-72.

Auvinen, M., Jarvinen, K., Hotti, A., Okkeri, J., Laitinen, J., Janne, O.A., Coffino, P., Bergman, M., Andersson, L.C., Alitalo, K. & Holtta, E. (2003). *Int J Biochem Cell Biol*, **35,** 496-521.

Auvinen, M., Laine, A., Paasinen-Sohns, A., Kangas, A., Kangas, L., Saksela, O., Andersson, L.C. & Holtta, E. (1997). *Cancer Res*, **57,** 3016-25.

Auvinen, M., Paasinen, A., Andersson, L.C. & Holtta, E. (1992). *Nature*, **360,** 355-8.

Averous, J. & Proud, C.G. (2006). *Oncogene*, **25,** 6423-35.

Banholzer, R., Nair, A.P., Hirsch, H.H., Ming, X.F. & Moroni, C. (1997). *Mol Cell Biol*, **17,** 3254-60.

Barker, N. & Clevers, H. (2000). *Bioessays*, **22,** 961-5.

Barker, N. & Clevers, H. (2006). *Nat Rev Drug Discov*, **5,** 997-1014.

Bello-Fernandez, C., Packham, G. & Cleveland, J.L. (1993). *Proc Natl Acad Sci U S A*, **90,** 7804-8.

Bert, A.G., Grepin, R., Vadas, M.A. & Goodall, G.J. (2006). *Rna*, **12,** 1074-83.

Brabletz, T., Jung, A., Reu, S., Porzner, M., Hlubek, F., Kunz-Schughart, L.A., Knuechel, R. & Kirchner, T. (2001). *Proc Natl Acad Sci U S A*, **98,** 10356-61.

Brengues, M., Teixeira, D. & Parker, R. (2005). *Science*, **310,** 486-9.

Brown, E.J., Albers, M.W., Shin, T.B., Ichikawa, K., Keith, C.T., Lane, W.S. & Schreiber, S.L. (1994). *Nature*, **369,** 756-8.

Brugarolas, J., Lei, K., Hurley, R.L., Manning, B.D., Reiling, J.H., Hafen, E., Witters, L.A., Ellisen, L.W. & Kaelin, W.G., Jr. (2004). *Genes Dev*, **18,** 2893-904.

Brunn, G.J., Hudson, C.C., Sekulic, A., Williams, J.M., Hosoi, H., Houghton, P.J., Lawrence, J.C., Jr. & Abraham, R.T. (1997). *Science*, **277,** 99-101.

Burns, J., Barton, C., Wynford-Thomas, D. & Lemoine, N. (1993). *Epithelial Cell Biol*, **2,** 26-43.

Bushell, M., Stoneley, M., Kong, Y.W., Hamilton, T.L., Spriggs, K.A., Dobbyn, H.C., Qin, X., Sarnow, P. & Willis, A.E. (2006). *Mol Cell*, **23,** 401-12.

Buxade, M., Parra, J.L., Rousseau, S., Shpiro, N., Marquez, R., Morrice, N., Bain, J., Espel, E. & Proud, C.G. (2005). *Immunity*, **23,** 177-89.

Campbell, P.M. & Der, C.J. (2004). *Semin Cancer Biol*, **14,** 105-14.

Carter, M.S. & Sarnow, P. (2000). *J Biol Chem, Vol. 275*, pp 28301-7.

Casero, R.A., Jr., Frydman, B., Stewart, T.M. & Woster, P.M. (2005). *Proc West Pharmacol Soc*, **48,** 24-30.

Chang, F., Steelman, L.S., Lee, J.T., Shelton, J.G., Navolanic, P.M., Blalock, W.L., Franklin, R.A. & McCubrey, J.A. (2003). *Leukemia*, **17,** 1263-93.

Chappell, S.A., LeQuesne, J.P., Paulin, F.E., deSchoolmeester, M.L., Stoneley, M., Soutar, R.L., Ralston, S.H., Helfrich, M.H. & Willis, A.E. (2000). *Oncogene*, **19,** 4437-40.

Chen, J., Zheng, X.F., Brown, E.J. & Schreiber, S.L. (1995). *Proc Natl Acad Sci U S A*, **92,** 4947-51.

Cheng, J.Q., Lindsley, C.W., Cheng, G.Z., Yang, H. & Nicosia, S.V. (2005). *Oncogene*, **24,** 7482-92.

Chong, H., Vikis, H.G. & Guan, K.L. (2003). *Cell Signal*, **15,** 463-9.
Clemens, M.J., Bushell, M., Jeffrey, I.W., Pain, V.M. & Morley, S.J. (2000). *Cell Death Differ*, **7,** 603-15.
Coffino, P. (2001a). *Biochimie*, **83,** 319-23.
Coffino, P. (2001b). *Nat Rev Mol Cell Biol*, **2,** 188-94.
Coleman, C.S. & Pegg, A.E. (1998). *Methods Mol Biol*, **79,** 41-4.
Cox, A.D. & Der, C.J. (2002). *Cancer Biol Ther*, **1,** 599-606.
Culjkovic, B., Topisirovic, I., Skrabanek, L., Ruiz-Gutierrez, M. & Borden, K.L. (2005). *J Cell Biol*, **169,** 245-56.
Davis, R.J. (1995). *Mol Reprod Dev*, **42,** 459-67.
Derynck, R., Akhurst, R.J. & Balmain, A. (2001). *Nat Genet*, **29,** 117-29.
Duriez, P.J. & Shah, G.M. (1997). *Biochem Cell Biol*, **75,** 337-49.
Dyer, J.R., Michel, S., Lee, W., Castellucci, V.F., Wayne, N.L. & Sossin, W.S. (2003). *Nat Neurosci*, **6,** 219-20.
Eberle, J., Krasagakis, K. & Orfanos, C.E. (1997). *Int J Cancer*, **71,** 396-401.
Efimova, T., Broome, A.M. & Eckert, R.L. (2003). *J Biol Chem*, **278,** 34277-85.
Erdman, S.H., Ignatenko, N.A., Powell, M.B., Blohm-Mangone, K.A., Holubec, H., Guillen-Rodriguez, J.M. & Gerner, E.W. (1999). *Carcinogenesis*, **20,** 1709-13.
Eulalio, A., Behm-Ansmant, I. & Izaurralde, E. (2007). *Nat Rev Mol Cell Biol*, **8,** 9-22.
Feith, D.J., Bol, D.K., Carboni, J.M., Lynch, M.J., Sass-Kuhn, S., Shoop, P.L. & Shantz, L.M. (2005). *Cancer Res*, **65,** 572-8.
Feith, D.J., Origanti, S., Shoop, P.L., Sass-Kuhn, S. & Shantz, L.M. (2006). *Carcinogenesis*, **27,** 1090-8.
Feith, D.J., Shantz, L.M. & Pegg, A.E. (2001). *Cancer Res*, **61,** 6073-81.
Foat, B.C., Houshmandi, S.S., Olivas, W.M. & Bussemaker, H.J. (2005). *Proc Natl Acad Sci U S A*, **102,** 17675-80.
Fong, L.Y., Feith, D.J. & Pegg, A.E. (2003). *Cancer Res*, **63,** 3945-54.
Fong, L.Y., Nguyen, V.T., Pegg, A.E. & Magee, P.N. (2001). *Cancer Epidemiol Biomarkers Prev*, **10,** 191-9.
Fredlund, J.O., Johansson, M.C., Dahlberg, E. & Oredsson, S.M. (1995). *Exp Cell Res*, **216,** 86-92.
Fukuchi-Shimogori, T., Ishii, I., Kashiwagi, K., Mashiba, H., Ekimoto, H. & Igarashi, K. (1997). *Cancer Res*, **57,** 5041-4.
Fultz, K.E. & Gerner, E.W. (2002). *Mol Carcinog*, **34,** 10-8.
Gallego, J. (2002). *Curr Opin Drug Discov Devel*, **5,** 777-84.
Gebauer, F. & Hentze, M.W. (2004). *Nat Rev Mol Cell Biol*, **5,** 827-35.
Gerner, E.W., Ignatenko, N.A., Lance, P. & Hurley, L.H. (2005). *Ann N Y Acad Sci*, **1059,** 97-105.
Gerner, E.W. & Meyskens, F.L., Jr. (2004). *Nat Rev Cancer*, **4,** 781-92.
Giardiello, F.M., Hamilton, S.R., Hylind, L.M., Yang, V.W., Tamez, P. & Casero, R.A., Jr. (1997). *Cancer Res*, **57,** 199-201.
Gingras, A.C., Kennedy, S.G., O'Leary, M.A., Sonenberg, N. & Hay, N. (1998). *Genes Dev*, **12,** 502-13.
Gingras, A.C., Raught, B. & Sonenberg, N. (1999). *Annu Rev Biochem*, **68,** 913-63.
Gingras, A.C., Raught, B. & Sonenberg, N. (2001). *Genes Dev*, **15,** 807-26.
Gollob, J.A., Wilhelm, S., Carter, C. & Kelley, S.L. (2006). *Semin Oncol*, **33,** 392-406.

Grady, W.M. & Markowitz, S.D. (2002). *Annu Rev Genomics Hum Genet*, **3,** 101-28.
Graff, J.R., De Benedetti, A., Olson, J.W., Tamez, P., Casero, R.A., Jr. & Zimmer, S.G. (1997). *Biochem Biophys Res Commun*, **240,** 15-20.
Grens, A. & Scheffler, I.E. (1990). *J Biol Chem*, **265,** 11810-6.
Gruendler, C., Lin, Y., Farley, J. & Wang, T. (2001). *J Biol Chem*, **276,** 46533-43.
Guo, Y., Harris, R.B., Rosson, D., Boorman, D. & O'Brien, T.G. (2000). *Cancer Res*, **60,** 6314-7.
Hamilton, T.L., Stoneley, M., Spriggs, K.A. & Bushell, M. (2006). *Biochem Soc Trans*, **34,** 12-6.
Hardie, D.G. (2005). *Curr Opin Cell Biol*, **17,** 167-73.
Harris, C.C., Reddel, R., Pfeifer, A., Iman, D., McMenamin, M., Trump, B.F. & Weston, A. (1991). *IARC Sci Publ***,** 294-304.
Hashemolhosseini, S., Nagamine, Y., Morley, S.J., Desrivieres, S., Mercep, L. & Ferrari, S. (1998). *J Biol Chem*, **273,** 14424-9.
Hay, N. (2005). *Cancer Cell*, **8,** 179-83.
Hay, N. & Sonenberg, N. (2004). *Genes Dev*, **18,** 1926-45.
Hayashi, S., Murakami, Y. & Matsufuji, S. (1996). *Trends Biochem Sci*, **21,** 27-30.
Hayashi, S., Nishimura, K., Fukuchi-Shimogori, T., Kashiwagi, K. & Igarashi, K. (2000). *Biochem Biophys Res Commun*, **277,** 117-23.
Hayes, C.S., DeFeo, K., Lan, L., Paul, B., Sell, C. & Gilmour, S.K. (2006). *Oncogene*, **25,** 1543-53.
Hellen, C.U. & Sarnow, P. (2001). *Genes Dev*, **15,** 1593-612.
Heller, J.S., Fong, W.F. & Canellakis, E.S. (1976). *Proc Natl Acad Sci U S A*, **73,** 1858-62.
Herbert, T.P., Kilhams, G.R., Batty, I.H. & Proud, C.G. (2000). *J Biol Chem*, **275,** 11249-56.
Holcik, M., Graber, T., Lewis, S.M., Lefebvre, C.A., Lacasse, E. & Baird, S. (2005). *Rna*, **11,** 1605-9.
Holtta, E., Sistonen, L. & Alitalo, K. (1988). *J Biol Chem*, **263,** 4500-7.
Hurta, R.A. (2000). *Mol Cell Biochem*, **215,** 81-92.
Ignatenko, N.A., Zhang, H., Watts, G.S., Skovan, B.A., Stringer, D.E. & Gerner, E.W. (2004). *Mol Carcinog*, **39,** 221-33.
Ito, K., Kashiwagi, K., Watanabe, S., Kameji, T., Hayashi, S. & Igarashi, K. (1990). *J Biol Chem*, **265,** 13036-41.
Iwata, S., Sato, Y., Asada, M., Takagi, M., Tsujimoto, A., Inaba, T., Yamada, T., Sakamoto, S., Yata, J., Shimogori, T., Igarashi, K. & Mizutani, S. (1999). *Oncogene*, **18,** 165-72.
Jang, S.K., Pestova, T.V., Hellen, C.U., Witherell, G.W. & Wimmer, E. (1990). *Enzyme*, **44,** 292-309.
Jefferies, H.B., Fumagalli, S., Dennis, P.B., Reinhard, C., Pearson, R.B. & Thomas, G. (1997). *Embo J*, **16,** 3693-704.
Johannes, G. & Sarnow, P. (1998). *Rna*, **4,** 1500-13.
Kangas, A., Nicholson, D.W. & Holtta, E. (1998). *Oncogene*, **16,** 387-98.
Kim, Y.K., Hahm, B. & Jang, S.K. (2000). *J Mol Biol*, **304,** 119-33.
Kimball, S.R. & Jefferson, L.S. (2004). *Curr Opin Clin Nutr Metab Care*, **7,** 39-44.
Kingsnorth, A.N. (1986). *Ann R Coll Surg Engl*, **68,** 76-81.

Knauf, U., Tschopp, C. & Gram, H. (2001). *Mol Cell Biol*, **21,** 5500-11.
Kopnin, B. (1993). *Tumori*, **79,** 235-43.
Koromilas, A.E., Lazaris-Karatzas, A. & Sonenberg, N. (1992). *Embo J*, **11,** 4153-8.
Krug, U., Ganser, A. & Koeffler, H.P. (2002). *Oncogene*, **21,** 3475-95.
Kullmann, M., Gopfert, U., Siewe, B. & Hengst, L. (2002). *Genes Dev*, **16,** 3087-99.
Lachance, P.E., Miron, M., Raught, B., Sonenberg, N. & Lasko, P. (2002). *Mol Cell Biol*, **22,** 1656-63.
Larue, L. & Delmas, V. (2006). *Front Biosci*, **11,** 733-42.
Lazaris-Karatzas, A., Montine, K.S. & Sonenberg, N. (1990). *Nature*, **345,** 544-7.
Lazaris-Karatzas, A. & Sonenberg, N. (1992). *Mol Cell Biol*, **12,** 1234-8.
Lee, H.C., Kim, M. & Wands, J.R. (2006). *Front Biosci*, **11,** 1901-15.
Lee, J.T., Jr. & McCubrey, J.A. (2002). *Leukemia*, **16,** 486-507.
Lee, M.H. & Yang, H.Y. (2001). *Cell Mol Life Sci*, **58,** 1907-22.
Li, W., Zhu, T. & Guan, K.L. (2004). *J Biol Chem*, **279,** 37398-406.
Lockhart, D.J., Dong, H., Byrne, M.C., Follettie, M.T., Gallo, M.V., Chee, M.S., Mittmann, M., Wang, C., Kobayashi, M., Horton, H. & Brown, E.L. (1996). *Nat Biotechnol*, **14,** 1675-80.
Lopatin, A.N., Makhina, E.N. & Nichols, C.G. (1994). *Nature*, **372,** 366-9.
Loreni, F., Thomas, G. & Amaldi, F. (2000). *Eur J Biochem*, **267,** 6594-601.
Lovkvist Wallstrom, E., Takao, K., Wendt, A., Vargiu, C., Yin, H. & Persson, L. (2001). *Biochem J*, **356,** 627-34.
Lucerna, M., Pomyje, J., Mechtcheriakova, D., Kadl, A., Gruber, F., Bilban, M., Sobanov, Y., Schabbauer, G., Breuss, J., Wagner, O., Bischoff, M., Clauss, M., Binder, B.R. & Hofer, E. (2006). *Cancer Res*, **66,** 6708-13.
Malumbres, M. & Barbacid, M. (2003). *Nat Rev Cancer*, **3,** 459-65.
Mamane, Y., Petroulakis, E., LeBacquer, O. & Sonenberg, N. (2006). *Oncogene*, **25,** 6416-22.
Mamane, Y., Petroulakis, E., Rong, L., Yoshida, K., Ler, L.W. & Sonenberg, N. (2004). *Oncogene*, **23,** 3172-9.
Manni, A., Grove, R., Kunselman, S. & Aldaz, M. (1995a). *Cancer Lett*, **92,** 49-57.
Manni, A., Wechter, R., Grove, R., Wei, L., Martel, J. & Demers, L. (1995b). *Breast Cancer Res Treat*, **34,** 45-53.
Manzella, J.M. & Blackshear, P.J. (1990). *J Biol Chem*, **265,** 11817-22.
Manzella, J.M., Rychlik, W., Rhoads, R.E., Hershey, J.W. & Blackshear, P.J. (1991). *J Biol Chem*, **266,** 2383-9.
Marderosian, M., Sharma, A., Funk, A.P., Vartanian, R., Masri, J., Jo, O.D. & Gera, J.F. (2006). *Oncogene*, **25,** 6277-90.
Martin, D.E., Soulard, A. & Hall, M.N. (2004). *Cell*, **119,** 969-79.
Martin-Blanco, E. (2000). *Bioessays*, **22,** 637-45.
Martinez, M.E., O'Brien, T.G., Fultz, K.E., Babbar, N., Yerushalmi, H., Qu, N., Guo, Y., Boorman, D., Einspahr, J., Alberts, D.S. & Gerner, E.W. (2003). *Proc Natl Acad Sci U S A*, **100,** 7859-64.
Marton, L.J. & Pegg, A.E. (1995). *Annu Rev Pharmacol Toxicol*, **35,** 55-91.
Matsufuji, S., Matsufuji, T., Miyazaki, Y., Murakami, Y., Atkins, J.F., Gesteland, R.F. & Hayashi, S. (1995). *Cell*, **80,** 51-60.
McKendrick, L., Morley, S.J., Pain, V.M., Jagus, R. & Joshi, B. (2001). *Eur J Biochem*,

268, 5375-85.
Megosh, L., Halpern, M., Farkash, E. & O'Brien, T.G. (1998). *Mol Carcinog*, **22,** 145-9.
Merrill, M.K., Dobrikova, E.Y. & Gromeier, M. (2006). *J Virol, Vol. 80*, pp 3147-56.
Merrill, M.K. & Gromeier, M. (2006). *J Virol*, **80,** 6936-42.
Mitchell, S.A., Brown, E.C., Coldwell, M.J., Jackson, R.J. & Willis, A.E. (2001). *Mol Cell Biol*, **21,** 3364-74.
Mitchell, S.A., Spriggs, K.A., Bushell, M., Evans, J.R., Stoneley, M., Le Quesne, J.P., Spriggs, R.V. & Willis, A.E. (2005). *Genes Dev*, **19,** 1556-71.
Miyazono, K., Suzuki, H. & Imamura, T. (2003). *Cancer Sci*, **94,** 230-4.
Mohan, R.R., Challa, A., Gupta, S., Bostwick, D.G., Ahmad, N., Agarwal, R., Marengo, S.R., Amini, S.B., Paras, F., MacLennan, G.T., Resnick, M.I. & Mukhtar, H. (1999). *Clin Cancer Res*, **5,** 143-7.
Moon, D.O., Park, C., Heo, M.S., Park, Y.M., Choi, Y.H. & Kim, G.Y. (2007). *Int Immunopharmacol*, **7,** 36-45.
Moon, R.T. (2005). *Sci STKE*, **2005,** cm1.
Morgensztern, D. & McLeod, H.L. (2005). *Anticancer Drugs*, **16,** 797-803.
Morley, S.J. & Naegele, S. (2002). *J Biol Chem*, **277,** 32855-9.
Morrison, D.K. (2001). *J Cell Sci*, **114,** 1609-12.
Moshier, J.A., Skunca, M., Wu, W., Boppana, S.M., Rauscher, F.J., 3rd & Dosescu, J. (1996). *Nucleic Acids Res*, **24,** 1149-57.
Murakami, Y., Matsufuji, S., Kameji, T., Hayashi, S., Igarashi, K., Tamura, T., Tanaka, K. & Ichihara, A. (1992). *Nature*, **360,** 597-9.
Murakami, Y., Nishiyama, M. & Hayashi, S. (1989). *Eur J Biochem*, **180,** 181-4.
Murata, T., Hijikata, M. & Shimotohno, K. (2005). *Virology*, **340,** 105-15.
Newman, R.M., Mobascher, A., Mangold, U., Koike, C., Diah, S., Schmidt, M., Finley, D. & Zetter, B.R. (2004). *J Biol Chem*, **279,** 41504-11.
Nilsson, J.A., Keller, U.B., Baudino, T.A., Yang, C., Norton, S., Old, J.A., Nilsson, L.M., Neale, G., Kramer, D.L., Porter, C.W. & Cleveland, J.L. (2005). *Cancer Cell*, **7,** 433-44.
Nilsson, J.A., Maclean, K.H., Keller, U.B., Pendeville, H., Baudino, T.A. & Cleveland, J.L. (2004). *Mol Cell Biol*, **24,** 1560-9.
Nishimura, K., Nakatsu, F., Kashiwagi, K., Ohno, H., Saito, T. & Igarashi, K. (2002). *Genes Cells*, **7,** 41-7.
O'Brien, T.G., Simsiman, R.C. & Boutwell, R.K. (1975). *Cancer Res*, **35,** 1662-70.
Okuda, T., Shurtleff, S.A., Valentine, M.B., Raimondi, S.C., Head, D.R., Behm, F., Curcio-Brint, A.M., Liu, Q., Pui, C.H., Sherr, C.J. & et al. (1995). *Blood*, **85,** 2321-30.
Oldham, S.M., Clark, G.J., Gangarosa, L.M., Coffey, R.J., Jr. & Der, C.J. (1996). *Proc Natl Acad Sci U S A*, **93,** 6924-8.
Paraskeva, C., Corfield, A.P., Harper, S., Hague, A., Audcent, K. & Williams, A.C. (1990). *Anticancer Res*, **10,** 1189-200.
Park, M.H., Wolff, E.C. & Folk, J.E. (1993). *Trends Biochem Sci*, **18,** 475-9.
Pegg, A.E. (1988). *Cancer Res*, **48,** 759-74.
Pegg, A.E. (2006). *J Biol Chem*, **281,** 14529-32.
Pegg, A.E., Feith, D.J., Fong, L.Y., Coleman, C.S., O'Brien, T.G. & Shantz, L.M. (2003). *Biochem Soc Trans*, **31,** 356-60.

Pegg, A.E., Shantz, L.M. & Coleman, C.S. (1995). *J Cell Biochem Suppl*, **22,** 132-8.
Pendeville, H., Carpino, N., Marine, J.C., Takahashi, Y., Muller, M., Martial, J.A. & Cleveland, J.L. (2001). *Mol Cell Biol*, **21,** 6549-58.
Pera, P.J., Kramer, D.L., Sufrin, J.R. & Porter, C.W. (1986). *Cancer Res*, **46,** 1148-54.
Petros, L.M., Howard, M.T., Gesteland, R.F. & Atkins, J.F. (2005). *Biochem Biophys Res Commun*, **338,** 1478-89.
Peyssonnaux, C. & Eychene, A. (2001). *Biol Cell*, **93,** 53-62.
Pollard, K.J., Samuels, M.L., Crowley, K.A., Hansen, J.C. & Peterson, C.L. (1999). *Embo J*, **18,** 5622-33.
Powell, B.C., Nesci, A. & Rogers, G.E. (1991). *Ann N Y Acad Sci*, **642,** 1-20.
Proud, C.G. (2004). *Curr Top Microbiol Immunol*, **279,** 215-44.
Pyronnet, S. (2000). *Biochem Pharmacol*, **60,** 1237-43.
Pyronnet, S., Dostie, J. & Sonenberg, N. (2001). *Genes Dev*, **15,** 2083-93.
Pyronnet, S., Gingras, A.C., Bouisson, M., Kowalski-Chauvel, A., Seva, C., Vaysse, N., Sonenberg, N. & Pradayrol, L. (1998). *Oncogene*, **16,** 2219-27.
Pyronnet, S., Pradayrol, L. & Sonenberg, N. (2000). *Mol Cell*, **5,** 607-16.
Pyronnet, S., Pradayrol, L. & Sonenberg, N. (2005). *Cell Mol Life Sci*, **62,** 1267-74.
Pyronnet, S., Vagner, S., Bouisson, M., Prats, A.C., Vaysse, N. & Pradayrol, L. (1996). *Cancer Res*, **56,** 1742-5.
Qin, C., Samudio, I., Ngwenya, S. & Safe, S. (2004). *Mol Carcinog*, **40,** 160-70.
Ray, P.S., Grover, R. & Das, S. (2006). *EMBO Rep*, **7,** 404-10.
Richter, J.D. & Sonenberg, N. (2005). *Nature*, **433,** 477-80.
Rommel, C., Clarke, B.A., Zimmermann, S., Nunez, L., Rossman, R., Reid, K., Moelling, K., Yancopoulos, G.D. & Glass, D.J. (1999). *Science*, **286,** 1738-41.
Ross, G., Dyer, J.R., Castellucci, V.F. & Sossin, W.S. (2006). *J Neurochem*, **97,** 79-91.
Rousseau, D., Kaspar, R., Rosenwald, I., Gehrke, L. & Sonenberg, N. (1996). *Proc Natl Acad Sci U S A*, **93,** 1065-70.
Ruggero, D., Montanaro, L., Ma, L., Xu, W., Londei, P., Cordon-Cardo, C. & Pandolfi, P.P. (2004). *Nat Med*, **10,** 484-6.
Russell, D. & Snyder, S.H. (1968). *Proc Natl Acad Sci U S A*, **60,** 1420-7.
Ruvinsky, I. & Meyuhas, O. (2006). *Trends Biochem Sci*, **31,** 342-8.
Sabatini, D.M., Erdjument-Bromage, H., Lui, M., Tempst, P. & Snyder, S.H. (1994). *Cell*, **78,** 35-43.
Saghir, A.N., Tuxworth, W.J., Jr., Hagedorn, C.H. & McDermott, P.J. (2001). *Biochem J*, **356,** 557-66.
Saito, T., Hascilowicz, T., Ohkido, I., Kikuchi, Y., Okamoto, H., Hayashi, S., Murakami, Y. & Matsufuji, S. (2000). *Biochem J*, **345 Pt 1,** 99-106.
Scheper, G.C. & Proud, C.G. (2002). *Eur J Biochem*, **269,** 5350-9.
Scheper, G.C., van Kollenburg, B., Hu, J., Luo, Y., Goss, D.J. & Proud, C.G. (2002). *J Biol Chem*, **277,** 3303-9.
Segditsas, S. & Tomlinson, I. (2006). *Oncogene*, **25,** 7531-7.
Seidel, E.R. & Ragan, V.L. (1997). *Br J Pharmacol*, **120,** 571-4.
Shahbazian, D., Roux, P.P., Mieulet, V., Cohen, M.S., Raught, B., Taunton, J., Hershey, J.W., Blenis, J., Pende, M. & Sonenberg, N. (2006). *Embo J*, **25,** 2781-91.
Shantz, L.M. (2004). *Biochem J*, **377,** 257-64.
Shantz, L.M., Coleman, C.S. & Pegg, A.E. (1996a). *Cancer Res*, **56,** 5136-40.

Shantz, L.M., Holm, I., Janne, O.A. & Pegg, A.E. (1992). *Biochem J*, **288 (Pt 2),** 511-8.
Shantz, L.M., Hu, R.H. & Pegg, A.E. (1996b). *Cancer Res*, **56,** 3265-9.
Shantz, L.M. & Pegg, A.E. (1994). *Cancer Res*, **54,** 2313-6.
Shantz, L.M. & Pegg, A.E. (1998). *Cancer Res*, **58,** 2748-53.
Shantz, L.M. & Pegg, A.E. (1999). *Int J Biochem Cell Biol*, **31,** 107-22.
Shi, Y., Sharma, A., Wu, H., Lichtenstein, A. & Gera, J. (2005). *J Biol Chem, Vol. 280*, pp 10964-73.
Shimogori, T., Suzuki, T., Kashiwagi, K., Kakinuma, Y. & Igarashi, K. (1996). *Biochem Biophys Res Commun*, **222,** 748-52.
Shin, S.Y., Bahk, Y.Y., Ko, J., Chung, I.Y., Lee, Y.S., Downward, J., Eibel, H., Sharma, P.M., Olefsky, J.M., Kim, Y.H., Lee, B. & Lee, Y.H. (2006). *Embo J*, **25,** 1093-103.
Smith, M.K., Trempus, C.S. & Gilmour, S.K. (1998). *Carcinogenesis*, **19,** 1409-15.
Spriggs, K.A., Bushell, M., Mitchell, S.A. & Willis, A.E. (2005). *Cell Death Differ*, **12,** 585-91.
Stein, U., Arlt, F., Walther, W., Smith, J., Waldman, T., Harris, E.D., Mertins, S.D., Heizmann, C.W., Allard, D., Birchmeier, W., Schlag, P.M. & Shoemaker, R.H. (2006). *Gastroenterology*, **131,** 1486-500.
Stoecklin, G., Gross, B., Ming, X.F. & Moroni, C. (2003). *Oncogene*, **22,** 3554-61.
Stolovich, M., Tang, H., Hornstein, E., Levy, G., Cohen, R., Bae, S.S., Birnbaum, M.J. & Meyuhas, O. (2002). *Mol Cell Biol*, **22,** 8101-13.
Stoneley, M., Chappell, S.A., Jopling, C.L., Dickens, M., MacFarlane, M. & Willis, A.E. (2000a). *Mol Cell Biol*, **20,** 1162-9.
Stoneley, M., Subkhankulova, T., Le Quesne, J.P., Coldwell, M.J., Jopling, C.L., Belsham, G.J. & Willis, A.E. (2000b). *Nucleic Acids Res*, **28,** 687-94.
Stoneley, M. & Willis, A.E. (2004). *Oncogene*, **23,** 3200-7.
Sunkara, P.S., Bowlin, T.L., Rosenberger, A.L. & Fleischmann, W.R., Jr. (1989). *J Biol Response Mod*, **8,** 170-9.
Sunkara, P.S. & Rosenberger, A.L. (1987). *Cancer Res*, **47,** 933-5.
Suzuki, T., He, Y., Kashiwagi, K., Murakami, Y., Hayashi, S. & Igarashi, K. (1994). *Proc Natl Acad Sci U S A*, **91,** 8930-4.
Takigawa, M., Enomoto, M., Nishida, Y., Pan, H.O., Kinoshita, A. & Suzuki, F. (1990). *Cancer Res*, **50,** 4131-8.
Tang, X., Kim, A.L., Feith, D.J., Pegg, A.E., Russo, J., Zhang, H., Aszterbaum, M., Kopelovich, L., Epstein, E.H., Jr., Bickers, D.R. & Athar, M. (2004). *J Clin Invest*, **113,** 867-75.
Tempero, M.A., Nishioka, K., Knott, K. & Zetterman, R.K. (1989). *Cancer Res*, **49,** 5793-7.
Terada, N., Patel, H.R., Takase, K., Kohno, K., Nairn, A.C. & Gelfand, E.W. (1994). *Proc Natl Acad Sci U S A*, **91,** 11477-81.
Tinton, S.A., Schepens, B., Bruynooghe, Y., Beyaert, R. & Cornelis, S. (2005). *Biochem J*, **385,** 155-63.
Tobias, K.E., Shor, J. & Kahana, C. (1995). *Oncogene*, **11,** 1721-7.
Topisirovic, I., Guzman, M.L., McConnell, M.J., Licht, J.D., Culjkovic, B., Neering, S.J., Jordan, C.T. & Borden, K.L. (2003). *Mol Cell Biol*, **23,** 8992-9002.
Topisirovic, I., Ruiz-Gutierrez, M. & Borden, K.L. (2004). *Cancer Res*, **64,** 8639-42.

Ueda, T., Watanabe-Fukunaga, R., Fukuyama, H., Nagata, S. & Fukunaga, R. (2004). *Mol Cell Biol*, **24,** 6539-49.
Van Steeg, H., Van Oostrom, C.T., Hodemaekers, H.M., Peters, L. & Thomas, A.A. (1991). *Biochem J*, **274 (Pt 2),** 521-6.
Venables, J.P. (2006). *Bioessays*, **28,** 378-86.
Vita, M. & Henriksson, M. (2006). *Semin Cancer Biol*, **16,** 318-30.
Vogelstein, B., Fearon, E.R., Hamilton, S.R., Kern, S.E., Preisinger, A.C., Leppert, M., Nakamura, Y., White, R., Smits, A.M. & Bos, J.L. (1988). *N Engl J Med*, **319,** 525-32.
Walhout, A.J., Gubbels, J.M., Bernards, R., van der Vliet, P.C. & Timmers, H.T. (1997). *Nucleic Acids Res*, **25,** 1493-501.
Walsh, D. & Mohr, I. (2004). *Genes Dev*, **18,** 660-72.
Waskiewicz, A.J., Flynn, A., Proud, C.G. & Cooper, J.A. (1997). *Embo J*, **16,** 1909-20.
Wennerberg, K., Rossman, K.L. & Der, C.J. (2005). *J Cell Sci*, **118,** 843-6.
White, M.W., Kameji, T., Pegg, A.E. & Morris, D.R. (1987). *Eur J Biochem*, **170,** 87-92.
Wong, S.C., Lo, E.S., Lee, K.C., Chan, J.K. & Hsiao, W.L. (2004). *Clin Cancer Res*, **10,** 1401-8.
Wynford-Thomas, D. (1997). *Horm Res*, **47,** 145-57.
Yee, L.D., Kacinski, B.M. & Carter, D. (1989). *Semin Diagn Pathol*, **6,** 110-25.
Yoon, A., Peng, G., Brandenburger, Y., Zollo, O., Xu, W., Rego, E. & Ruggero, D. (2006). *Science*, **312,** 902-6.
Yunmbam, M.K. (1998). *Oncol Rep*, **5,** 1431-7.
Zhao, B. & Butler, A.P. (2001). *Mol Carcinog*, **32,** 92-9.
Zimmermann, S. & Moelling, K. (1999). *Science*, **286,** 1741-4.
Zirvi, K.A., Dasmahapatra, K.S., Atabek, U. & Lyons, M.A. (1989). *Clin Exp Metastasis*, **7,** 591-8.
Zou, T., Mazan-Mamczarz, K., Rao, J.N., Liu, L., Marasa, B.S., Zhang, A.H., Xiao, L., Pullmann, R., Gorospe, M. & Wang, J.Y. (2006). *J Biol Chem*, **281,** 19387-94.

VITA

Sofia S. Origanti

Education

B.Sc. (Zoology), Department of Zoology, Stella Maris College,
Madras University, Chennai, India (1995-1998).
M.Sc. (Zoology), Department of Zoology, Loyola College,
Madras University, Chennai, India (1998-2000).
Ph.D. (Candidate), Department of Molecular Biology and Biochemistry,
Wesleyan University, Middletown, CT (2000-2002).
Ph.D. (Physiology), Department of Physiology, Penn State University,
Hershey, PA (2002-2007)

Publications

1. **Origanti S**, Shantz LM. Ras-transformation of RIE-1 cells activates cap-independent translation of ODC. In press, Cancer Research.

2. **Origanti S**, Kuhn SS, Shantz LM. Activated Ras regulates stability of ODC RNA through the PI3K/mTOR pathway. (Manuscript in preparation).

3. Feith D, **Origanti S**, Shoop PC, Kuhn SS, and Shantz LM. Antizyme inhibition of spontaneous skin tumorigenesis induced by MEK: Effects on tumor cell proliferation and Apoptosis. *Carcinogenesis*. 2006, May, 27:1090-8. [PDF]

4. Ionescu C, **Origanti S**, and McAlear, M. The yeast rRNA biosynthesis factor Ebp2p is also required for efficient nuclear division. *Yeast*. 2004, 21: 1219-1232. [PDF]